

NUMERICAL ANALYSIS OF DISPLACEMENT OF LATERALLY LOADED PILES  
SUBJECTED TO DYNAMIC LOADING

MSc. In GEOTECHNICAL ENGINEERING

LIDIYA WOLDE DENDIR

HAWASSA UNIVERSITY, HAWASSA, ETHIOPIA

JUNE, 2022

NUMERICAL ANALYSIS OF DISPLACEMENT OF LATERALLY LOADED PILES  
SUBJECTED TO DYNAMIC LOADING

LIDIYA WOLDE DENDIR

A THESIS PROPOSAL SUBMITTED TO  
HAWASSA UNIVERSITY  
DEPARTMENT OF CIVIL ENGINEERING,  
HAWASSA INSTITUTE OF TECHNOLOGY, SCHOOL OF  
GRADUATE STUDIES, HAWASSA UNIVERSITY,  
HAWASSA, ETHIOPIA

IN PARTIAL FULFILLMENT OF THE  
REQUIREMENTS FOR THE  
DEGREE OF  
MASTER OF SCINCE IN GEOTECHNICAL ENGINEERING

JUNE, 2022

**HAWASSA UNIVERSITY**  
**SCHOOL OF GRADUATE STUDIES**  
**ADVISORS' APPROVAL SHEET**

This is to certify that the thesis entitled ‘‘Numerical analysis of displacement of laterally loaded piles subjected to dynamic loading’’ submitted in partial fulfillment of the requirements for the degree of Master’s with specialization in Geotechnics, the Graduate Program of the School of Civil Engineering, and has been carried out by Lidiya Wolde Dendir Id.No GPGeotR/016/11, under our supervision. Therefore, we recommended that the student has fulfilled the requirements, and hence here can submit the thesis to the school.

M U JAGADEESHA

Name of major advisor

\_\_\_\_\_

Signature

\_\_\_\_\_

Date

Mr. Bereket Bezabih

Name of co-advisor

\_\_\_\_\_

Signature

\_\_\_\_\_

Date

**HAWASSA UNIVERSITY**  
**SCHOOL OF GRADUATE STUDIES**  
**EXAMINERS' APPROVAL SHEET**

We, the undersigned, members of the Board of Examiners of the final open defense by Lidiya Wolde Dender have read and evaluated her thesis “Numerical analysis of displacement of laterally loaded piles subjected to dynamic loading”, and examined the candidate. This is, to certify that the thesis has been accepted in partial fulfillment of the requirement for the degree.

M U JAGADEESHA

Name of Major Advisor

Signature

Date

Moltot Zewudie (PhD)

Name of Internal Examiner

Signature

Date

Tigist Guracha (Msc)

Name of the Chairperson

Signature

Date

Argaw Asha (PhD)

Name of External Examiner

Signature

Date

SGS Approval

Signature

Date

## **DECLARATION**

I hereby declare that this thesis is my original work and has not been presented for a thesis degree in any other university, and all sources of material used for this thesis have been duly acknowledged.

Name: Lidiya Wolde Dendir

Signature: \_\_\_\_\_

This MSc in Geotechnical Engineering or equivalent thesis has been submitted for examination with my approval as a thesis advisor.

Name: M U JAGADEESHA

Signature: \_\_\_\_\_

Place    Hawassa University,  
              Institute of Technology,  
              Hawassa.

Date    June, 2022

## **ACKNOWLEDGEMENT**

Above anyone and everything, I praise my almighty God, who enabled me to succeed in my work. Then I would like to express my special thanks gratitude to my advisor M U JAGADEESHA and my co-advisor Mr. Bereket Bezabih for their constructive comments, advice, and encouragement throughout this work. I want to forward my deep appreciation to Hawassa University Institute of Technology and Ethiopian Road Authority (ERA) for giving me a chance to learn, getting knowledge, and finish my research work with financial support.

My deepest thanks also go to my dearest families, friends, and classmates for the invaluable and heartfelt gratitude contributions they made for this research work feasible. I thank me for believing in me. Furthermore, I thank all those who directly or indirectly contributed to the success of this work.

## TABLE OF CONTENTS

ACKNOWLEDGEMENT .....	I
LISTS OF ABBREVAIATIONS AND ACRONYM .....	VI
LIST OF TABLES.....	IX
LIST OF FIGURES .....	X
LIST OF FIGURE IN THE APPENDIX.....	XII
ABSTRACT.....	XIII
1. INTRODUCTION .....	1
1.1 Background .....	1
1.2 Statement of the Problem.....	3
1.3 Objectives.....	3
1.3.1 General Objective.....	3
1.3.2 Specific Objectives .....	3
1.4 Significance of the Study .....	4
1.5 Scope and Limitations of the Study .....	4
1.6 Thesis Organization .....	5
2. LITERATURE REVIEW .....	6
2.1 Introduction.....	6
2.2 Dynamic Analysis of Laterally Loaded Pile .....	6
2.3 Estimation of Dynamic Loads.....	7
2.3.1 Machine Loads .....	7
2.3.2 Wave Forces and Wind Forces.....	8
2.3.3 Earthquake Forces .....	8
2.4 Method of Analysis for Laterally Loaded Pile.....	10
2.4.1 Theory of Vibration.....	10

2.5 Wave Propagation in Elastic Medium.....	12
2.5.1 Equation of Motion.....	12
2.5.2 Damping .....	14
2.5.3 Ground Response.....	15
2.6 Soil-Pile Interaction Analyses Approach .....	16
2.7 Kinematic interaction.....	18
2.8 Analysis of Kinematic Interaction of Pile Foundations .....	19
2.8.1 Dynamic Soil-Structure Interaction.....	20
2.8.2 Time Domain Vs Frequency Domain Analysis.....	22
2.9 Linear, Non Linear and equivalent Linear Analysis .....	22
2.9.1 Direct and Multi-Step Approach .....	23
2.9.2 1D, 2D and 3 D Analysis.....	23
<u>2.10 Available Analysis Methods for Dynamic Lateral Loading of Piles .....</u>	<u>24</u>
2.10.1 Winkler Model.....	24
2.10.2 p-y Curve .....	25
2.10.3 Continuum Model.....	26
2.11 Critical pile length.....	29
2.12 Dynamic analysis of batter pile.....	31
2.13 Prior Works on Dynamic Laterally Loaded Piles .....	32
2.13.1 Equivalent Cantilever Beam.....	32
2.13.2 Beam on Elastic Foundation (Sub Grade Reaction).....	32
2.13.3 Approximate Analytical Approach.....	33
2.14 Plaxis 3-D Model validation .....	37
2.14.1 Hetlant Wind Monopile.....	37
3. MATERIAL AND METHODS.....	42

3.1 General Approach .....	42
3.2 Finite Element Method.....	42
3.2.1 Element Formulation.....	42
3.2.2 Time Integration .....	44
3.3 Constitutive Models .....	45
3.3.1 Linear Elastic Model .....	46
3.3.2 Mohr Coulomb Model.....	46
3.3.3 Hardening soil model (HS).....	46
3.3.4 Hardening soil model with small strains (HSsmall).....	47
3.4 Boundary Conditions .....	47
3.4.1 Static Boundary Conditions.....	47
3.4.2 Dynamic Boundary Condition.....	47
3.4.3 Rayleigh Damping Parameters and Damping Ratio.....	48
3.5 Materials Modeled in PLAXIS .....	48
3.5.1 Steel Piles .....	48
3.5.2 Soil.....	49
3.5.3 Geometry of Soil Model.....	50
3.6 Input Motion .....	51
3.7 Soil volume in PLAXIS 3D was modeled Mesh .....	53
4. RESULT AND DISCUSSION .....	56
4.1 Effect of pile length.....	56
4.2 Effect of pile length on free head pile.....	60
4.3 Effect of pile length on fixed head pile.....	62
4.4 Effect of batter angle.....	63
4.5 Effect of Negative batter pile on Head Deflection of Pile .....	64

4.6 Effect of positive batter pile on Head Deflection of Pile .....	65
4.7 Final displacement for free head and fixed head single pile .....	68
5. SUMMARY AND CONCLUSION .....	69
5.1 Summary .....	69
5.2 Conclusion .....	70
5.3 Recommendation.....	71
REFERENCES .....	72
APPENDEX.....	77

## LISTS OF ABBREVIATIONS AND ACRONYM

3D	Three dimensional
2D	Two dimensional
1D	One dimensional
$A_{\text{LOOP}}$	Area of hysteretic loop
$\beta$	Tuning ratio
C	Cohesion
C	Viscose damping coefficient
c	Translational vibrational stiffness
CPT	Cone penetration test
D	Pile diameter (m)
$\epsilon$	Volumetric strain
EI	Flexural rigidity of pile
$E_p$	Yonge's modulus of pile
E	Modulus of elasticity
$E_{50}$	Tri-axial loading stiffness
$E_{ur}$	Tri-axial unloading stiffness
$E_{ode}$	Odometer loading stiffness
F	Force (KN)
$G_o^{\text{ref}}$	Small strain shear modulus
G	Shear modulus
Hz	Herze
HS	Hardening soil model

$\tau$	Shear stress
K	Stiffness
$k_s$	Static soil modulus
$\kappa$	Spring constant of soil
L/d	Slenderness ratio
$l_e$	Tangent (average) element size
LE	Linear elastic
L	Length (m)
$l_c$	Effective pile length
M	Mass matrix
MC	Mohr-coulumb
m	Mass of pile element per unit length
$\eta$	Viscosity
$\rho$	Mass density of a material
p-y	Soil resistance per unit length
p-wave	Primary wave
Q	Excitation force
R	Width of pile
r	Eccentricity of unbalance weight
SPT	Standard penetration test
SDOF	Single degree of freedom
S-wave	Secondary wave
T	Thickness

$u, \dot{u}, \ddot{u}$	Displacement, velocity, acceleration
$\nu$	Poisson's
$V_s$	Shear wave velocity
$W_D$	Dissipated energy
$W_s$	Maximum strain energy
$\omega$	Angular frequency
$\lambda, \mu$	Lame's constant
$\nabla^2$	Laplacian operator
$\xi$	Damping ratio of the system
$\gamma, \gamma_s$	Shear strain, shear wave velocity
$\phi, \psi, \Pi$	Friction angle, angle of dilatancy

## LIST OF TABLES

Table 2- 1 effective pile slenderness ration for fixed-head piles .....	30
Table 2- 2 effective pile length slenderness ratio for free-head piles .....	30
Table 3-1 Pile parameters used for analysis.....	49
Table 3-2 Soil parameter used for analysis.....	50
Table 3-3 List of geometrical coordinates .....	51
Table 3-4 Relative element size and the resulting element dimension.....	53
Table 4-1 classification of short and long free head pile in terms of effective pile length.....	57
Table 4-2 classification of short and long fixed head pile in terms of effective pile length.....	57
Table 4-3 comparison pile top displacement for negative and positive batter pile under earthquake loading .....	67

## LIST OF FIGURES

Figure 2- 1 Sketch of soil-pile-interaction problems (after Gazetas and Mylonakis 1998).....	17
Figure 2- 2 the superposition theorem for soil-pile-interaction problems a) kinematic interaction b)inertial interaction (after Gazetas and Mylonakis 1998).....	17
Figure 2- 3 Seismic soil-pile-foundation-structure interaction: the whole system (Gazetas et al1993) .....	19
Figure 2- 4 Seismic soil-pile foundation-structure interaction: kinematic seismic response analysis(Gazetas et al 1993) .....	20
Figure 2- 5 Idealized Soil models (Gazetas 1984).....	20
Figure 2- 6 Salient features of dynamic soil-pile interaction (wolf, 1985).....	21
Figure 2- 7 Soil- structure system Wolf, 1985.....	21
Figure 2- 8 Beam on elastic foundation.....	24
Figure 2- 9 3-D FEM model used by Bentley and Naggar [2000] a) Plan view b) Front cross sectional view .....	29
Figure 2- 10 Laboratory test setup.....	38
Figure 2- 11 linearly increasing stiffness profile for soil model.....	39
Figure 2- 12 3D modeling of wind-turbine Monopile .....	40
Figure 2- 13 Time-series of pile top displacement for 0 kPa overburden pressure using LE. .	41
Figure 2- 14 Time-series of pile top displacement for 0 kPa overburden pressure using Hss.	41
Figure 3-1 Basic 10 node tetrahedral element in Plaxis3D.....	43
Figure 3-2 Adopted mesh for analysis .....	44
Figure 3-3 Stiffness profile used in the analysis.....	50
Figure 3-4 Input acceleration time history used as base excitation .....	52
Figure 3-5 Earthquake acceleration- time records applied to the bottom of the model.....	52
Figure 3-6 3D mesh generation .....	54
Figure 3-7 Plaxis 3d modeling and analysis steps .....	55
Figure 4-1 lateral displacement of 4m free headed short pile Vs dynamic time. ....	58
Figure 4-2 lateral displacement of 16m free headed long pile Vs dynamic time. ....	59
Figure 4-3 lateral displacement of 8m fixed headed long pile Vs dynamic time. ....	59

Figure 4-4 lateral displacement of 20m fixed headed long pile Vs dynamic time. ....	60
Figure 4-5 Pile head deflection of free headed pile .....	61
Figure 4-6 Pile head deflection of fixed headed pile .....	62
Figure 4-7 the effect of pile head fixity condition on maximum head deflection of pile .....	63
Figure 4-8 3D modeling negative batter pile .....	64
Figure 4-9 Pile top displacement Vs negative batter angle .....	65
Figure 4-10 3D modeling positive batter pile .....	66
Figure 4-11 Pile top displacement Vs batter angle .....	67
Figure 4-12 the effect of pile head fixity condition on the final displacement of pile .....	68

**LIST OF FIGURE IN THE APPENDIX**

Figure B- 1 Pile head displacement for 4m free headed pile..... 79

Figure B- 2 Pile head displacement 8m free headed pile ..... 79

Figure B- 3 Pile head displacement 12m free headed pile ..... 80

Figure B- 4 Pile head displacement 20m free headed pile ..... 80

Figure B- 5 Pile head displacement 24m free headed pile ..... 81

Figure B- 6 Pile head displacement 4m fixed headed ..... 81

Figure B- 7 Pile head displacement 8m fixed headed ..... 82

Figure B- 8 Pile head displacement 12m fixed headed ..... 82

Figure B- 9 Pile head displacement 16m fixed headed ..... 83

Figure B- 10 Pile head displacement 20m fixed headed ..... 83

Figure B- 11 Pile head displacement 24m fixed headed ..... 84

## ABSTRACT

In this paper, the behavior of a vertical pile for both free headed and fixed head condition and batter pile subjected to lateral earthquake load are modeled with finite element software. The paper attempts to examine the effect of vertical and batter angle on its deflection magnitude with different pile length and magnitude under earthquake loading. The overall response of vertical and batter pile subjected to lateral earthquake load are investigated using 3D finite element method was applied for numerical modeling and plaxis3D software is utilized to evaluate the lateral displacement of pile. For this analysis, the length of the pile varies between 4m-24m with 4m interval and the batter angle vary  $5^0$ - $25^0$ . The effective pile length ( $l_c$ ) values differentiate the pile as short and long pile for both free head and fixed head conditions. also the analysis done on batter pile Two cases were considered; one case considered positive batter pile with pile length 8m the and two case considers negative batter with pile length 8m. The built-in material models of the Finite Element (FE) program PLAXIS were used to capture the head displacement of pile and for the seismic loading a real strong motion record of Hollister earthquake is adopted largely for its small duration. Dynamic analysis carried out using linear-elastic soil material model used for both pile and soil. The analysis indicates that the head deflection on a pile decrease with increasing pile length because of soil stiffness increase within the depth for fixed head and free head pile. Short pile has higher deflection than long flexible pile for both fixed head and free head condition. For the increasing in negative batter angle decreases the pile head displacement This behavior is due batter pile generally have higher horizontal stiffness, mainly due to the fact that inclined pile provide partial horizontal resistance and the upper soil support in a negative battered pile is enormous. For the increasing in positive batter angle increasing the pile head displacement This behavior is due the soil reaction at the ground level is zero for positive batter pile

**Key words:** vertical pile, batter pile, FEM, earthquake loading

# 1. INTRODUCTION

## 1.1 Background

Pile foundations are used to transfer super-structural loads to underlying soil or rock. Mostly deep foundations are adopted when the load of the superstructures is heavy or the bearing capacity of the soil is very low. Pile foundations are safer than other foundation types for supporting structures in seismic prone areas.

If the load acting on the pile is axial, it is transferred to the base of the pile and through the pile shaft as base resistance and shaft or skin friction, respectively. Laterally loaded piles transfer the load to the surrounding soil mass through the lateral resistance of soil. When lateral loads are applied on the pile, the pile tries to shift in the direction of the applied load, pressing against the soil. This will generate normal stress, shear stress, and strain in the soil. The external force is resisted by the soil resistance around the pile. Failure of short pile occurs when the lateral of the soil has been exceeded. In cases of long pile, the failure associated the moment at one or more points exceeds the moment of resistance and the failures takes place by formation of hinges along the pile length. This lateral deflection of pile depends on the soil resistance and the soil resistance in turn depends on the pile deflection and this interdependence is known as soil- pile interaction.

Soil-pile interaction can be kinematic and /or inertial (Kramer, 1996) (Poulos, 2013). The inertial interaction is the phenomenon in which inertial forces developed in the structure by its own vibrations generate primarily base shears, bending moments, and axial loads which in turn cause deformations in the surrounding soil surrounding of foundation system. Kinematic interaction results from the propagating nature of seismic disturbances in the form of waves, which makes the soil motion at any given instant generally different from point to point. Design of pile foundation under seismic load should include the effect of ground motion and inertial load. For such cases, dynamic soil-pile interaction analysis becomes important to assess the dynamic response of pile foundation.

Analysis of pile structure is mostly done for vertical piles corresponding to their vertical loads. When the structure is loaded laterally, i.e. the lateral load per pile exceeds the limiting value, batter piles are used in combination with vertical piles. Generally, a pile carries much larger axial loads than lateral loads. Standing from this, a designer expects to transfer a portion of the lateral load to axial load, thereby increasing the lateral capacity of a pile. Batter piles convert overturning moments into compression and tension forces. Therefore, it is better to analyze the batter (inclined) piles to meet the maximum resistance capacity of piles for both vertical and lateral loads of applications in engineering developments to handle such loads under control without hazard.

In this study, pile head displacement vertical and batter pile was investigated by analyzing the effects of the three parameters which were length of pile for both include short rigid and long flexible pile condition, for free head and fixed head pile. Batter pile analysis on long pile Since the study of the pile head displacement and soil-pile interaction was focused on sand, this study considered drained conditions.

For this study, a 3D numerical model of a pile and the surrounding soils have been analyzed in the PLAXIS 3D (Brinkgreve and Swolfs (2013)). 2011. The validation of the 3D finite element model is examined by comparing the results with those from the experimental data conducted on offshore wind turbine by (Hetland & Ekisund, 2015) to make a comparison with current study of laterally loaded piles under seismic excitation.

Effective pile length ( $L_c$ ) value differentiate the pile as short rigid pile and long flexible pile. The analysis is performed on single pile considering different pile length 4m,8,12,16,20,24 for each length analysis is performed for both fixed and free head condition by considering 0.4 diameter and using the same procedure to analyze for positive and negative batter pile foundation. The sub soil comprised medium dense sand whose behavior represent by linearly elastic model for small strain analysis and pile foundations subjected to seismic excitation under the bottom of the model to consider the effect of interaction.

## **1.2 Statement of the Problem**

The lateral load capacity of pile foundations is critically important in the design of civil structures which may be subjected to earthquake load. Information about the lateral behavior of piles under dynamic loading condition. It is noted that there is limited literature reporting on pile behavior under lateral dynamic load.

This paper investigates the importance of analysis of pile under seismic excitation using simple soil model for kinematic interaction by considering short and long pile and fixed and free head pile condition and advantage of using batter pile under dynamic earthquake taking in account of both positive and negative batter pile condition. Such analyses are valuable in leading to a better understanding of the details of piled under seismic excitation load using simple constitutive model to make simple and understandable the complex nature of seismic analysis.

## **1.3 Objectives**

### **1.3.1 General Objective**

- The overall objective of this study is focused on the investigation of the behavior of laterally loaded piles under dynamic loading conditions using 3D numerical analysis.

### **1.3.2 Specific Objectives**

- Determine deflection magnitude dynamic loading for short and long pile
- To determine the deflection magnitude for free headed and constrained piles under dynamic load
- To determine the deflection magnitude for batter pile under dynamic loading condition

#### 1.4 Significance of the Study

pile foundation analysis by its self very complicated problem when a pile foundation subjected to earthquake lateral load make it more complex the problem involving knowledge of soil mechanics, soil dynamics and vibration theories. The emphasis of this study is to understand the dynamic lateral behavior of single vertical and batter pile under seismic induced vibration, the pile exited in horizontal direction 3d dynamic implicit finite element analysis wear carried out using linear elastic soil model.

The finding of this study had a significant impact on piled analysis in a linear elastic approach rather than an advance soil model gives information about the pile head displacement of vertical single pile under dynamic excitation. Evaluating the parameters that affect pile flexibility gives a noticeable understanding of piled foundations performance subjected to dynamic loading. In addition, the study was used as a reference by those researchers who want to conduct studies on the future details of laterally loaded pile foundations and related issues. Thus, the results presented in this paper can serve as a guideline to produce a safe and economical design for pile under seismic load in small strain condition.

#### 1.5 Scope and Limitations of the Study

This paper focuses on laterally loaded piles under the dynamic conditions when the pile is vertical and inclined at an angle  $\beta$ .

- **Loading type:** dynamic lateral loads
- **Soil parameter:** the soil is simulating using linear elastic mode for all analysis
- **Pile head fixity:** the analysis was carried out for both fixed head and free head vertical single pile and batter pile.
- **Pile depth and batter angle:** the pile length is 4m,8m,12m,16m, 20m, 24m batter angle vary from  $50^{\circ}$   $10^{\circ}$ ,  $15^{\circ}$ ,  $20^{\circ}$ ,  $25^{\circ}$ degrees for both negative and positive batter pile
- **Drainage condition:** Drained analysis was conducted for all layers of ground material

## **1.6 Thesis Organization**

In Chapter 1, a brief background to the dynamic lateral response of piles is presented. The statement of the problem, the objective, scope, and methodology of the study are concisely presented.

In Chapter 2, a summary of a literature review of relevant topics (piles under dynamic lateral loads, seismic-soil-pile interaction, soil-structure interaction, dynamic analysis of batter pile) is provided.

In Chapter 3, detailed descriptions of the pile and soil properties and materials used for the development of the proposed model with a description of PLAXIS 3D, the FE software used, validation of proposed model are presented

In chapter 4, parametric study and analysis of laterally loaded pile is discussed in details.

In chapter 5, summery, conclusions and recommendations of the present study are given followed by the references.

## **2. LITERATURE REVIEW**

### **2.1 Introduction**

Due to the continuous nature of soils and geological material, their dynamic behavior is often understood in the context of wave propagation. While most structures can be idealized as a set of discretized masses with corresponding stiffness's, soils in most cases cannot. Therefore, in order to fully understand the dynamical behavior of soils, elastic wave propagation must be considered. Materials consist of atoms which can be vibrated about their position of equilibrium. When the particles produce a unison movement, they can be considered to create a mechanical wave. Such waves will propagate through a material until it reaches the material boundaries, where they will be reflected or transmitted depending on the boundary conditions. In an infinite elastic medium there is considered to be only two types of waves: P-waves and S-waves. In an elastic half space, however, boundary conditions are introduced, which leads to two additional types of waves. These are called Rayleigh and Love waves. While Rayleigh waves are known to exist in a homogeneous elastic half-space, Love waves require a surficial layer of lower S-wave velocity and is therefore outside the scope of this thesis.

### **2.2 Dynamic Analysis of Laterally Loaded Pile**

Piles are often subjected to lateral dynamic loading originating from various sources. These loads include wind loads, water waves, earthquake loads and machine loading from buildings and bridges. Unlike the conventional attributes required to characterize static loading i.e. force magnitude, direction and line of action, dynamic loads require frequency for complete description. Common frequency ranges of interest are 0 -10 Hz for earthquake loading, 0-1 Hz for water waves and winds and 5- 200 Hz for machine loading, (El Naggar & Bentely, 2000).

The design criteria used to design safe and economical foundations relates to the dynamic responses of the foundation, which are expressed in terms of the limiting amplitude of vibration at a particular frequency or a limiting value of peak velocity of peak acceleration, (Richarts, Hall Jr, & Woods, 1970).

Most building and bridge design codes however, opt to adopt factored static loads to address the effects of dynamic loading. Such an approach may yield satisfactory results for low frequency loading but fails to address resonance, nonlinearity, damping and soil-pile interactions for

medium to high frequency loading conditions (El Naggar & Bentely, 2000; El Naggar & Bentely, 2000). Furthermore, (Richart, 1962) put forward a general limit of displacement amplitudes for a particular frequency of vibration in which he pointed out the magnitudes involved are much smaller than the displacement usually considered in the design of foundations for static loads.

Hence the analysis and design of dynamically loaded foundations should adopt a rigorous approach to determine the dynamic response in terms of stresses, strains deflection and so on. To this end (Poulos & Davis, Pile Foundation Analysis and Design, 1980) laid out the following steps; definition of dynamic loads, selection of appropriate method and selection of soil and foundation parameters to be used in the analysis. These steps shall be discussed here under as it pertains to dynamic laterally loaded piles. At the end of this section the various models proposed to analyses dynamic laterally loaded piles including physical model tests and the pertinent conclusions shall be reviewed and presented.

### **2.3 Estimation of Dynamic Loads**

Dynamic loads on foundations can be categorized in to two classes; loads directly applied to the foundation, and loads applied to the foundation through the soil, (Poulos & Davis, Pile Foundation Analysis and Design, 1980); (Nair, 1969). Directly applied loads include machine loads, wind and water waves loads, whereas earthquake loads constitute loads applied to the foundation through the soil.

#### **2.3.1 Machine Loads**

Machine loads in foundations can be from rotary machines such as turbines, centrifugal pumps, axial compressors, generators etc. Rotary machines operate at a constant speed for long durations of time. Although these machines are design with minimal unbalanced force, in practice they often produce unbalanced force during rotation. Reciprocating machine induce vibratory force on to their support due to the need to decelerate and accelerate moving parts, (Richarts, Hall Jr, & Woods, 1970). A typical expression for unbalanced forces due to machine loads is given as;

$$F(t) = wr\omega^2 \sin(\omega t) \dots\dots\dots 2.1$$

where  $F(t)$  Is the force,  $w$  is the unbalanced weight,  $r$  the eccentricity the unbalanced weight,  $\omega$  is the angular velocity  $t$  is time.

The equations of motion for most discrete systems with stiffness,  $k$ , viscous damping coefficient  $c$ , is given as;

$$m \frac{\partial^2 u}{\partial t^2} + c \frac{\partial u}{\partial t} + ku = F(t) \dots\dots\dots 2.2$$

where  $u$  Is displacement

When  $c$  and  $k$  are constants, the second order differential equations is linear and a closed form solution is readily available and allows the principle of superposition to be used. However, when either  $c$  or  $k$  or bot are not constants, the problem becomes nonlinear and requires numerical solution.

**2.3.2 Wave Forces and Wind Forces**

According to (Morison, O'Brien, Johnson, & Schaff, 1950), the wave force on piles has two components, one depending on friction or drag and the other on inertia forces. Despite the fact that the assumption for the drag component contradicts the computations of inertia forces, a more refined analysis has not delivered better results, (Poulos & Davis, Pile Foundation Analysis and Design, 1980). A recent and comprehensive guideline to compute dynamic wave forces and wind forces is presented in (American Petroleum Institute, 2003)

**2.3.3 Earthquake Forces**

Poulos & Davis (1980) present three approaches to estimate earthquake forces. The first approach is the use of factored static loads at the surface, second equivalent dynamic load at the surface, often assumed sinusoidal in characteristics and the third one component base excitation. They reckon the first two approaches do not have any rational bases. Besides, the use of single seismic coefficient of static loads ignores the vertical variation in the value of the seismic coefficient, (Poulos & Davis, Pile Foundation Analysis and Design, 1980) (Seed & Martin, 1966).

Under ideal circumstances, analysis of ground response, which is used to predict earthquake induced forces, will include modeling the seismic event from the rapture mechanism to

propagation of stress waves and determine the reaction of the soils above the bed rock supporting the structure of interest, (Kramer, 1996). In practice, empirical methods are used based on the characteristics of recorded earthquakes to predict the bedrock motion at the site and the response of overlaying soil and its interaction with structure is analyzed.

If the total displacement of a single degree of freedom discrete mass,  $m$  supported on a base undergoing base vibration in a time period  $t$  is given by,  $u_t$ , it may be presumed that  $u_t$  composed of the base movement  $u_b$  and the displacement mass relative to the base  $u$  i.e.  $u_t = u_b + u$ . Taking the second derivatives of the displacements;

$$\frac{\partial^2 u_t}{\partial t^2} = \frac{\partial^2 u_b}{\partial t^2} + \frac{\partial^2 u}{\partial t^2} \dots\dots\dots 2.3$$

In the absence of an external excitation i.e.  $F(t) = 0$ , the equation of motion for the single degree of freedom system is

$$m \frac{\partial^2 u_t}{\partial t^2} + c \frac{\partial u}{\partial t} + ku = 0 \dots\dots\dots 2.4$$

Substituting the value of  $\frac{\partial^2 u_t}{\partial t^2}$  and rearranging, the equation of motion for a base excitation can be written as

$$m \frac{\partial^2 u_t}{\partial t^2} + c \frac{\partial u}{\partial t} + ku = -m \frac{\partial^2 u_b}{\partial t^2} \dots\dots\dots 2.5$$

Hence, base shaking can be represented as an external excitation of magnitude  $F(t) = -m \frac{\partial^2 u_b}{\partial t^2}$

Because the deformations associated with horizontal base excitation are primarily shear deformations, the real system can be considered as a discrete system based on a column of soil having a unit cross sectional area and height equal to depth of the soil layer, (Penzien, Shaffey, & Parmelee, 1964); (Poulos & Davis, Pile Foundation Analysis and Design, 1980). In this approach, the whole soil mass may be lumped at discrete points along the depth of the layer and linkages connecting adjacent masses consist of springs and dashpots.

## 2.4 Method of Analysis for Laterally Loaded Pile

### 2.4.1 Theory of Vibration

Vibrating systems can be categorized into rigid systems and compliant systems. In rigid systems all points within the system move in phase while in compliant systems different points within the system move out of phase. Compliant system can be further divided into discrete systems, whose mass can be considered to be concentrated at finite points hence finite degree of freedom, and continuous systems in which the mass distribution is continuous, hence infinite degree of freedom.

A discrete system where one dimension is adequate to completely describe the motions is referred to as single degree of freedom motion, SDOF. A typical example would be a spring dashpot system attached to mass,  $m$  with spring stiffness  $k$  and viscous damping coefficient  $c$  and subjected to excitation force  $Q(t)$ . The equation of motion for such a system using Leibniz's notation shall be;

$$m\ddot{u}(t) + c\dot{u}(t) + ku(t) = Q(t) \dots\dots\dots 2.6$$

Where,  $u(t)$  displacement from the equilibrium position. The differential equation is linear if the dashpot coefficient and stiffness are independent of displacement,  $u(t)$ , velocity,  $\dot{u}(t)$  or acceleration,  $\ddot{u}(t)$  enabling a closed form solution and use of principle of superposition. However, if the equation is nonlinear numerical methods are required to solve it.

The solution to the equation of motion of a vibrating system with damping ( $c > 0$ ) and external excitation force, say harmonic characteristics,  $Q(t) = Q_o \sin \bar{\omega}t$ , can be found by complementary solution. Assuming initial static equilibrium,

$$u(t) = e^{-\xi\omega_o t} (C_1 \sin \omega_d t + C_2 \cos \omega_d t) + C_3 \sin \bar{\omega}t + C_4 \cos \bar{\omega}t \dots\dots\dots 2.7$$

where

$$\omega_o = \sqrt{\frac{k}{m}} \quad \text{Un-damped free natural circular frequency of the system}$$

$$\xi = \frac{c}{2\sqrt{km}} \quad \text{Damping ratio of the system}$$

$$\omega_d = \omega_o \sqrt{1 - \xi^2} \quad \text{Damped circular natural frequency}$$

$$\bar{\omega} \quad \text{Frequency of the external excitation force}$$

$$C_1, C_2, C_3 \ \& \ C_4 \quad \text{Integration constants}$$

$$C_1 =$$

$$\frac{Q_o \bar{\omega}}{k \omega_d} \frac{\beta^2 - 1}{(\beta^2 - 1)^2 + (2\xi\beta)^2} \dots\dots\dots 2.8$$

$$C_2 =$$

$$\frac{Q_o}{k} \frac{2\xi\beta}{(\beta^2 - 1)^2 + (2\xi\beta)^2} \dots\dots\dots 2.9$$

$$C_3 =$$

$$\frac{Q_o}{k} \frac{\beta^2 - 1}{(\beta^2 - 1)^2 + (2\xi\beta)^2} \dots\dots\dots 2.10$$

$$C_4 =$$

$$\frac{Q_o}{k} \frac{-2\xi\beta}{(\beta^2 - 1)^2 + (2\xi\beta)^2} \dots\dots\dots 2.11$$

$$\beta = \frac{\bar{\omega}}{\omega_o} \quad \text{Tuning ratio}$$

It is pertinent to note that the solution has two components, a transient component which will die out after certain time and a steady-state component which is out of phase with the excitation external frequency. The steady state part of the solution can be given as;

$$u(t) = A \sin(\bar{\omega}t + \phi) \dots\dots\dots 2.12$$

where

$$A = \frac{Q_o}{k} \frac{1}{\sqrt{(\beta^2 - 1)^2 + (2\xi\beta)^2}}$$

$$\phi = \tan^{-1} \left( -\frac{2\xi\beta}{1 - \beta^2} \right)$$

The value of  $Q_o/k$  is the amplitude of the system under static loading, hence the accompanying coefficient for the steady-state part of the response,  $\frac{1}{\sqrt{(\beta^2-1)^2+(2\xi\beta)^2}}$  can be considered as a magnification factor,  $M$  for the amplitude. Note that it is a function of the damping coefficient and the tuning ratio. If there is no damping, the amplitude will go to infinity as the tuning ratio approaches unity i.e., resonance. In practice however, there is always damping and the maximum magnification for a given damping ratio will be occur when,  $\beta = \sqrt{1 - \xi^2}$ ;

$$M_{max} = \frac{1}{2\xi\sqrt{1-\xi^2}} \dots\dots\dots 2.13$$

The above solution is presented for a case of harmonic loading. In the event when the loading is a general periodic loading, Fourier transformation can be used to convert any periodic loading into a sum of harmonic loadings and principle of superposition can be used to determine the response of the system to the overall periodic excitation (Kramer, 1996).

## 2.5 Wave Propagation in Elastic Medium

### 2.5.1 Equation of Motion

In an infinite (unbounded) medium there are two types of waves are known to exist. These are the primary (longitudinal) waves, P-Waves, and secondary (shear) waves, S-Waves. The particle displacement in p-waves is parallel to the direction of wave propagation, whereas in the case of s-waves the particle displacement is orthogonal to the direction of wave propagation.

When the medium is bounded (elastic half space) other types of waves are observed. These include Rayleigh waves (surface waves), Love waves etc. The characteristics of these waves are treated in standard text books on continuum mechanism and shall not be repeated here. In the interest of continuity, however the basic equations shall be presented hereunder.

The equation of motion for stress wave propagation in a three dimensional isotropic, linearly elastic solid is given as;

$$\rho \frac{\partial^2 u}{\partial t^2} = (\lambda + \mu) \frac{\partial \bar{\epsilon}}{\partial x} + \mu \nabla^2 u \dots\dots\dots 2.14$$

$$\rho \frac{\partial^2 v}{\partial t^2} = (\lambda + \mu) \frac{\partial \bar{\epsilon}}{\partial y} + \mu \nabla^2 v \dots\dots\dots 2.15$$

$$\rho \frac{\partial^2 w}{\partial t^2} = (\lambda + \mu) \frac{\partial \bar{\epsilon}}{\partial z} + \mu \nabla^2 w \dots \dots \dots 2.16$$

where

$\lambda, \mu$       Lamé's constants

$\rho$             Mass density of the material

$u, v$  and  $w$    Displacements in  $x, y$  and  $z$  directions

$\bar{\epsilon}$             Volumetric strain

$\nabla^2$           Laplacian Operator

The wave equation for irrotational, dilatational wave i.e. p-waves can be found by differentiating the three equations of motions with respect to  $x, y$  and  $z$  and adding both sides and rearranging yields;

$$\frac{\partial^2 \bar{\epsilon}}{\partial t^2} = \frac{\lambda + 2\mu}{\rho} \nabla^2 \bar{\epsilon} \dots \dots \dots 2.17$$

The velocity of propagation of p-waves is given by,  $v_p = \sqrt{\frac{\lambda + 2\mu}{\rho}}$  or in terms of shear modulus,  $G$  and Poisson's Ratio  $\nu$ ,

$$v_p = \sqrt{\frac{2G(1-\nu)}{\rho(1-2\nu)}} \dots \dots \dots 2.18$$

The equation of motion for s-waves is given by eliminating the volumetric strain parameter from the equation of motion equations in a given direction, say  $x$ ;

$$\rho \frac{\partial}{\partial t^2} \left( \frac{\partial w}{\partial y} - \frac{\partial v}{\partial z} \right) = \mu \nabla^2 \left( \frac{\partial w}{\partial y} - \frac{\partial v}{\partial z} \right) \dots \dots \dots 2.19$$

The speed of propagation of s-waves is given by,  $v_s = \sqrt{\frac{\mu}{\rho}} = \sqrt{\frac{G}{\rho}}$ .

Detail treatment of the subject including surface waves, Loves waves etc., dispersion, reflection and refraction of these waves at various boundary conditions is presented in standard books such as, (Kramer, 1996)

### 2.5.2 Damping

Damping refers to dissipation of energy as a result of propagation the wave through a medium. The cause of dissipation can be attributed to friction, heat or plastic deformation and is not completely understood. Such a damping is often called material damping and/or viscous damping. For the purposes of viscoelastic wave propagation, soils are usually modeled as Kelvin-Voigt Solids. The stress- strain properties of such a material in shear are given by;

$$\tau = G\gamma + \eta \frac{\partial \gamma}{\partial t} \dots\dots\dots 2.20$$

where

$\tau$  Shear stress

$\gamma$  Shear strain

$\eta$  Viscosity

Another form of energy dissipation is radiation damping or geometric damping. This refers to the loss of energy due to the propagation of the wave energy into an ever increasing larger volume of mass of material. Essential distinguishing feature from material damping is that in material damping, the energy is transformed to other forms.

A number of factors influence damping in structures. These include vibration amplitude, material of construction, fundamental period of vibration, mode shape of structural configuration etc., (Elnashai & Di Sarini, 2015). In classical damping approach, where an appropriate idealization of similar damping mechanism is distributed throughout the structure, a mass and stiffness proportional damping such as Rayleigh damping can be adopted to estimate energy dissipation in the structure.

$$C = \alpha M + \beta K \dots\dots\dots 2.21$$

The damping ratio of the system for mass proportional damping  $\alpha$  can be related to modal damping ratio as;

$$\xi_n = \frac{\alpha}{2} \frac{1}{\omega_n} \dots\dots\dots 2.22$$

Equation 2.22 shows the value of  $\alpha$  can be chosen to obtain a specified value of damping ratio  $\xi_i$  for the  $i^{\text{th}}$  mode of vibration,  $\omega_i$ . Similarly, the modal damping ratio for stiffness proportional damping can be related to the coefficient  $\beta$  as;

$$\xi_n = \frac{\beta}{2} \omega_n \dots \dots \dots 2.23$$

Hence the overall damping ratio for the  $n^{\text{th}}$  mode of vibration of a system is given as;

$$\xi_n = \frac{\alpha}{2} \frac{1}{\omega_n} + \frac{\beta}{2} \omega_n \dots \dots \dots 2.24$$

The values of  $\alpha$  and  $\beta$  can be determined for a specified damping ratios,  $\xi_i$  and  $\xi_j$  for the  $i^{\text{th}}$  and  $j^{\text{th}}$  modes. However, experimental measurements show damping ratios do not vary with frequencies as stipulated in equations shown above. Hence, a single damping ratio can be used over a range of frequencies.

$$\alpha = \xi \frac{2\omega_i\omega_j}{\omega_i+\omega_j} \text{ and } \beta = \xi \frac{2}{\omega_i+\omega_j} \dots \dots \dots 2.25$$

In applying the method, the modes,  $i$  and  $j$  with specified damping ratios should be selected to ensure a reasonable value for the damping ratio in all modes contributing significantly to the dynamic response of the structure. For instance, if five modes are considered for the analysis, and roughly the same damping ratio is adequate for all modes the  $i^{\text{th}}$  and  $j^{\text{th}}$  modes should be the first and the fourth modes, (Chopra, 2012).

### 2.5.3 Ground Response

Local soil conditions influence the characteristics of dynamic forces originating from natural causes like earthquakes, and consequently the interaction with structures (Wolf, 1985). The ground response analysis determines the control motion (free field motion) which enables to establish the most important parameter for the structure i.e. whether it is peak ground acceleration, frequency content or duration of motion.

As stress waves traverse geologic materials with varied properties, they are reflected and refracted. By the time they reach the ground surface, one can assume the waves are dominated by shear waves propagating vertically from the bed rock, (Kramer, 1996). In such a case 1 D

analysis suffices. Depending on the complexity of the problem, a 2D or 3D linear or nonlinear ground response analysis can be adopted.

A typical 1 D linear response analysis involves the use of a transfer function which is used to express various output response parameters such as displacement, velocity, acceleration, stress and strains to an input parameter such as bedrock acceleration. A known time history of bedrock motion is first presented as a Fourier series. Each term of the series is then multiplied by the transfer function to produce the output surface ground motion. The output is then expressed in the time domain using inverse Fourier transformation.

For problems in which one dimensional wave propagation assumption is not acceptable (site close to the source of excitation), sloping or irregular ground surfaces, when heavy or stiff structures are present and/or for embedded structures, walls and tunnels a 2D or 3D response analysis shall be adopted (Kramer, 1996).

## **2.6 Soil-Pile Interaction Analyses Approach**

An earthquake geotechnical engineer faces numerous challenges in foundation design for seismic excitation because of the complexity of the problem. To handle this type of problem, the earthquake geotechnical engineer needs skills in soil mechanics, foundation engineering, and soil-pile- interaction.

Figure 2-1 shows the soil-pile-interaction problem and its key features. Since the forces that result from soil-pile-interaction govern structural response, these forces should be determined with accurate analyses. Soil-pile-interaction analyses can be carried out in two ways: either by modeling the structure and soil together with appropriate interface behavior as shown in Figure 2-1 or by using the principle of superposition as shown in Figure 2-2. The superposition approach has two steps that address two different mechanisms, kinematic and inertial interaction. This approach is based on the assumption that the system remains linear. Superposition is exactly valid for linear soil, pile, and structure (Whitman, 197). However, superposition is approximately valid for moderately nonlinear systems under engineering approximations, because pile deformations due to lateral loading transmitted from the structure vanish very rapidly with depth.

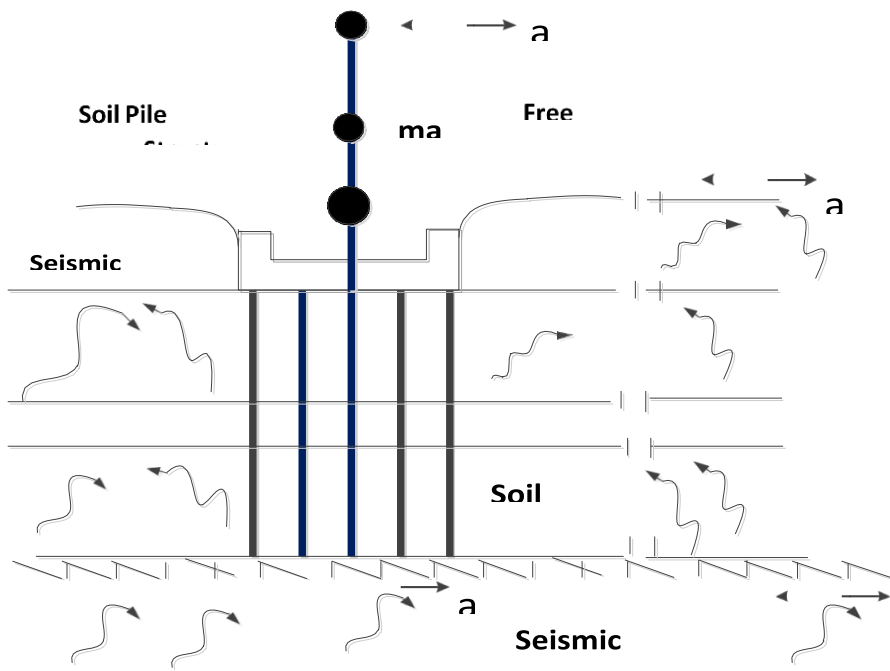


Figure 2- 1 Sketch of soil-pile-interaction problems (after Gazetas and Mylonakis 1998).

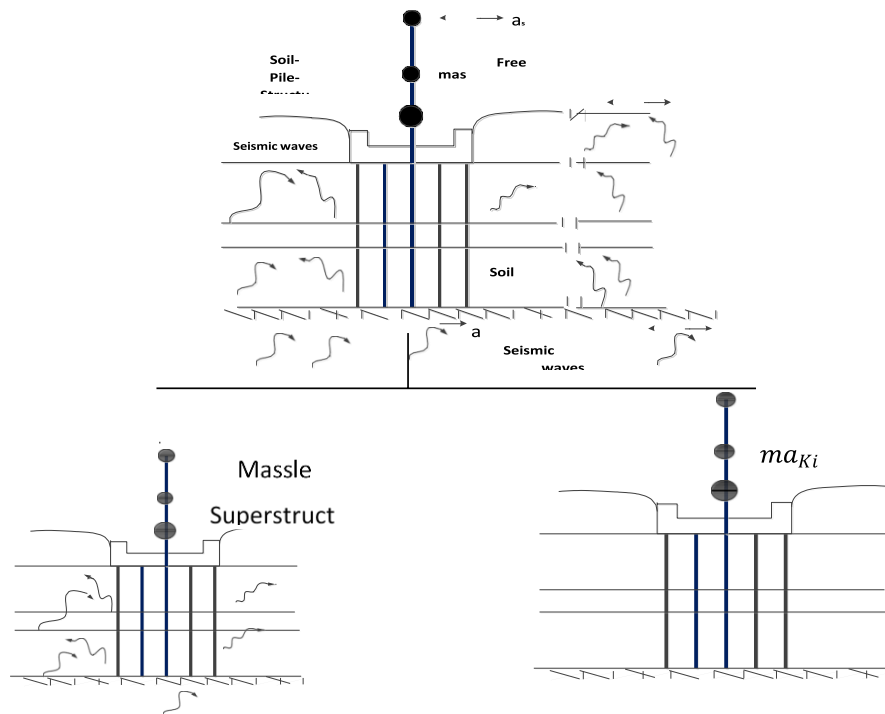


Figure 2- 2 the superposition theorem for soil-pile-interaction problems a) kinematic interaction b) inertial interaction (after Gazetas and Mylonakis 1998)

## 2.7 Kinematic interaction

In the free-field, an earthquake will cause soil displacements in both the horizontal and vertical directions. The kinematic interaction or scattering effect happens due to the inability of the foundation, owing to its stiffness and rigidity, to conform to the free-field ground motion causing variation of ground motion with depth and scattering of waves at the corners of the foundation. The other causes of these deviations are base-slab averaging, in which spatially variable ground motions within the building envelope are averaged within the foundation footprint due to the stiffness and strength of the foundation system and embedment effect, in which foundation-level motions are reduced as a result of ground motion reduction with depth below the free surface (Kramer 1996).

Horizontally propagating waves have negligible impacts in kinematic interaction effects on pile foundations, as wave length of practical interest,  $\lambda > 6d$  where  $d$  is the pile diameter, so that the base slab averaging effect is negligible for piles, moreover, the axial stiffness of piles is considerably high (Dobry and Gazetas 1988). But, vertically propagating SH waves have considerable impact on piles and it has been found that the kinematic interaction between pile and soil has, in general, two consequences (Dobry and Gazetas 1998):

- It filters out low-period (i.e. high frequency) components of the motion while at the same time it induces a rotational component at the pile head.
- It induces axial, bending, and shear deformation on piles. Bending is significant at two locations: at the top of fixed-head piles and at the interfaces of soil layers with sharply different stiffness's.

So, the kinematic response of a pile or pile group needs to be calculated at the pile head and at depth separately. The response at the pile head is an input into the inertial response analysis; and the response at depth may be used to assess the structural requirement of the pile in the intermediate and deep zones.

Kinematic interaction effects are exactly zero for shallow foundations in a seismic environment consisting exclusively of vertically propagating shear waves or dilatational waves; but more pronounced in pile and very stiff embedded shallow foundations of structures having two or more subterranean levels (Kramer & Stewart 2004; NIST GCR 12-917-21 2012). Gazetas

(1984) has demonstrated that when piles are flexible with respect to the surrounding soil, kinematic interaction is significant for small to medium frequencies.

## 2.8 Analysis of Kinematic Interaction of Pile Foundations

Kinematic interaction effects are described by a frequency dependent transfer function relating the FFM to the FIM of a hypothetical system which differs from the complete actual system in that, the mass of the superstructure is set equal to zero. The kinematic interaction is solved using the displacement and rotation kinematic interaction factors given by Gazetas (1984) for three soil models. So, calculation of the kinematic response of piles comprises of finding the FFM and calculation of the interaction factors to modify this FFM to get the FIM. The FIM is then simply obtained by multiplying the free-field response spectra with the calculated interaction factors.

### Free-field ground motion

Normally the free field motion at a specific location is obtained by 1D, 2D or 3D wave propagation theories. However, in the frequency domain analysis response spectra can be used as a FFM (Han 2004).

### Pile head motion

Kinematic interaction is expressed in terms of kinematic amplification factors as (Gazetas 1984):

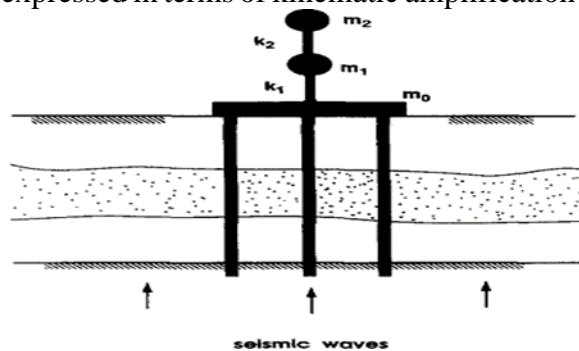


Figure 2- 3 Seismic soil-pile-foundation-structure interaction: the whole system (Gazetas et al 1993)

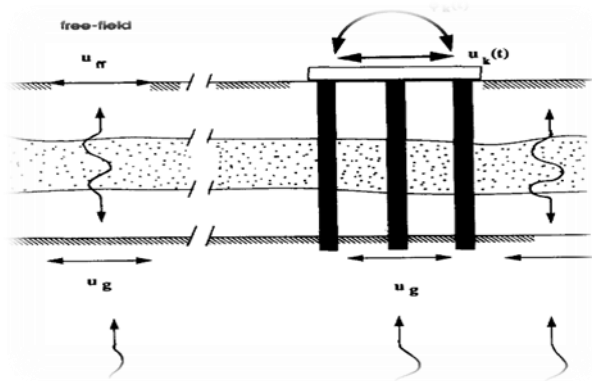


Figure 2- 4 Seismic soil-pile foundation-structure interaction: kinematic seismic response analysis(Gazetas et al 1993)

Simplified kinematic interaction factors for the three types of soil models as shown in Figure 2-5, which idealize different distributions of Young's modulus with depth are given as a function of the following frequency parameters (Gazetas 1984). However, this study focuses on constant stiffness distribution model, i.e. Soil model C shown in Figure 2-5.

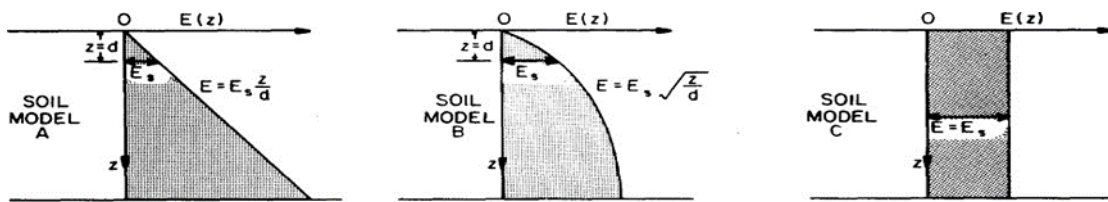


Figure 2- 5 Idealized Soil models (Gazetas 1984)

### 2.8.1 Dynamic Soil-Structure Interaction

Unlike structural dynamics, which determines the stress and displacement of structures to dynamic loads using a discretized dynamic model with finite degree of freedom, foundations interact with the soil, which is unbounded semi-infinite medium. The structure itself and the boundaries reflect the vibrations prohibiting use of simple assumptions in static analysis.

Wolf (1985) presents a demonstration of the salient features of dynamic soil- structure interaction as follows. Consider structures erected on rock out crop and soil mass along with assumed a free field response shown in the figure 2-6 below. Assume the structures are close enough so that the excitation reaching them is the same and consists of a horizontal motion propagating vertically, the particle motion and propagation as shown by the arrow.

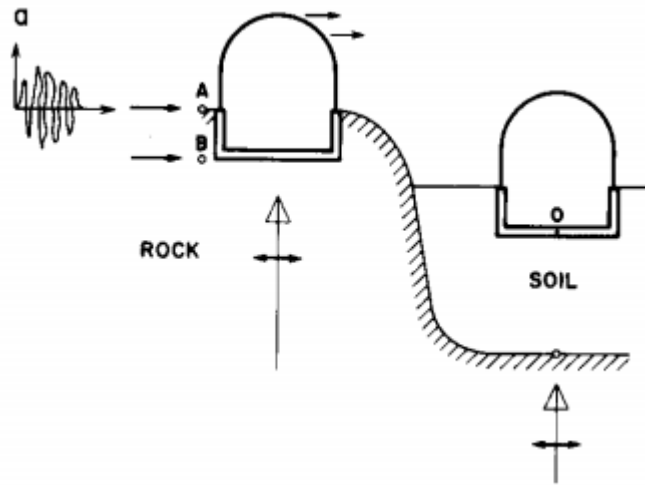


Figure 2- 6 Salient features of dynamic soil-pile interaction (wolf, 1985)

For the structure on the rock, the horizontal motion can be applied directly to the base of the structure i.e. due to the stiffness of the rock; the base motion will be the same as the free field motion of the excitation force. As a result, the input acceleration resulting in the applied inertial horizontal loads will be constant over the height of the structure. During the excitation an overturning moment and transverse shear acting at the base will develop, but non rocking motion at the base. Hence, the structural response depends only the properties of the structures.

For the structure founded on the soil, however the motion of the base of the structure at O is different from the free field response at A because of the coupling of the soil-structure system. Figure 2-6 presents three effects. First the motion of the site without the structure and excavation at D & E, i.e. the free field response is determined from the rock motion at C. In general the motion is amplified depending on the frequency content of the excitation resulting an increase in the horizontal displacement towards the free surface.

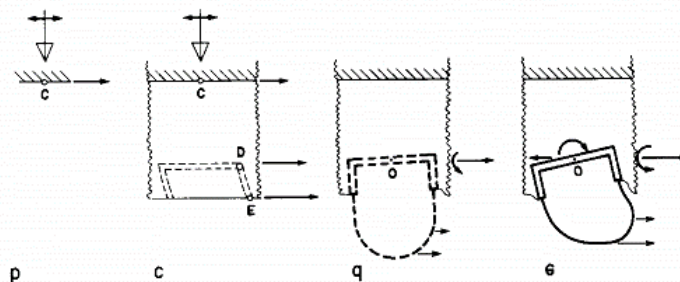


Figure 2- 7 Soil- structure system Wolf, 1985

Second excavation and construction will modify the response to the excitation. The rigid base will experience some average horizontal displacement and rocking component. The horizontal displacement leads to acceleration (inertial loads) which varies with the height of the structure, i.e. kinematic interaction. Third the inertial loads applied to the structure will lead to an overturning moment and transverse base shear acting at point O. A detailed account of the effect of local site condition is presented in (Kramer, 1996)

### **2.8.2 Time Domain Vs Frequency Domain Analysis**

The response of soil-structure system to dynamic loading is known to be frequency dependent. Two approaches can be adopted to evaluate the overall system response, frequency domain analysis and time domain analysis. In frequency domain analysis, the response of soil –structure system is evaluated at each excitation frequency. Once the responses at all frequencies of interest are identified, the overall response is evaluated using the principle of superposition, (Elnashai & Di Sarini, 2015). The approach presumes linear behavior in order to apply principle of superposition.

In time domain analysis the entire soil-structure system is analyzed at each time steps of excitation using numerical integration. At each step force equilibrium and displacement compatibility are ensured hence inelastic behavior of the components can be accurately represented.

### **2.9 Linear, Non Linear and equivalent Linear Analysis**

The selection of analysis method depends on many factors. These include the level of nonlinearity involved in the system, the required level of accuracy, level of uncertainty in the input parameters and available computational power, (Elnashai & Di Sarini, 2015). The linear approach has computational efficiency and has been used widely through transfer functions to model ground response and soil-structure interactions. The approach depends on the principle of superposition and cannot be used to analyze the nonlinear behavior of soils. To improve the linear approach by accounting for the known non-linear behavior of soil, the actual hysteretic stress-strain curve for dynamically loaded soil can be approximated by equivalent linear properties,  $G$  (the secant shear modulus) and  $\xi$  damping ratio which produce the same amount of energy loss as in a single hysteretic loop, (Kramer, 1996). These values are continually

adjusted for the appropriate strain magnitude for each time increment but remain constant within the same increment. Hence constant values of these variables can be used for each soil layer.

Most structures supported on piles such as high rise buildings and bridges are expected to behave in inelastic manner under design dynamic excitation. Hence need to be analyzed using none linear models. Many soil-structures models adopt a near field and far field formulation for the soil. The near field soil is modeled in a nonlinear model whereas the far field soil may be assumed to behave in linear manner. Detailed account of the material models is presented in the materials and methods section of this report.

### **2.9.1 Direct and Multi-Step Approach**

Direct approach accounts for both kinematic and inertial interactions the soil structure system using numerical models like finite elements. A single model is used to evaluate the dynamic response. The excitation or ground acceleration can be applied on the structure or on the boundary of the soil domain, (Elnashai & Di Sarini, 2015); (Zhang, et al., 2008).The various strength and limitation of this approaches are discussed in the materials and methods section of this report.

In the multi-step approach the dynamic response of the soil-structure system is evaluated in two steps, the kinematic and inertial interactions, (Wolf, 1985); (Elnashai & Di Sarini, 2015).In the kinematic analysis component, the structure is assumed to have no mass but stiffness. In the inertia analysis component the forces resulting from the kinematic interaction and the original excitation are applied to the structure with its mass, (Kramer, 1996). Since this approach relies on the principle of superposition, the soil needs to be linearly elastic.

### **2.9.2 1D, 2D and 3 D Analysis**

The ground motion to which surface structures are subjected to can be simplified as a vertically propagating shear wave with horizontal vertical motion, unless the structures very close to the source of the disturbance. Hence a 1 D modeling of the system can be applied in such cases for level or gently sloping ground surfaces to establish the ground response and soil-structure interaction.

For sloping natural or ground surfaces, heavy structures, stiff embedded structures invalidate the assumption of one dimensional wave propagation and require 2D analysis. When the soil

property or the problem boundary varies with lateral direction, a 3 D analysis is warranted to realistically evaluate the dynamic response, (Kramer, 1996).

## 2.10 Available Analysis Methods for Dynamic Lateral Loading of Piles

In this section, methods of modeling the dynamic behavior of a single pile under lateral loads are explained. These are Beam on Non-linear Winkler Foundation (BNWF), Continuum Methods, and Boundary Element Method (BEM), and Finite Element Method (FEM).

### 2.10.1 Winkler Model

In 1867, Winkler proposed this model, which was introduced as Beam on Winkler Foundation (BWF). This model characterizes the soil as a series of independent linearly elastic spring, soil-pile contact at any point along the pile length, there is a relationship between deflection and forces, and the contact stress at other points is independent

(Hetenyi, 1946) presented analytical solutions for beams on a foundation with a fourth-order differential equation governing the beam deflection (Eq.2.29). The input parameters of the solution are the length and elastic modulus of the beam, the spring constant of the foundation (soil), and the magnitude and distribution of the applied load (Figure 0-8). At the end of the solution, shear force, bending moment, and deflection along the span of the beam can be found.

$$EI \frac{d^4 y}{dx^4} + ky = q \dots\dots\dots 2.29$$

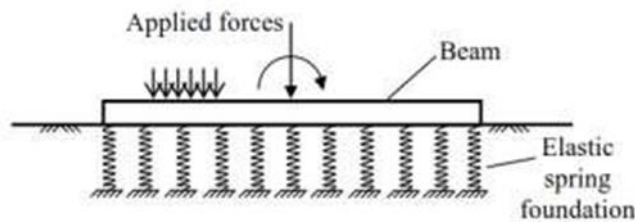


Figure 2- 8 Beam on elastic foundation

The Beam-On-Winkler foundation approach can also be called the subgrade-reaction approach because the foundation spring constant can be related to the modulus of subgrade reaction of a soil mass (Terzaghi, 1955). Terzaghi suggested values of the subgrade modulus that can be used in the standard beam equation, which is used to compute bending moment and deflection. Vesic (1961) presented an elastic solution of infinite beams on elastic isotropic sub-grades acted upon by concentrated loads and obtaining the analytical solutions (contact pressure, shear force,

bending moment, and deflection). He suggested the Winkler model is given an accurate result for long beams by comparing his solution with the Winkler method solutions. Therefore, the Winkler model gives an accurate result for the sub-grade. Analysis to evaluate factors affecting the sub-grade reaction modulus  $K_h$  and suggesting a procedure to obtain constant (average) soil reaction as a function of the Soil Young's Modulus which can be used for the analysis of the Beam Winkler Foundation.

Novak (1974) used generalized Winkler model to simulate the dynamic soil-pile interaction system. The analysis is done based on linear elasticity of the soil-pile system. The analytical approach is to establish the dimensionless parameters of the problem and obtain closed-form formulas for pile stiffness and damping. In Novak analysis, all components of the motion in a vertical plane were considered, i.e. horizontal and vertical translations and rotations of the pile head.

This model is assumed that both piles and soil can treat as nonlinear manner during the exciting, since the seventies, Matlock et al. (1978) extended the concept of BNWF to seismic analysis, develop the analysis of the dynamics program SPASM8, and explaining the use of p-y methods for the lateral stiffness of soil-pile model used for seismic analysis. Wang et al. (1998), Polam et al., 1998 and Hutchinson et al., 2004 were used p-y element models for dynamic analysis. According to p-y models, cyclic soil degradation should be using. For executing this analysis, the common linear modal analysis should be replaced by an iterative nonlinear time domain analysis, as expected non-linear response cannot be feasible by linear modal analysis (Brown et al., 2001).

### **2.10.2 p-y Curve**

Design engineers often prefer to use the Beam-On-Dynamic-Winkler-Foundation (BDWF) model for design purposes rather than the FE method or elastic continuum solutions. BDWF methods use traditional semi-empirical p-y curves such as those developed by Matlock (1970) and Reese et al. (1974). These curves represent the nonlinear soil behavior by a series of nonlinear springs, where the  $p$  refers to soil pressure per unit length of pile and the  $y$  refers to deflection. The loading in the pile is traditionally applied as a factored static load at the pile-top. This review focuses on p-y curves developed within this approach that is, obtained from static tests. It is important to note, however, that pseudo-static loading may be correct for low

frequency vibration design, but response may change significantly when seismic loading generates the introduction of soil nonlinearity, damping, and pile-soil interaction. Other authors (Naggar and Novak 1996, Brown et al. 2001) have developed p-y methods that can deal with dynamic loading.

Most of the existing standard p-y curves were developed based on full-scale lateral load tests on a relatively small range of pile diameters. However, Juirnarongrit (2002) showed that in dense weakly cemented sand, the pile diameter effect on the p-y curves at displacement levels below the ultimate soil resistance is insignificant. Beyond this range, an increment in the pile diameter increases the ultimate soil resistance. Existing p-y curves predict the response of the laterally loaded piles well in weakly cemented sand but are inappropriate for large diameter piles. These existing p-y curves have been incorporated into commercial programs such as COM624P (Wang and Reese 1993), LPILE (Reese et al. 2000), and FLPIER (University of Florida 1996). Deflection and moment along the pile can be found for a given load by using these commercial programs. The literature review presented herein focuses on the existing p-y curves for laterally loaded piles and methods to find p-y curves from numerical analysis.

### **2.10.3 Continuum Model**

Continuum approach, analysis of laterally loaded piles are done by treating the surrounding soil of pile as a three-dimensional continuum. Continuum approach is attractive because the interaction of pile and surrounding soil is conceptually more attractive than the beam-on-foundation approach. After all, the interaction of the pile and the surrounding soil is in reality three dimensional. The main advantage of continuum models is modeling the effect of radiation damping; the disadvantage of the model is only practicable for visco-elastic material.

This method is extremely useful to obtain a better understanding on the soil-pile interaction phenomenon and to obtain analytical expressions of parameters such as the sub-grade reaction modulus (Vesić, 1961), that can be used in the Winkler models.

Tajimi (1966) describes a dynamic soil-pile interaction solution based on elastic continuum theory. He used a linear Kelvin-Voigt visco-elastic stratum to model the soil and ignored the vertical components of the response.

In 1974, Novak developed an approximate continuum model to explain soil-pile interaction. The

soil is assumed as a group of independent thin infinite horizontal layers that extended to infinity. As each plane is considered independent, this model may be viewed as a generalized Winkler model.

Nogami and Novak (1980) investigated the coefficients of dynamic soil reaction to pile motion treating the soil as a three-dimensional continuum, to compare with Winkler model (where the soil is modeled as discrete springs and dashpots).

One of the first applications of finite element analysis to piles was done by Yeigan and Wright (1973) who introduced two-dimensional nonlinear soil models to analyses elastic piles. They have used the model to develop the lateral soil resistance –displacement relationships (p-y curves) for pile foundations.

The advantage of the finite element approach is used in the analysis of the soil-pile interaction model of pile and pile groups with a superstructure response even if in dynamic loading conditions. The finite element is model the soil profile as 3-D and analyses the effect. Soil is treated as a continuum mass in the finite element method. Randolph (1981) presented the results of his parametric studies on the response of laterally loaded piles embedded in an elastic soil continuum. The finite element modeling result is fitted with algebraic equation solutions. Wu & Finn (1997) used a quasi-3D finite element program for the analysis of dynamic soil–pile–structure interaction. An eight-node brick element is used to represent the soil continuum, and a two-node beam element is used to simulate the piles.

Currently, the most useful continuum based method of analysis available method. Several investigators are done different forms of the finite element method. Desai and Appel (1976) presented a three- dimensional finite element solution with interface elements for the laterally loaded pile problem. Kooijman and Vermeer (1988) used a quasi-dimensional analysis for the analysis of pile-soil contact on elastoplastic soil behavior. Bhowmik and Long (1991) developed two-dimensional and three- dimensional finite element models that used a bounding surface plasticity soil model and provided for soil-pile gapping. Brown and Shie (1991) used a three-dimensional finite element model to analyze the group effects on the modification of p-y curves. Bransby (1999) used two-dimensional finite element analysis to develop a p-y curve at different depths of infinitely long pile embedded in undrained soil, and the soil behavior linear elastic soil and power-law soil.

Bentley & El Naggar (2000) implemented a finite element model by modeling the soil as a homogeneous elastic medium and to evaluate the effect of soil they were using the Drucker-Prager failure criteria. They are applying the dynamic load in the horizontal direction at the bottom of the model, and discontinuity conditions at the pile-soil interface by introducing a contact element that enables to slippage gapping

Bentley & El Naggar (2000) studied the effects of kinematic interaction on the input motion at the foundation level. The 3-D model used in their study is shown in Figure 2.7. In this study, they included pile-soil separation, slippage, soil plasticity, and 3-D wave propagation. By considering the symmetry one half of the actual model was developed in order to reduce the computing time. Kelvin elements were used to simulate the infinite soil medium. Soil was modelled as linear and elastoplastic material using the Drucker-Prager failure criterion. Linear elastic cylindrical piles were considered for this study. Two different types of soil-pile interfaces were considered either as perfectly bonded soil-pile interface and frictional interface. The Coulomb frictional model was used to incorporate the frictional interface behavior. Two recorded earthquake motions were used at the base of the model to simulate the seismic motion in the model. The authors have concluded that the elastic kinematic interaction for a single pile slightly amplifies the free field transfer function, i.e. the ratio of soil to bedrock motion.

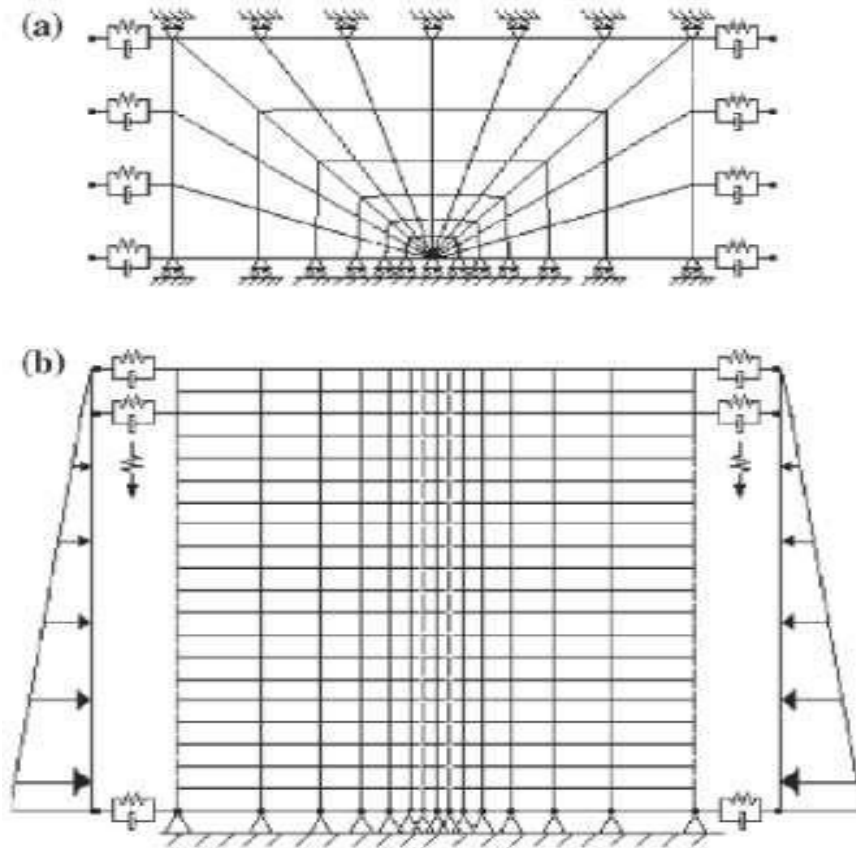


Figure 2- 9 3-D FEM model used by Bentley and Naggar [2000] a) Plan view b) Front cross sectional view

Maheshwari et al. (2004) used a 3D FE model to obtain the pile response under seismic excitation and a load applied to the pile cap and column base, considering the nonlinearity effects of the soil material and pile-soil interaction in the dynamic behavior of a single pile and pile groups. Figure 2.8 shows one of the FE mesh.

Boundary Element Method (BEM) has been used in the laterally loaded piles in evaluation. Ben Jamma and Shiojiri (2000) analyzed the dynamic behavior of a single pile embedded in an infinite half-space and the pile-soil system by the mixing of the finite element method and a hybrid thin layer element. Basile (2003) identify the advantage of the boundary element method for soil-pile interaction modeling and evaluation.

### 2.11 Critical pile length

Piles may be classified as long or short in accordance with effective pile length  $\langle l_c \rangle$ . The embedded length of pile is denoted by  $\langle L \rangle$ . A short pile behaves as a rigid body and rotates as a

unit under lateral loads. In the case of a long pile, the length beyond a particular depth loses its significance under lateral loads. The pile behavior is dependent on the effective pile length  $l_c$  of the pile.

Kuhlemeyer (1979) defined the critical pile length for free head piles, as the length corresponding to the point where a fixed tip pile and a pinned tip pile have the same pile head swaying stiffness. This length is a function of the pile-soil relative stiffness, and for static conditions, it is equal to (Kuhlemeyer 1979):

$$\frac{lc}{d} = 1.7 \left( \frac{Ep}{Es} \right)^{0.25} \dots\dots\dots 2.30$$

Similarly, Randolph (1981) and Gazetas (1991b), as cited by Syngros (2004), defined the active length as the depth below which pile deflections are less than one-thousandth of the top deflections and came up with different expressions. The formulas are given in Equation (2.31) and Equation (2.32) for Randolph (1981) and Gazetas (1991b), respectively (for a Poisson’s ratio of 0.4)

$$\frac{lc}{d} = 1.25 \left( \frac{Ep}{Es} \right)^{2/7} \dots\dots\dots 2.31$$

$$\frac{lc}{d} = 2 \left( \frac{Ep}{Es} \right)^{0.25} \dots\dots\dots 2.32$$

For piles with  $L \leq l_c$ , referred to as “short piles”, the pile head deformation varies with change in length. This implies the pile-head stiffness also varies with change in length. But for piles with  $L > l_c$ , which is referred as “long piles”, the pile head stiffness remains constant because there will not be any change in pile head deformation due to length variation.

Table 2- 1 effective pile slenderness ration for fixed-head piles

Model	Kuhlemeyer(1979)	Syngros(2004)	Gazetas(1991)	Guo(2001)
$\frac{lc}{d}$	$1.7 \left( \frac{Ep}{Es} \right)^{0.25}$	$1.6 \left( \frac{Ep}{Es} \right)^{0.28}$	$2 \left( \frac{Ep}{Es} \right)^{0.25}$	$1.057 \left( \frac{Ep}{Es} \right)^{0.25}$

Table 2- 2 effective pile length slenderness ratio for free-head piles

Model	Guo(2001)	Syngros(2004)	Mylonakis G.(2001)
$\frac{lc}{d}$	$1.5 \left( \frac{Ep}{Gs} \right)^{0.25}$	$2.4 \left( \frac{Ep}{Es} \right)^{0.25}$	$1.5 \left( \frac{Ep}{Es} \right)^{0.25}$

## **2.12 Dynamic analysis of batter pile**

Piles are classified as vertical/plumb/ and batter depending on the alignment of a pile with the vertical axis. Batter piles are inclined with some angle from the vertical axis and they further more classified as positive and negative batter piles depending on the loading direction and pile inclination. Piles are called "Pile battered reverse", if the lateral load acts opposite to the direction of pile inclination (negative batter angle), and "Pile battered forward", if the lateral load acts in the direction of the pile inclination (positive batter angle) (Zhang et al 2002).

Batter piles have been used for a long time to resist large lateral loads from winds, water waves, soil pressures, and impacts. Their distinct advantage over vertical piles is that they transmit the applied lateral loads partly in axial compression, rather than only through shear and bending. Thus, batter piles offer larger stiffness and bearing capacity than same-diameter-and-depth vertical piles a superiority of particular importance when the near surface soils are soft and/or the lateral load is large.

Until 1990's, batter piles were used to carry lateral loads, especially when lateral loads were large, unsupported pile length and weak soils present at the ground surface. In 1990's following the poor performance of batter piles in series of earthquakes, some engineers began advising against the use of batter piles (Mahmoud G. et al 2014). However, once the reason for the poor performance of batter piles understood, engineers develop design strategies to address these problems. Using these strategies, batter piles have once again become an important weapon in the engineer's field for the designing foundations subjected to lateral loads.

The poor performance of batter piles during some of the earthquakes was due to the design analyses which assumed the head of the pile to be "pinned", i.e. free to rotate, and thus was not designed to sustain any moment loading. However, pile head was subjected to large shear and moment loads, resulting in failure. Thus, the performance of batter piles could be improved by strengthening the in the present study, the dynamic lateral behavior of batter piles subjected to machine vibrations has been studied. 3D dynamic finite element analyses have been performed using ABAQUS with excellent pre and post processing features. Lateral dynamic loading is applied in both x (along batter) and z (across batter) directions in the form of sweep load to study the influence of batter direction on the behavior of soil pile system considering a range of

working frequency and force levels. Twenty-four different cases were considered by changing the direction and force level.

### **2.13 Prior Works on Dynamic Laterally Loaded Piles**

Poulos & Davis (1980), (Prakash & Sharma, 1990) lay out three approaches to analyses single piles subjected to lateral dynamic loads. These are the equivalent cantilever approach, beam on elastic foundation approach and approximate analytical approach.

#### **2.13.1 Equivalent Cantilever Beam**

In the equivalent cantilever approach the natural frequency and amplitude of vibration can be determined by standard methods. However, no information can be determined on stress, moments and displacements along the length of the pile for dynamic loads. (Hayashi, 1973), (Prakash & Sharma, 1969) and (Prakash & Gupta, 1970) attempted to determine the natural frequency of the soil-pile system under the assumption massless equivalent cantilever with a concentrated mass at the top using the top using Rayleigh's method. The approach is arbitrary, (Prakash & Sharma, 1990).

#### **2.13.2 Beam on Elastic Foundation (Sub Grade Reaction)**

Beam on elastic (subgrade) approach considers time dependent loading and analyzes by a numerical, finite difference method, the moments, stresses and displacements along the length of the pile. As the extension of the static approach for linear elastic and nonlinear p-y method of analysis, the soil is modeled as a Winkler medium. For dynamic effects the inertia and damping characteristics are added to the finite difference equation. Inertial forces of the soil medium are assumed to be included in the elastic spring restraints. Inertial properties of the pile and soil damping are represented as additional forces, (Poulos & Davis, 1980). For the appropriate initial condition of displacement, velocity and acceleration of a particular problem, the finite difference equation can be solved for each time increment.

Tucker (1964) presented a numerical simulation of a sinusoidal lateral pile, loaded at the mud line model test by (Gaul, 1958). The numerical model constituted 10 elements with each load cycle represented in 20 time increments and frequency of load ranging between 1- 200Hzs. The peak moment curve for 1Hz agrees with the results of Gaul (1958)'s model results. The analysis

showed the bending moments increase significantly as frequency approached the natural frequency of the system.

The nonlinear solution based on subgrade reaction has been presented with non-dimensional solution for cyclic loading Matlock and Reese (1961). A number of models were developed to address the nonlinear soil behavior and the soil-structure conditions that develop.

EL Naggar & Novak (1996) presented a nonlinear analysis using the subgrade reactions model ( $p - y$  curves) which will account for discontinuity condition at the soil pile interface (slippage and gap formation during vibration) using two series connected spring-dashpot systems (inner field and field). Their interface model is capable to interact with the soil and pile independently on both sides. They adopted the previous solution by (Novak & Sheta, 1980) to determine the stiffness under their inner field and (Novak, Nogami, & Aboull-Ella, 1978) explicit solution for soil horizontal complex stiffness for cylinder embedded in a linear viscoelastic medium. Computed lateral dynamic response compares favorably with field measured data. Furthermore, stiffness and damping are affected by level of loading. Nonlinearity reduces pile stiffness and damping.

El Naggar & Bentely (2000) modified the model and solution developed by (EL Naggar & Novak, 1996) to utilize existing or developed  $p - y$  curves for cyclic or static loadings to represent the nonlinear behavior of soil adjacent to the piles. Their model uses unit load transfer to account for nonlinearity in time domain and incorporate both material and radiation damping. The developed dynamic  $p-y$  curve is able to represent dynamic soil reaction using a predefined static  $p - y$  curve.

### **2.13.3 Approximate Analytical Approach**

Novak (1974) derived lateral stiffness and damping constants for single piles in translational, rotational and coupled rotation and translational vibration with soil modulus constant with depth, (Prakash & Sharma, 1990). (Novak & El-Sharnouby, 1983) Extended these solutions to include parabolic variation of soil shear modulus. The stiffness and damping coefficients were given as a function of parameters which themselves depended on poisons ratio and slenderness  $L/d$  for various end conditions. The stiffness and damping constant for translation vibration given in equation 2.33 and 2.34.

$$k = \frac{E_p I_p}{d^3} f_1 \dots\dots\dots 2.33$$

$$c = \frac{E_p I_p}{d^2 v_s} f_2 \dots\dots\dots 2.34$$

where  $k$  Translational vibration Stiffness

$c$  Translation Vibration Damping

$E_p$  Young's Modulus of Pile

$I_p$  Moment of Inertia of Pile Cross section

$d$  Pile Diameter

$v_s$  Shear Wave velocity

$f_1, f_2$  Parameters for Stiffness and Damping respectively

It was shown that the dependence of stiffness and damping is insignificant and the most important parameters are the Young's Modulus, Moment of Inertia of the section and slenderness of the piles i.e. L/d.

Ghazzaly, Hwong, & O'Neal (1976) gave the equation of motion of a pile under lateral dynamic load as in equation 2.31, where z is the axis along pile length and y is lateral deflection.

$$\frac{\partial^2}{\partial z^2} \left( EI \frac{\partial^2 y}{\partial z^2} \right) + m \frac{\partial^2 y}{\partial t^2} + c \frac{\partial y}{\partial t} + ky = 0 \dots\dots\dots 2.35$$

where  $EI$  Flexural rigidity of pile

$m$  Mass of the pile element per unit length

$c$  Viscous damping coefficient

$k$  Spring constant of the soil

$y, z$  and  $t$  Longitudinal and transverse coordinates and time respectively

The authors estimated the values of  $c$  and  $k$  as follows;

$$\bar{c} = \frac{3.4r^2}{1-\nu} \sqrt{G\rho} \quad \& \quad \bar{k}_s = k_s \dots\dots\dots 2.36$$

- where
- $k_s$       Static Soil Modulus
  - $R$         Pile Diameter/Width of Pile
  - $G$         Shear Modulus of Soil
  - $\rho$         Mass Density of Soil
  - $\nu$         Poisson's ratio
- $$r^2 = \frac{hR}{\pi} \quad h \text{ length of pile increment}$$

Hence the equation of motion becomes;

$$\frac{\partial^2}{\partial z^2} \left( EI \frac{\partial^2 y}{\partial z^2} \right) + m \frac{\partial^2 y}{\partial t^2} + \frac{3.4r^2}{h(1-\nu)} \frac{\partial y}{\partial t} + k_s y R = 0 \dots\dots\dots 2.37$$

Yang and Jeremić (2002) conducted numerical analyses using finite element method on single laterally loaded pile in elastic-plastic soil model. Pile behavior was tested in uniform sand, clay and layered soil deposits. Based on the results obtained from numerical analysis authors developed p-y curves and compared them with p-y curves obtained by McVay et al. (1990) and Reese et al. (1974). Pile was modeled to be made of aluminum, squared shape with 0.429 m in width and about 12 m long with 11.3 m embedded in the soil. The authors concluded that the use of three dimensional finite element model, with the use of very simple constitutive soil model can give good approximation of laterally loaded pile behavior.

The authors solved the equation of motion using finite difference method and compared the results with test data by (Gaul, 1958) and others. They found the solutions acceptable for low amplitude vibrations. The difference between computed and observed deflection at the pile head where less than 17% and 10% for cohesion-less and cohesive soils respectively.

In the beginning, Czerniak (1957) defined short rigid pile as the one where the embedded length does not exceed ten times its lateral dimension. Matlock and Reese (1960), described short rigid and long flexible pile through stiffness factors (both for cohesive and cohesion-less soil depending upon the bending stiffness of the pile and modulus of subgrade reaction of the

surrounding soil. Later on, Carter and Kulhawy (1992) proposed limiting criteria for short pile based on the  $L/d$  ratio of the pile, considering the effective Young's modulus of the pile and equivalent shear modulus of the surrounding soil.

Zhang et al. (1999) performed a centrifuge lateral load tests on single batter piles in sand with different relative density sands. Five pile inclinations were modelled:  $7^\circ$  and  $14^\circ$  at a negative pile batter, vertical, and  $7^\circ$  and  $14^\circ$  at positive pile batter. The effects of pile batter and soil density on lateral resistance were studied. Pile batter had significant effects in dense sands, but minor effects in loose sands. The lateral pile resistance was influenced by pile batter and soil density. Based on the centrifuge test results, the resistance increases over vertical piles were 4, 14, 24, and up to 50% in very loose, loose, medium-dense, and dense sands, respectively, at positive  $14^\circ$  batter. In contrast, the resistance decreases over vertical piles were 4, 5, 15, and up to 35%, respectively, at negative  $14^\circ$  batter. The effects of pile batter were significant in medium- dense and dense sands, but minor in loose and very loose sands,

Hazzar et al. (2015) presented numerical models to investigate the effect of the batter angle on the behavior of laterally loaded batter piles in sand soil. The numerical models were conducted using the computer program FLAC 3D and the model were verified using centrifuge model testing data. The verified numerical model was used to perform a parametric study considering different variations of batter angle and soil density to evaluate the lateral capacity of steel batter piles subjected to lateral loads. Based on the results of this parametric study, the lateral capacities of the batter piles in sandy soils under lateral loads are influenced by the both pile batter angle and sand density.

Murthy (1965) developed a relationship between vertical and batter piles using an instrumented model batter pile installed in the sand, the batter angles varied within 0 to  $\pm 45^\circ$  range. In these relationships, Murthy (1965) introduced important factors as pile material modulus of elasticity, second moment of area, pile length, pile diameter, free head of the pile, soil internal friction angle, soil density, and batter angle. The results reported that lateral resistance of a negative batter pile is higher than a positive batter pile.

Ranjan et al. (1980) carried out Laboratory tests on single and group batter piles in sand. The results revealed that, the negative batter piles offer more resistance than positive batter piles,

and a group of one vertical pile and one batter pile (positive or negative) has more resistance to lateral deflection compared to a similar pile group consisting two vertical piles.

Zhang et al. (1999) performed a centrifuge lateral load tests on single batter piles in sand with different relative density sands Five pile inclinations were modelled:  $7^{\circ}$  and  $14^{\circ}$  at a negative pile batter, vertical, and  $7^{\circ}$  and  $14^{\circ}$  at positive pile batter. The effects of pile batter and soil density on lateral resistance were studied. Pile batter had significant effects in dense sands, but minor effects in loose sands. The lateral pile resistance was influenced by pile batter and soil density. Based on the centrifuge test results, the resistance increases over vertical piles were 4, 14, 24, and up to 50% in very loose, loose, medium-dense, and dense sands, respectively, at positive  $14^{\circ}$  batter. In contrast, the resistance decreases over vertical piles were 4, 5, 15, and up to 35%, respectively, at negative  $14^{\circ}$  batter. The effects of pile batter were significant in medium- dense and dense sands, but minor in loose and very loose sands,

Lv et al. (2011) carried out experimental work to study the lateral bearing capacity of negative batter pile under different batter and different constraints at pile head. These piles were embedded in sand. The pile batter angle to vertical,  $\beta$ , is  $0^{\circ}$ ,  $10^{\circ}$  or  $20^{\circ}$ . The analysis indicates that (1) the lateral capacity of the negative batter pile decreases as the batter angle decreases when the pile head is only horizontal movement (translational), (2) the lateral capacity of the negative batter translational pile is more than that of the positive batter.

## **2.14 Plaxis 3-D Model validation**

The software, which is used for developing the model, must be validated before its result is accepted and applied to simulate the real world problems. Validation is the only way to justify the predictions of a numerical model to the true physics concerned (Sinha 2013). This section used to assess the ability of Plaxis 3D the finite element approach in analyzing laterally loaded single pile under earthquake loading and to verify certain details of the finite element such as pile displacement damping coefficient. Verification example was worked out to compare the result obtained by finite element analysis to those obtained from laboratory investigation

### **2.14.1 Hetlant Wind Monopile**

Dynamic testing of a steel pipe installed in dry sand has been carried out in the Foundations Laboratory at NTNU. Preparations and test-setup was performed during the spring of 2014 as a

part of a project thesis (Hetland (2014)). The aim was to determine important characteristics of the model pile, as well as important material properties relevant to the dynamic behavior of the model pile. The laboratory work conducted by Hetland is used to verify the capability of the numerical model to simulate the dynamic behavior of pile foundations. The work of Hetland was concerned with the dynamic behavior of offshore mono pile wind turbines.

The laboratory model implemented a simulation of the actual case study with scale 1:20 as illustrated in figure 2-10.

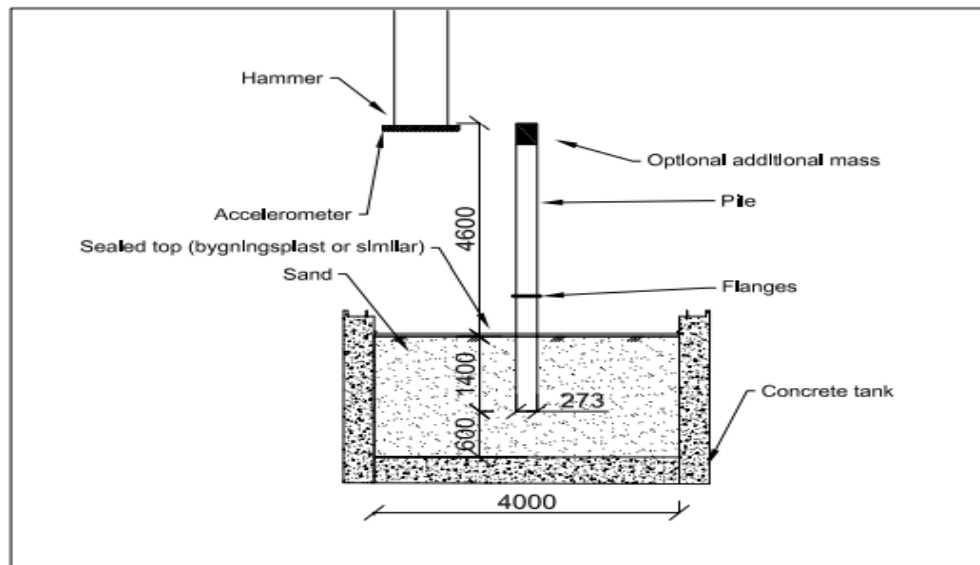


Figure 2- 10 Laboratory test setup

The Foundations Laboratory consists of a 4x4 m wide and 2m deep contain sand bin from glaziflviaal deposit in hokksund, Norway figure 2-10 show the assigned sand property according to laboratory with concrete walls. Meanwhile, the linear Elastic Model used in PLAXIS is only capable of considering a linear increase of stiffness with depth. Therefore, soil profile in PLAXIS is divided into 0.5 m thick sub-layers as shown in Figure 2-10.

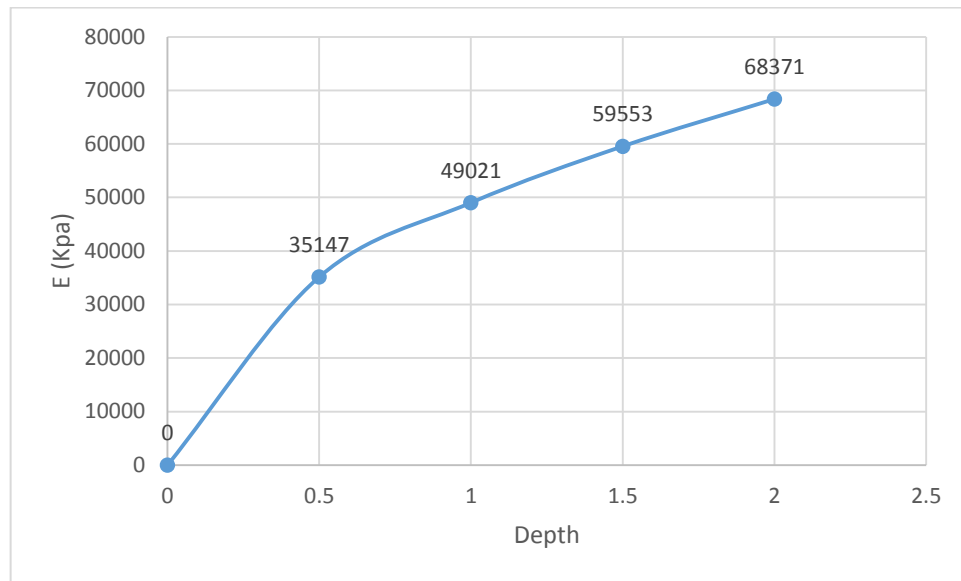


Figure 2- 11 linearly increasing stiffness profile for soil model

To model the wind turbine mono pile, a steel pile is used with an outer diameter of 0.273 m and a wall thickness of 4 mm. The steel pile is installed in the middle of the sand tank. It has an embedded length of 1.4 m and a free length of 4.6 m. The pipe is attached to a flange connection positioned 0.6 m above the soil and another flange is located at the pipe top (Figure 2-11). The maximum meshing size used in the finite element analysis is determined using the rule established by Kramer. This rule relates the maximum meshing size to the shortest wavelength considered in the analysis Numerical modeling.

Validates the simulation of the piles using numerical finite element program (plaxis3D software). The linear elastic material model is a relatively simple model, requiring few input parameters. In order to better estimate the stiffness profile of the sand, four different layers were defined show in figure 3-4 0 to 0.5, 0.5 to 1, 1 to 1.5, 1.5 to 2m by soil stiffness is linearly increasing stiffness

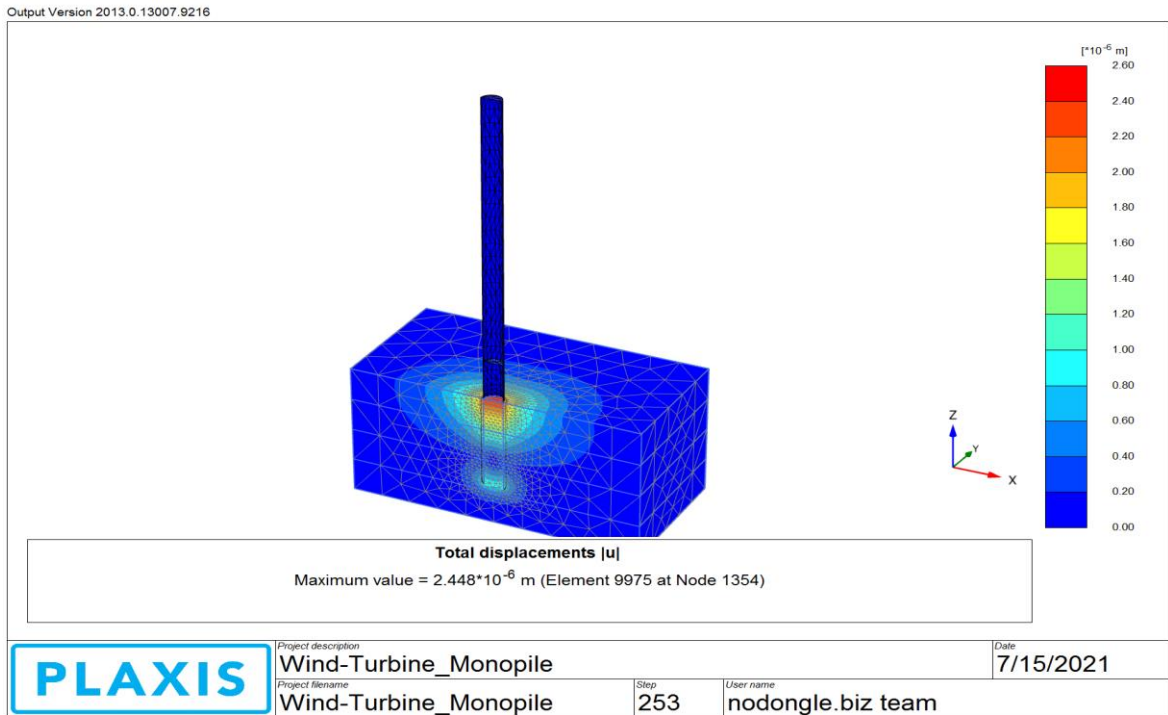


Figure 2- 12 3D modeling of wind-turbine Monopile

The geometry of the FE-model can be seen in figure3-4. The boundaries of the Finite Element Model were defined by the points  $x = [-2, 2]$  and  $y = [0, 2]$ . The other model properties used was the default values from PLAXIS. To create the soil volume, a single borehole was defined with boundaries  $z = [0, -2]$ . The conditions were considered to be uniform throughout the soil with regards to soil properties with the exception of soil stiffness. The pile was created using the polycurve function, making a half circle with a radius of 0.1365 m, and extruding the half circle from  $Z = [4.6, -1.4]$ . It was then defined as a plate and material properties.

The dynamic response of the pile top was found using the finite element model. The time-series of the pile top displacement in x-direction for 0 overburden pressure can be seen in figure 2-13. The laboratory results were successfully back-calculated. Especially the Eigen frequency was well estimated using the numerical model described in this thesis. Assuming small-strain stiffness was found to represent the stiffness profile of the Hokksund sand in a good manner.

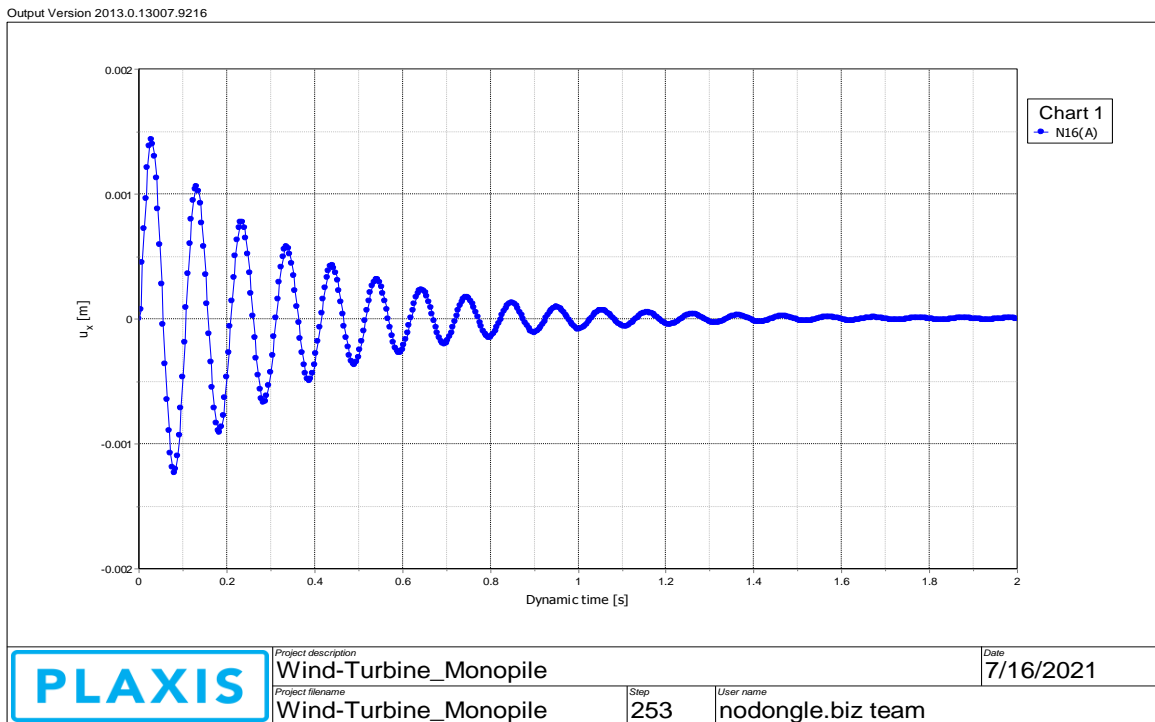


Figure 2- 13 Time-series of pile top displacement for 0 kPa overburden pressure using LE.

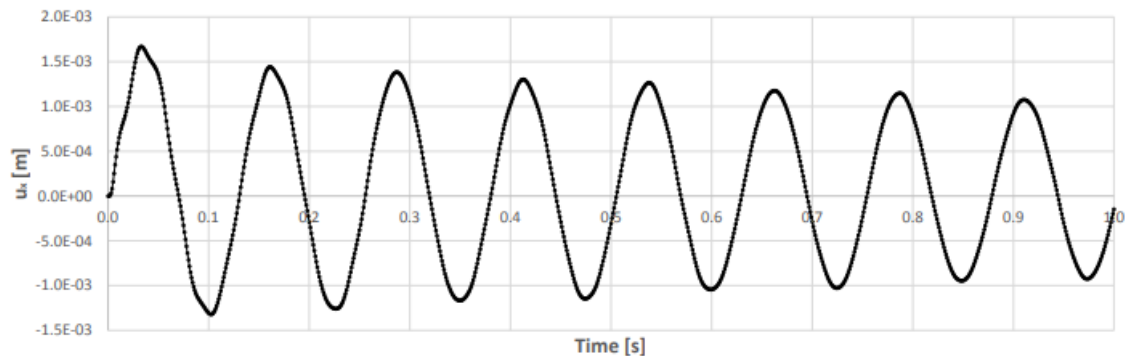


Figure 2- 14 Time-series of pile top displacement for 0 kPa overburden pressure using Hss.

By taking the same data from literature the analysis of hetland monopole by using plaxis 3D were done and the result demonstrated that the analysis result of pile top displacement is  $1.53 \times 10^{-3}$  for linear elastic model which show a good agreement with the HSS model analysis as show figure 2-14 after review the result obtained from the developed numerical model agreed with advanced numerical model (HSS) therefore, PLAXIS 3D results are reliable adopted for my analysis.

### 3. MATERIAL AND METHODS

#### 3.1 General Approach

In this research project, the finite element tools that will be used in the study, i.e. PLAXIS 3D is validated by using an experimental data conducted on offshore wind turbine by (Hetland & Ekisund, 2015). A model for the study is proposed using steel pipe pile (vertical and batter) embedded in sand soil. A range of pile lengths, batter angles, load amplitude and frequencies are modelled to study the impact of various attributes in the pile's dynamic lateral load capacity. Finally, the results the analysis are summarized and compared with previous works and code provision, and conclusions are drawn based on relevant findings.

#### 3.2 Finite Element Method

The finite element method is used to solve the time dependent movement of volume under the influence of the input dynamic force or prescribed displacement. The continuum is divided into a number of elements, which consist of a number of nodes. Each node has a number of degrees of freedom which correspond to displacement, velocity or other attribute under consideration. Equilibrium equations, constitutive relationships and compatibility conditions are used to solve for the unknowns.

The general equation of motion for dynamic analysis in PLAXIS 3D is given as;

$$M\ddot{u} + C\dot{u} + Ku = F \dots\dots\dots 3.1$$

Where  $M$  is the mass matrix,  $C$  is the damping matrix,  $K$  is the stiffness matrix,  $F$  the dynamic input force,  $\ddot{u}, \dot{u}, u$  are the acceleration, velocity and displacement vectors. The damping coefficient is defined as two part, i.e. mass and stiffness Rayleigh damping.

$$C = \alpha M + \beta K \dots\dots\dots 3.2$$

##### 3.2.1 Element Formulation

PLAXIS 3D uses a 10 node tetrahedral basic element for the soil volume. Special elements are employed for structures such as beams, plates geo-grids etc. PLAXIS 3D also deploys a 16 node interface element to model soil-structure interaction. The elements are generated through automated mesh generation process.

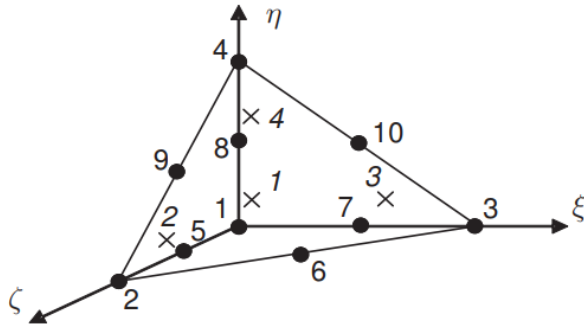


Figure 3-1 Basic 10 node tetrahedral element in Plaxis 3D

The mesh generator requires a global mesh parameter that is required to define a target (average) element size  $l_e$ .

$$l_e \frac{r_e}{20} \sqrt{(x_{max} - x_{min})^2 + (y_{max} - y_{min})^2 + (z_{max} - z_{min})^2} \dots \dots \dots 3.3$$

Where  $r_e$  a coefficient for relative element size factor for very course to very fine mesh sizes.

It is considered good practice to refine the finite element mesh in areas where large deformation gradients are expected. This allows us to have more accurate results with minimum calculation time. Based on this principle, the mesh around the pile was refined, as shown in Figure 3-2.

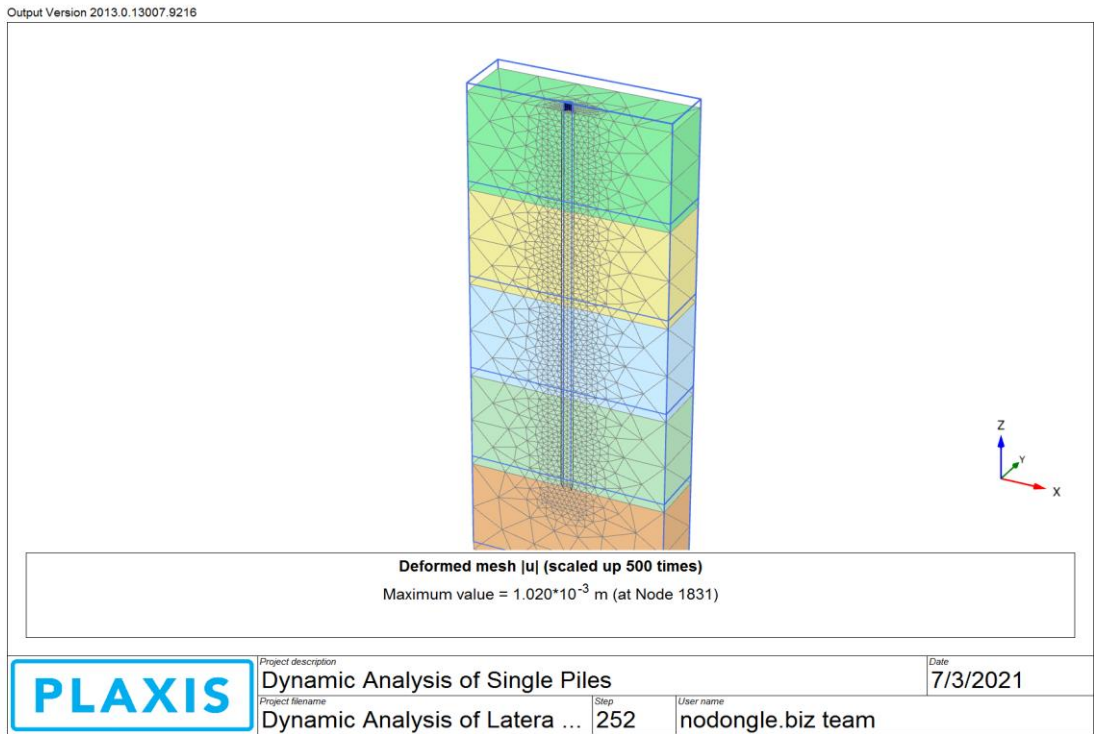


Figure 3-2 Adopted mesh for analysis

### 3.2.2 Time Integration

In dynamic analysis, the most important factor for the accuracy and stability of the numerical procedure is the time integration formulation. Newmark's implicit time integration scheme is adopted. With this method the displacement and velocity at time  $t + \Delta t$  are respectively as;

$$u^{t+\Delta t} = u^t + \dot{u}^t \Delta t + \left( \left( \frac{1}{2} - \alpha \right) \ddot{u}^t + \alpha \ddot{u}^{t+\Delta t} \right) \Delta t^2 \dots \dots \dots 3.4$$

$$\dot{u}^{t+\Delta t} = \dot{u}^t + \left( (1 - \beta) \ddot{u}^t + \beta \ddot{u}^{t+\Delta t} \right) \Delta t \dots \dots \dots 3.5$$

Where  $\Delta t$  is the integration time step. The coefficients  $\alpha$  and  $\beta$  (not the same as Rayleigh Coefficients) determine the accuracy of the numerical time integration. The general range of values for a stable solution is given as;

$$\beta \geq 0.5 \text{ and } \alpha \geq \frac{1}{4} \left( \frac{1}{2} + \beta \right)^2 \dots \dots \dots 3.6$$

The recommended values are  $\alpha = 0.25$  and  $\beta = 0.5$

### 3.2.2.1 Critical Time Step

There is a constraint to the time step that can be used in dynamic finite element analysis. If the time step is too large, the results will show deviations and the calculations be unreliable, (PLAXIS 3D, 2013b). The critical time step depends on the maximum frequency and the coarseness of the finite element mesh. Generally, the following expression can be used for a single element.

$$\Delta t_{\text{critical}} = \frac{l_e}{\alpha \sqrt{\frac{E(1-\nu)}{\rho(1+\nu)(1-2\nu)} \sqrt{1 + \frac{B^4}{4S^2} - \frac{B^2}{2S^2} \left[ 1 + \frac{1-2\nu 2S}{4 B^2} \right]}}} \dots\dots\dots 3.7$$

Where

B and S Largest dimension and surface area of the finite element

A Depends on element type(number of nodes)

P Material Mass Density

E,ν Young's Modulus and Poisson's Ratio

l<sub>e</sub> Average Length of the element

This critical time shall be selected so that a wave during single time step duration does not travel more than the minimum length of the element.

The time step used in PLAXIS 3D is equal to

$$\delta t = \frac{\Delta t}{m * n} \dots\dots\dots 3.8$$

Where Δt the relevant time interval identified for the relevant phase, m is the number of Additional steps and n is the number of dynamic sub-steps. It is important to define a proper number of such steps such that the dynamic signal used in loading is properly covered. In general it is recommended to choose Δt, m and n in such a way that the dynamic sun step time interval equal to the time interval used in the input signal.

### 3.3 Constitutive Models

A number of constitutive models are available in PLAXIS 3D. These range from simple models of Linear Elastic and Mohr-Coulomb (elasto-plastic) to advanced models. Although the use of

advanced models in analysis is expected to represent the reality of the soil better, these advanced models require large number of parameters whose accurate determination is challenging for natural materials. Hence, it is not always preferable to adopt advanced models, despite the promise of accurate results.

### **3.3.1 Linear Elastic Model**

The linear elastic model (LE) which requires Young's modulus ( $E$ ) and Poisson's ratio ( $\nu$ ), is applicable under the assumption of homogenous, isotropic material under loads causing small strains. To account for variation of Young's modulus with depth the soil layer may be divided into layers of uniform lateral properties. It can also be used to model stiff volumes in soils. The damping characteristics for dynamic loading is modeled using Rayleigh's damping coefficients  $\alpha$  and  $\beta$  for both the soil mass and structural elements. The highly nonlinear nature of soils under dynamic loads limits the application of the model.

An advantage of the linear elastic material model compared to the Mohr- Coulomb linear elastic perfectly plastic is that it enables better control over the model damping, seeing as Mohr Coulomb will introduce damping for plastic strains (Brinkgreve et al. (2013c)).

### **3.3.2 Mohr Coulomb Model**

The linear elastic perfectly plastic model (Mohr-Coulomb, MC) model requires the following parameters to define the soil;  $E$  and  $\nu$  for elasticity,  $c$  and  $\phi$  for soil plasticity and  $\psi$  angle of dilatancy. The model allows for a constant or a linearly varying stiffness. However, the model does not account for stress or strain dependency of stiffness or anisotropy.

### **3.3.3 Hardening soil model (HS)**

Hardening soil model (HS) is an advanced model to describe soil behavior. Strength behavior is represented by  $c$ ,  $\phi$  and  $\psi$ . Soil stiffness is represented much more accurately using three different stiffness input values: the tri-axial loading stiffness,  $E_{50}$ , the tri-axial unloading stiffness,  $E_{ur}$ , and the Oedometer loading stiffness,  $E_{Oed}$ . This model however, does not take into account softening of soil due to dilatancy and de-bonding effects. It models neither hysteretic and cyclic loading nor cyclic mobility. It also does not distinguishes between large stiffness at small strains and reduced strains at engineering load levels, (PLAXIS 3D, 2013).

### **3.3.4 Hardening soil model with small strains (HSsmall)**

Hardening soil model with small strains (HSsmall) is a modified HS model that accounts for the increase in stiffness of soils at small strains. This behavior is accounted for by using two additional parameters,  $G_0^{\text{ref}}$  a small strain shear modulus and  $\gamma_{0.7}$ , strain level at which the shear modulus has reduced 70% of  $G_0^{\text{ref}}$ . This model gives better estimates of displacement at design load levels. Under dynamic load modeling it introduces hysteretic material damping. In this project the HSsmall model shall be adopted.

## **3.4 Boundary Conditions**

### **3.4.1 Static Boundary Conditions**

The static boundary condition on the soil model are automatically applied by PLAXIS 3D as follows; (PLAXIS 3D, 2013b)

- Vertical model boundaries with their normal in the x direction are fixed in the x-direction ( $u_x = 0$ ) and free in y and z direction
- Vertical model boundaries with their normal in the y direction are fixed in y-direction ( $u_y = 0$ ) are free in z and x direction
- Vertical model boundaries with their normal in the x nor y direction are fixed in x- and y-direction ( $u_x = u_y = 0$ ) are free in z direction
- The model bottom boundary is fixed in all direction ( $u_x = u_y = u_z = 0$ ).
- The ‘ground surface’ is free in all direction

### **3.4.2 Dynamic Boundary Condition**

PLAXIS 3D allows for the dynamic boundaries to be either ‘viscous’ which absorb stress wave energy arriving at the boundary ‘none’ which will reflect the energy back into the soil. The appropriate boundary type shall be adopted for dynamic computation. An absorbent boundary is aimed to absorb the increasing stress in the boundaries caused by the dynamic loading; otherwise, it will be reflected inside the soil body. In PLAXIS, absorbent boundaries are generated by selecting the standard absorbent boundaries. In this model, the absorbent boundaries are generated at the left, right and the bottom boundary.

### 3.4.3 Rayleigh Damping Parameters and Damping Ratio

PLAXIS 3D uses Rayleigh damping coefficients to estimate the damping of the soil structure system, despite its limitations to accurately estimate hysteretic damping of the soil material. With Rayleigh damping only one damping ratio can be specified for the entire time series; the reduced damping ratio with reduced amplitude cannot be modeled, (Hetland & Ekisund, 2015).

The use of Rayleigh damping coefficients,  $\alpha$  and  $\beta$  results in a frequency dependent damping matrix. However, damping in soil is not frequency dependent and  $\alpha$  and  $\beta$  shall be selected in such a way that there is minimal variation over the range of frequencies of interest. Hudson, Idriss, & Beikae (1994) put forward which uses two frequencies to determine  $\alpha$  and  $\beta$ . The first frequency shall be fundamental frequency  $\omega_1$ . The second frequency is established as  $\omega_2 = n\omega_1$ , where n is next odd integer from the ratio of fundamental frequency and the predominant frequency of the input motion. The choice of two frequencies results in underdamping between  $\omega_1$  and  $\omega_2$  overdamping outside that range (Hudson, Idriss, & Beikae, 1994).

Kramer (1996) the fundamental frequency for a soil layer of depth H above a rigid half space is as;

$$\omega_1 = \frac{v_s}{4H} \dots\dots\dots 3.9$$

where  $v_s$  shear wave velocity

The damping ratio of the pile material is set  $\xi = 0.005$  based on experimental observation for steel pile piles, (Hetland & Ekisund, 2015). The damping ratio in the soil depends on the soil property and overburden pressure. Would be relatively time-consuming to perform. The Rayleigh coefficients indicate that the system damping is highly mass-proportional with an  $\alpha R$  with order.

## 3.5 Materials Modeled in PLAXIS

### 3.5.1 Steel Piles

Steel piles have been in wide use since 1890s. They have high strength and ductility which enables driving through hard soils and carry heavy loads. They are easy to splice hence ideal for depths greater than 18m. Up to 210m deep pile reported. Their major disadvantages are; relatively expensive to purchase, noisy to drive and susceptible corrosion. Steel piles are

available in H-piles or Pipe piles. They can be deployed as end bearing or friction piles. H-piles load capacity ranges between 400kN to 2000kN axial capacity with depth range 15-50m, ASTM A36. Circular pipe has diameters ranging between 200mm to 1220mm for plain section and 300mm to 900mm for filled piles. Their depth ranges between 10m to 50m. The load for circular steel pipe piles is 800kN to 2500kN for plain sections and 5000kN to 15,000kN for filled sections, ASTM A36.

A 400mm diameter steel pile with a plain section is adopted for this research. The length of the pile is varied from 4m to 24m. For batter pile simulation; the batter angle is varied between  $5^{\circ}$  to  $25^{\circ}$ .

Table 3-1 Pile parameters used for analysis

Parameter	symbol	Unit	Values
Steel pipe pile	-	-	-
Diameter	D	Mm	400
Thickness	T	Mm	4
Length	L	M	4-24
density	$\gamma$	kN/m <sup>3</sup>	78.5
Modulus of elasticity	E	MPa	2000000
Poissons ratio	$\nu$	NA	0.15
Pile head		NA	Free & fixed

The pile was created using the poly-curve function, making a half circle with a radius of 0.2m and extruding the half circle from Z=(4m-24m) it was then defined as plate and material properties were defined according to table 3.

### 3.5.2 Soil

The soil was defined by a single borehole, consisting of six different layers for the linear elastic model. The borehole 0 to -25 m depth and the ground water head was set to -25 m to ensure the ground water level was below the soil. The soil was modelled with linear elastic soil model. The soil properties used on the model is described on table 3.2.

Table 3-2 Soil parameter used for analysis

Parameters	symbol	unit	Value for sand
Model			Linear elastic
Drainage types	drained		
Saturated unit weight	$\gamma_{sat}$	KN/m <sup>3</sup>	20
Unsaturated unit weight	$\gamma_{unsat}$	KN/m <sup>3</sup>	20
Damping ratio	$\xi$	%	5

### 3.5.2.1 Soil Stiffness Profiles

The stiffness profile of sand relates to the effective stress level and follows a power rule as found in the appendix. In the linear elastic material model in PLAXIS 3D it is only possible to use linearly increasing stiffness with depth. This was solved by introducing six layers, and thus making the stiffness profiles piece-wise linear.

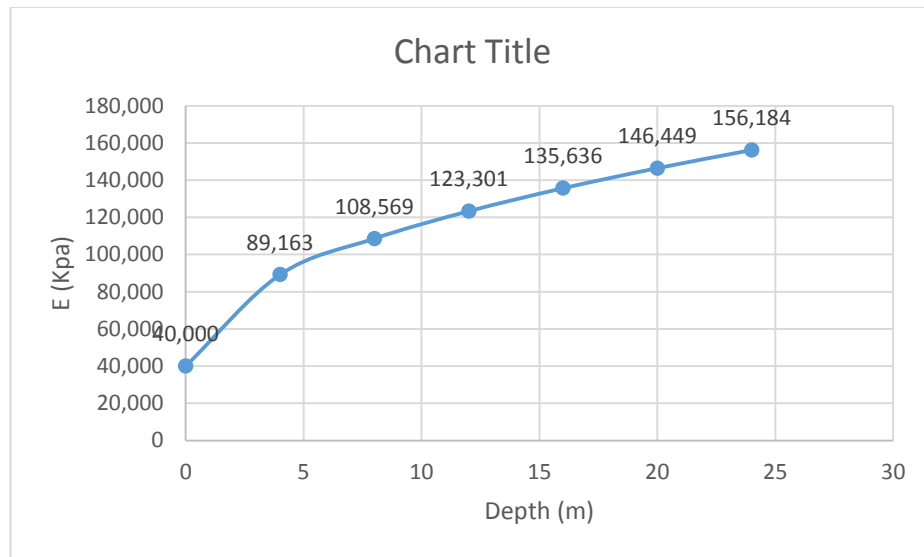


Figure 3-3 Stiffness profile used in the analysis

### 3.5.3 Geometry of Soil Model

Geometry of the soil model, i.e. the extents of the soil mass in all three orthogonal directions, shall be determined in such a way that the reflection of stress waves is minimize. Despite the use of appropriate boundary conditions in numerical models which absorb energy it is essential to constitute the boundaries far enough not to influence the structure. The soil in this analysis

has the extent as shown in Table 3.3. It is recommended to take advantage of geometrical and loading symmetries to reduce computation time. The other model properties used was the default values from PLAXIS.

Table 3-3 List of geometrical coordinates

Coordinates	Max	Min
X(m)	-5	5
Y(m)	0	3
Z(m)	-25	0

### 3.6 Input Motion

While designing of structures many types of loads are considered static and dynamic. One type of dynamic load on structures is the load that comes from external source, such as earthquakes. Since an earthquake record in our county only gives the magnitude, the data obtained cannot be used for soil-foundation structure interaction analysis.

Lateral dynamic loads on piles can be from machines like end turbines, environments like water wave and winds or earthquake. The nature of the loads can be transient, harmonic or periodic. Time history of earthquake loads can be adopted from artificial accelero-grams or real strong motion records. Artificial accelero-grams have an advantage over real time motion records as they allow the control of input motion attributes such as frequency content, amplitude and duration. However, real strong motion records have realistic low frequency content. In this research a real strong motion record of Hollister earthquake is adopted largely for its small duration to reduce computation time.

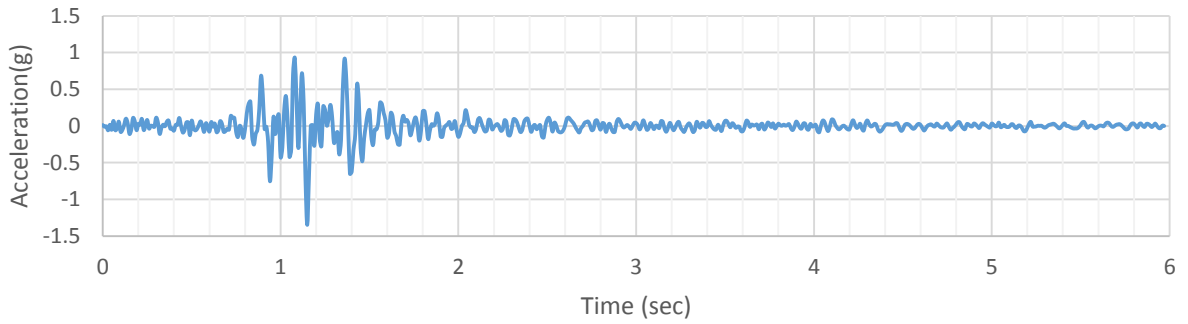


Figure 3-4 Input acceleration time history used as base excitation

Through the observation of the time history of the Hollister seismic wave acceleration shown in Figure 3-5, it is found that the greater acceleration is mainly concentrated in the first half of the time-history diagram and the dynamic load is applied to the bottom of the model, along the x-axis.

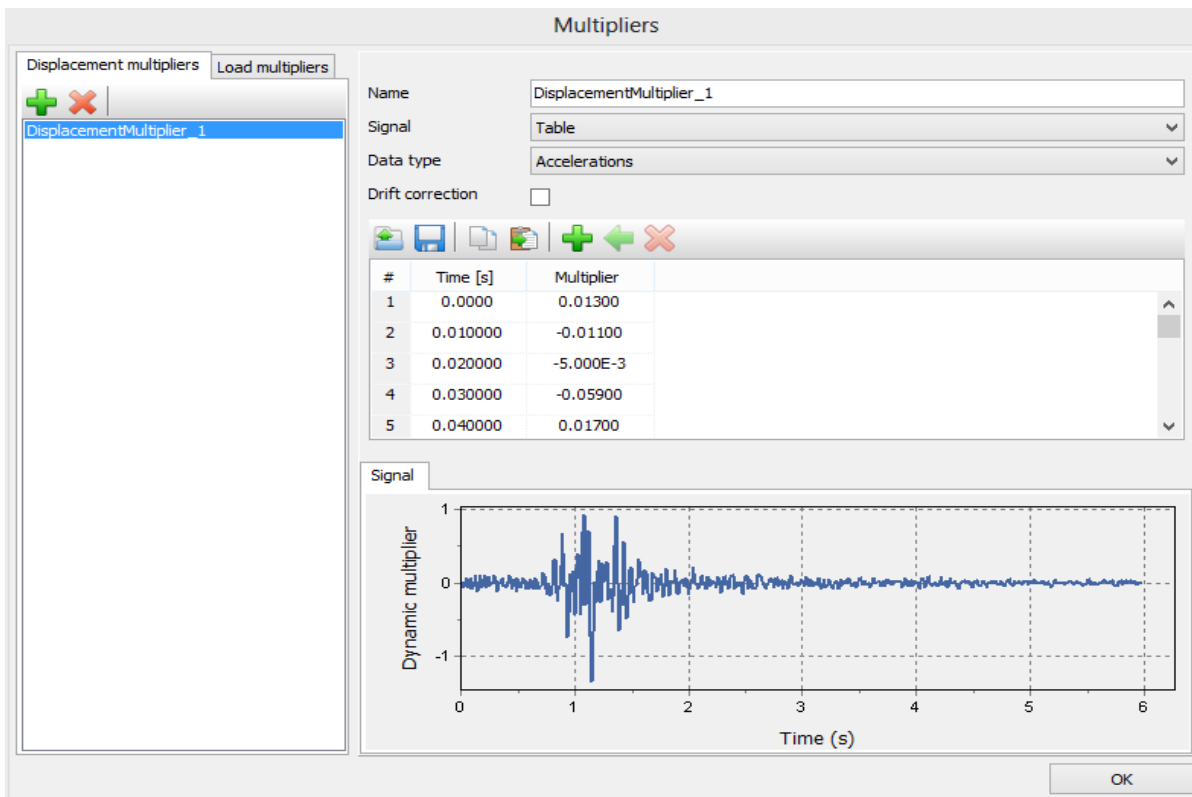


Figure 3-5 Earthquake acceleration- time records applied to the bottom of the model

### 3.7 Soil volume in PLAXIS 3D was modeled Mesh

By 10-node tetrahedral elements and the finite element mesh consists of a finite number of such elements. The characteristics of a finite element mesh are defined by its coarseness (fineness). Using a finer mesh will give more elements, more nodes and stress points and thus increase computational time. Therefore, significant understanding is needed to optimize the mesh such that it represents the problem in a sufficiently accurate manner without too much computational effort. There exists a parameter called target element dimension  $l_e$  defined

$$\text{by: } \frac{r_e}{20} \sqrt{(x_{max} - x_{min})^2 + (y_{max} - y_{min})^2 + (z_{max} - z_{min})^2} \dots\dots\dots 3.10$$

Based on a parameter called relative element size factor  $r_e$ ,  $r_e$  is defined by five different global levels. From the highest value of very coarse to the lowest value of very fine. The target element dimension  $l_e$  relates to the critical time step in dynamic calculations by equation (3.10). For description of the interpolation functions, its derivatives and the numerical integration of this element type, it is referred to Brinkgreve et al. (2013c). The finite element mesh was investigated based on the four global levels of relative element size. The resulting target element size was found in the general information tab in PLAXIS output mode and can be seen in table

Table 3-4 Relative element size and the resulting element dimension

Relative element size	Target element dimension(m)
Very course	3.176
coarse	2.382
medium	1.588
fine	1.111
Very fine	0.794

As shown on table 3-4 the target element dimension is show small change after medium element dimension it represent the problem in sufficient an accurate manner with soil layers of 5.0m - 24m thickness for the linear elastic soil model was needed in order to avoid problems with the flexibility of the elements. The mesh was refined in the area around the pile by defining a local fineness factor of 0.125. This allows for a more accurate determination of the deformation pattern of the pile

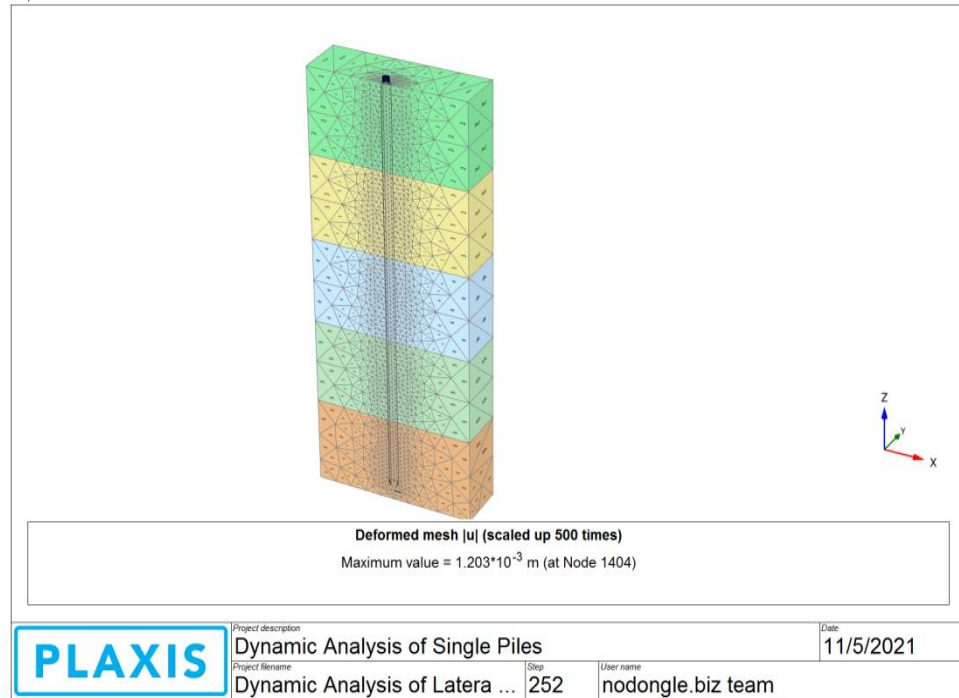


Figure 3-6 3D mesh generation

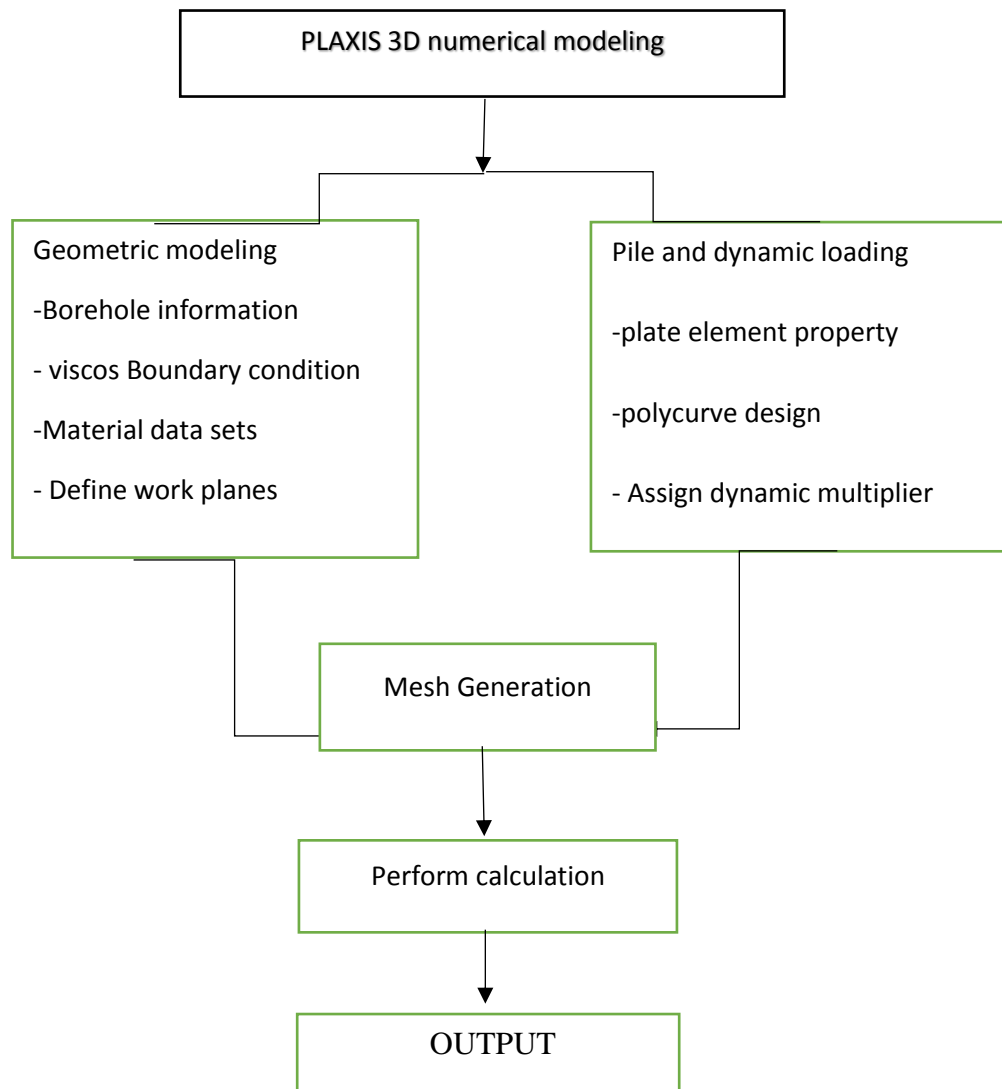


Figure 3-7 Plaxis 3d modeling and analysis steps

## 4. RESULT AND DISCUSSION

The lateral load behavior of a single pile due to dynamic loading is studied by using lateral load deflection curves. The curves are drawn for displacement for a given dynamic loads. In this chapter, a parametric study was conducted on a laterally loaded single vertical and batter pile under dynamic loading conditions using Plaxis 3D Foundation. One of the purposes for this study was to investigate the laterally loaded pile by varying; length of the piles, pile head fixity condition and batter pile angle under dynamic lateral loading. The analysis was performed on the model with the same characteristics except for pile length and batter angle.

The main objective of this study is to investigate the behavior of laterally loaded pile under dynamic lateral loading. As shown in chapter-3, a Plaxis 3D model has been developed to study the behavior of laterally loaded pile. In addition, to ensure the reliability of the results obtained by validated by using an experimental data conducted on offshore wind turbine by (Hetland & Ekisund, 2015) to make a comparison with current study of laterally loaded piles. In this chapter, the 3D finite element method results were compiled and presented.

### 4.1 Effect of pile length

The effective pile length under earthquake load is significantly amplified even compared to other dynamic loads. Hence an equation is developed by performing multiple regression analysis to estimate the effective pile length of long piles under earthquake load as given below:

$$\frac{le}{d} = \left(\frac{Ep}{Es}\right) 0.345 \dots\dots\dots 4.1$$

Similarly, Randolph (1981) and Gazetas (1991b), as cited by Syngros (2004), defined the active length as the depth below which pile deflections are less than one-thousandth of the top deflections and came up with different expressions. The formulas are given in Equation (4.34) and Equation (4.35) for Randolph (1981) and Gazetas (1991b), respectively

$$\frac{lc}{d} = 1.6 \left(\frac{Ep}{Es}\right)^{0.28} \dots\dots\dots 4.2$$

$$\frac{lc}{d} = 2 \left(\frac{Ep}{Es}\right)^{0.25} \dots\dots\dots 4.3$$

$$\frac{lc}{d} = 1.057 \left(\frac{Ep}{Es}\right)^{0.28} \dots\dots\dots 4.4$$

In which  $l_c$ =effective pile length,  $d$  = is pile diameter,  $E_p$ = is young's modulus of pile and  $E_s$  = is young's modulus of soil. The proposed equation can be used to find out the effective length of single pile subjected to seismic load. The model pile used in the present study are classified as short and long pile in terms of effective pile length  $\langle l_c \rangle$

For piles with  $L \leq l_c$ , referred to as “short piles”, the pile head deformation varies with change in length. This implies the pile-head stiffness also varies with change in length. But for piles with  $L > l_c$ , which is referred as “long piles”, the pile head stiffness remains constant because there will not be any change in pile head deformation due to length variation.

Table 4-1 classification of short and long free head pile in terms of effective pile length

Pile length(m) (L)	diameter	$l_c$ (eq 4.2)	$l_c$ (eq 4.3)	$l_c$ (4.4)	Description ( $L \leq l_c$ Short pile, $L > l_c$ , long pile)
4	0.4	6.95	6.5021	5.718	Short pile
8	0.4	6.95	6.727	5.718	Short pile
12	0.4	6.95	6.5021	5.718	Long pile
16	0.4	6.95	6.5021	5.718	Long pile
20	0.4	6.95	6.5021	5.718	Long [pile
24	0.4	6.95	6.5021	5.718	Long pile

Table 4-2 classification of short and long fixed head pile in terms of effective pile length

Pile length (m)	diameter	$l_c$ (eq)	$l_c$ (eq)	Description ( $L \leq l_c$ Short pile, $L > l_c$ , long pile)
4	0.4	8.072	5.04	Short pile
8	0.4	8.072	5.04	long pile
12	0.4	8.072	5.04	Long pile
16	0.4	8.072	5.04	Long pile
20	0.4	8.072	5.04	Long pile
24	0.4	8.072	5.04	Long pile

The pile response is observed by varying the length of a pile from 4m, 8m, 12m, 16m, 20m, and 24m so that both short pile behavior and long flexible pile behavior are captured as shown in Table 4-1 and Table 4-2. These six types of pile length have been simulated numerically for 0.4 pile diameter. The simulated output of the numerical analyses through PLAXIS 3D FE software, in the form, displacement at pile head Vs dynamic time is illustrated in Figures 4-1,4-2 and 4-3. Pile head assumed to be both free head and fixed head pile, for short and long pile, respectively are considered for the present analysis.

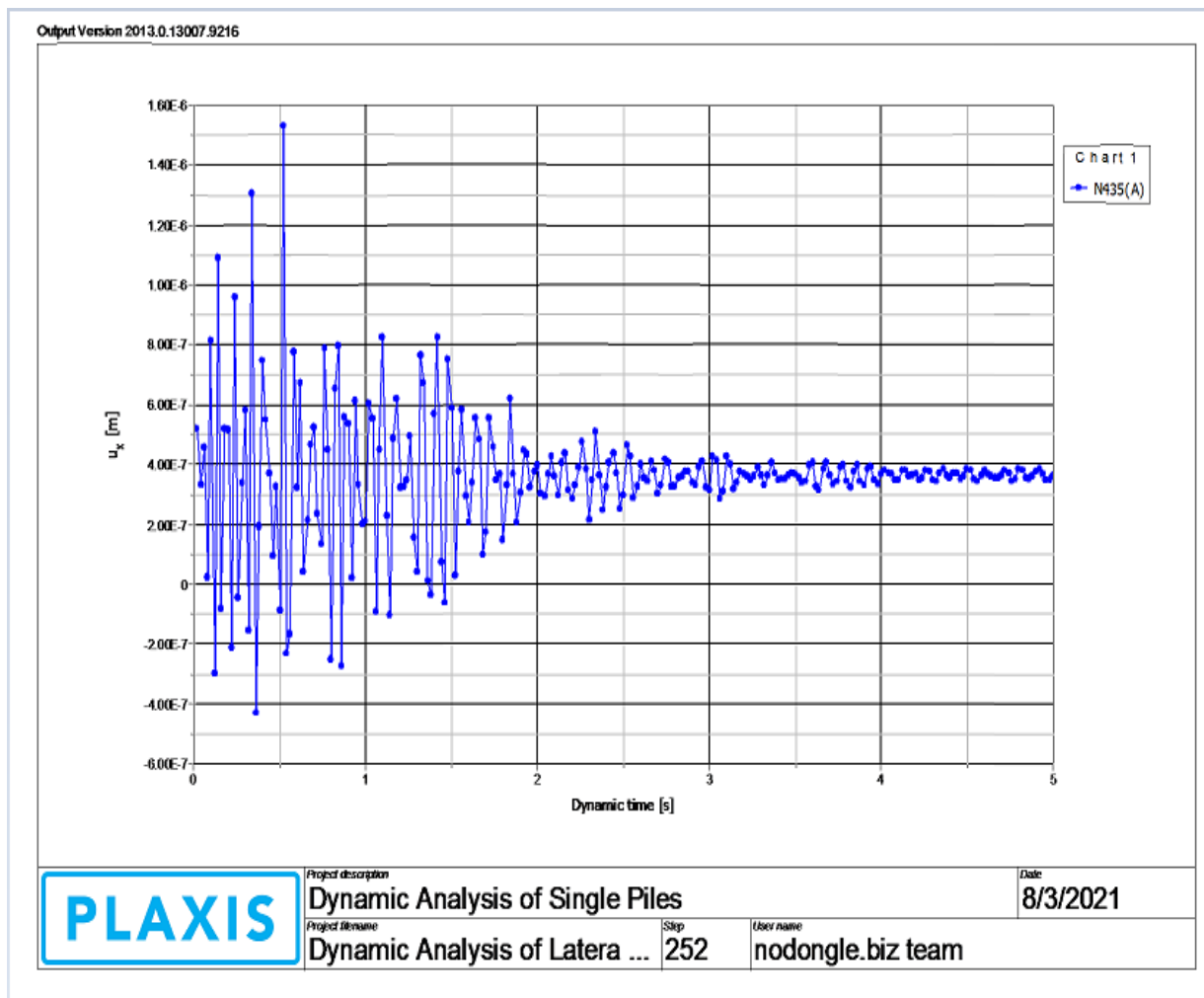


Figure 4-1 lateral displacement of 4m free headed short pile Vs dynamic time.

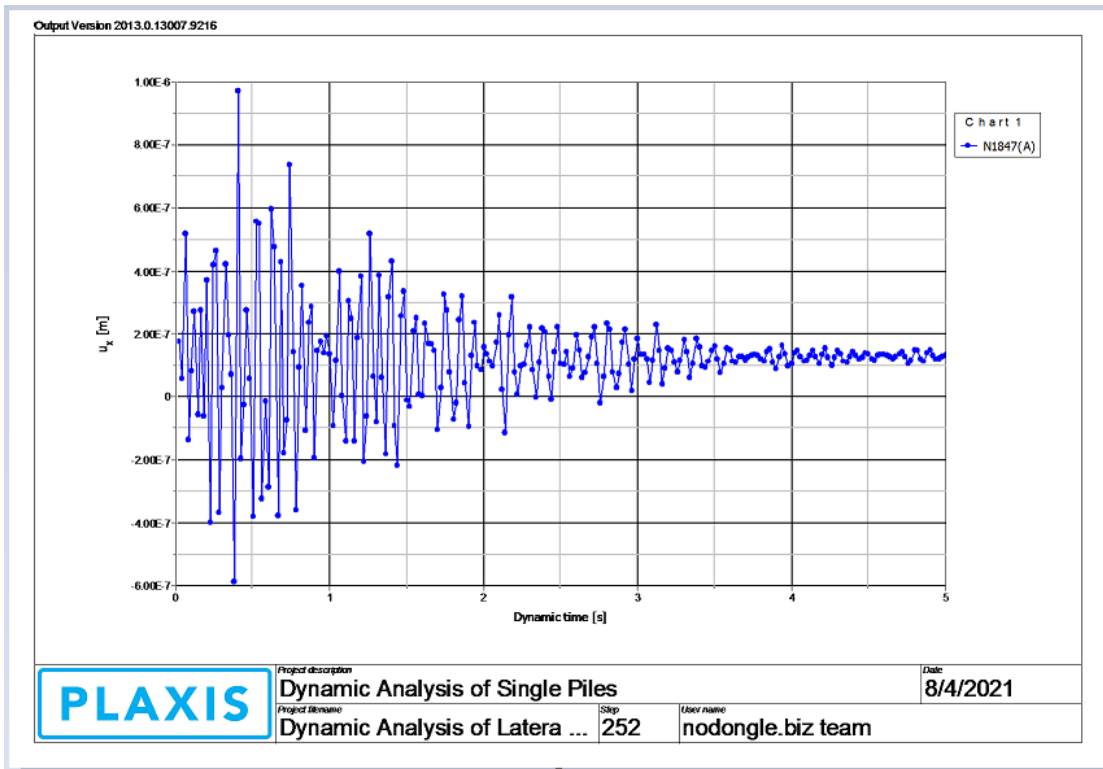


Figure 4-2 lateral displacement of 16m free headed long pile Vs dynamic time.

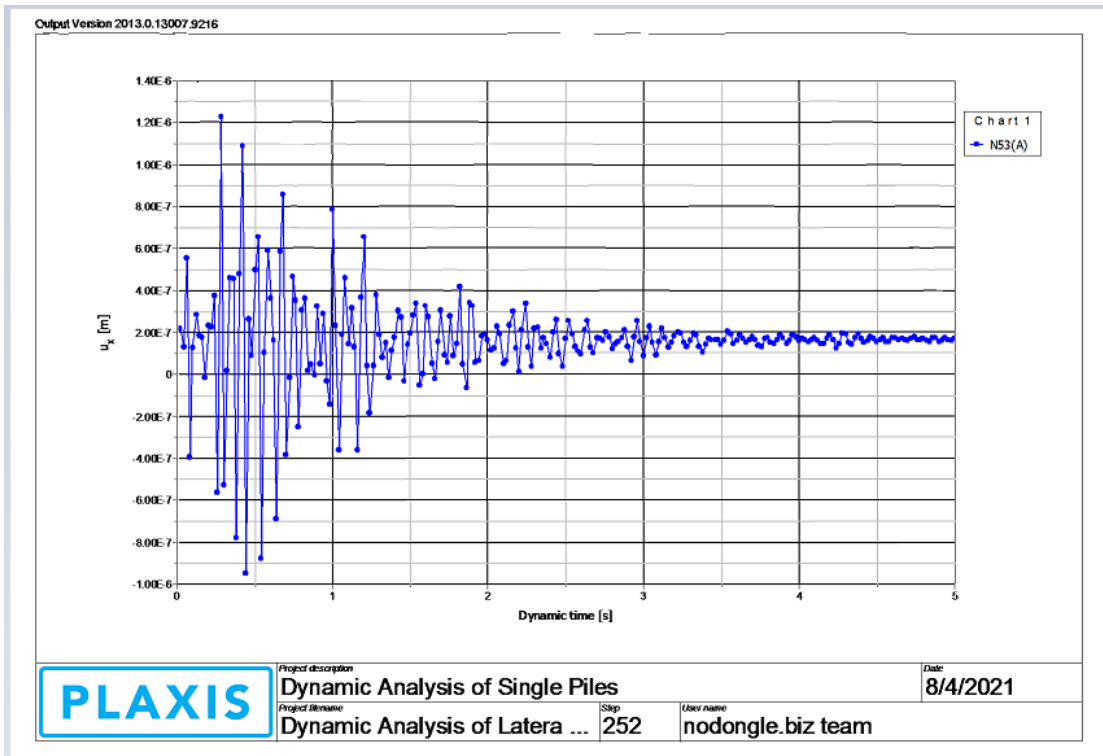


Figure 4-3 lateral displacement of 8m fixed headed long pile Vs dynamic time.

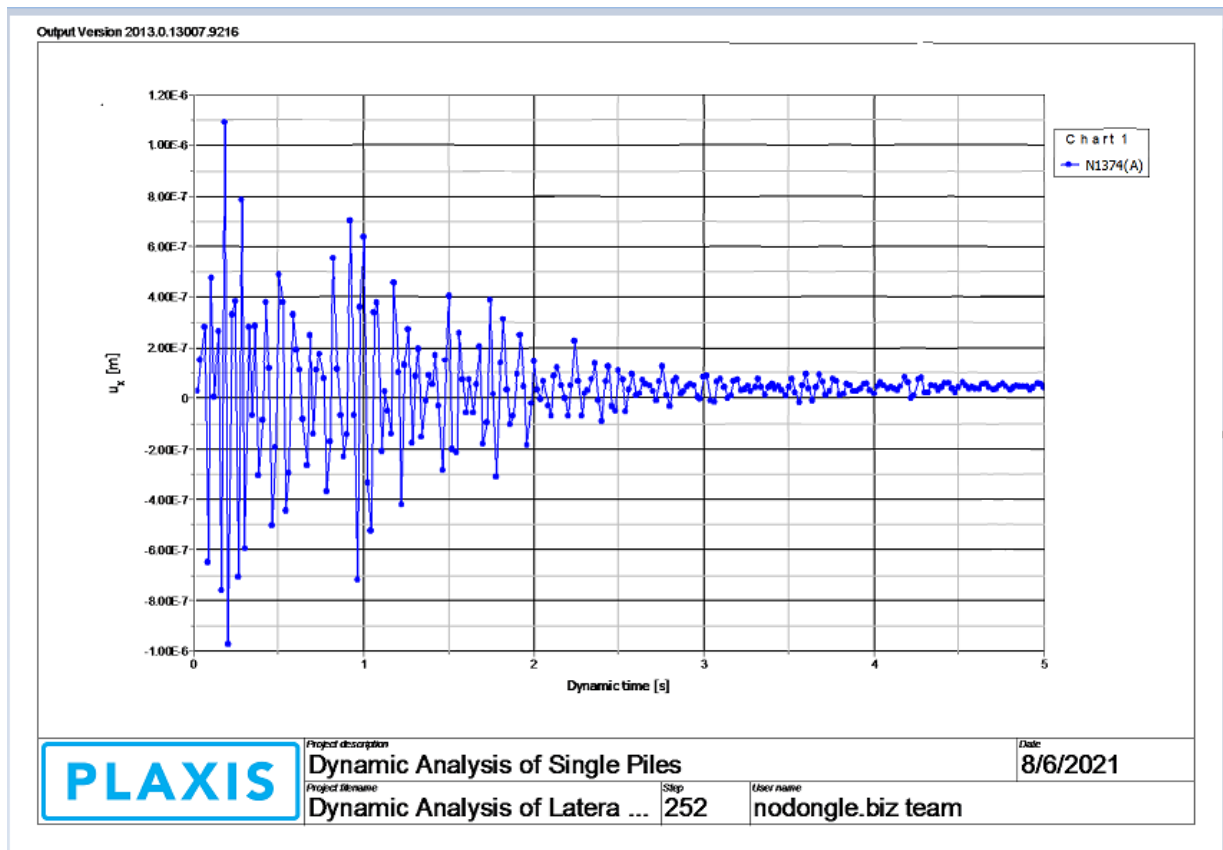


Figure 4-4 lateral displacement of 20m fixed headed long pile Vs dynamic time.

Figure 4-3 and Figure 4-4 shows the kinematic pile response at different embedment pile depth from short pile to long pile with interval of 4m. The lateral displacement of the pile shows decrement with the increase of embedment depth. This is attributed for the increase of stiffness of soil as depth increases and the deformation along the pile can be governed by stiffness of the surrounding soil and the amount of deflection can be influenced by the stiffness difference between pile and soil. Lateral deflection of pile decreased while down along the pile length.

#### 4.2 Effect of pile length on free head pile

Figure 4-5 shows the variation of maximum displacements along different pile lengths when the pile is head condition is free from the result, it is observed that as pile length increase the maximum displacement decreases.

the short rigid pile has a larger deflection as shown in figure 4-5 than the long flexible pile under free head condition This behavior is due to an increase in the depth of fixity and an increase in

the relative stiffness of the soil-pile system due to an increase in the embedded length of the pile also short rigid behavior resulting pile rotation.

The reduction has a similar pattern but with a different reduction rate. Increasing length from 4m to 8m, 8m to 12m, 12m to 16m, and 16m to 20m and 20m to 24m the percentage of reduction in pile head displacement 12.4%, 11.9%, 5.93%, 9.96% and 0.95% and for free headed pile short and long pile condition. 8m-24m (long flexible pile) pile length it is observed that the pile response is not affected by increase in length anymore which is dynamic lateral loads at pile heads do not deform piles over their entire length. Instead, pile deformations and stresses reduce to negligible proportions below a distance  $l_c$  called dynamic “effective length”, from the ground surface.

As shown in Table 4.1 the effective pile length value is 6.95m for free head pile the analysis result also show that the of length  $L > l_c$  commonly termed as flexible piles, the exact pile length  $L$ , has no influence on their response to lateral loads. It is found that pile head responses are smaller when the soil is stiffer. Generally, the long flexible pile has less pile head displacement than short rigid pile under seismic excitation.

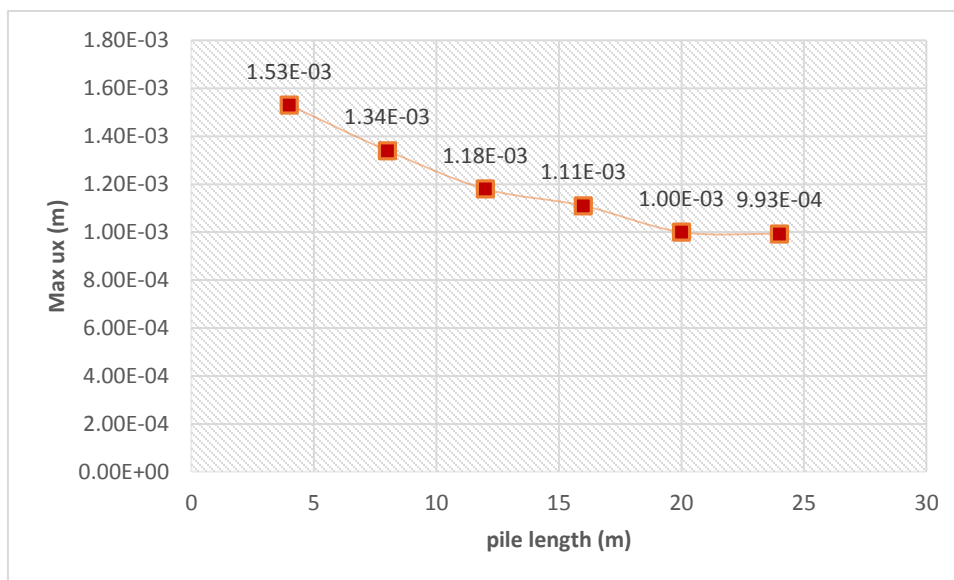


Figure 4-5 Pile head deflection of free headed pile

For 4m pile length show large lateral displacement than 20m pile length this is due to the reduction to the soil stiffens at shallow depth the laterally loaded pile installed in granular soil are subjected to more lateral displacement at shallow depth as compared to those installed in cohesive soil.

### 4.3 Effect of pile length on fixed head pile

For the increase in a pile, length decreases the pile head displacement. This behavior is due to an increase in the depth of fixity and an increase in the relative stiffness of the soil-pile system due to increase in the embedded length of the pile. As shown in figure 4-6 the displacement of short pile has given larger value than long pile.

The reduction has a similar pattern but with a different reduction rate. Increasing length from 4m to 8m, 8m to 12m, 12m to 16m, and 16m to 20m the percentage of reduction in pile head displacement 38.5%, 5.69%, 5.17%, 4.95% for free headed single pile foundation the reduction rate is almost similar at pile reach 8m -16m pile length and show a significant change in 20m pile length from the ground level because of as the depth increases, stiffness of the soil increases. Therefore, depth and deformation are inversely proportional to each other while the application of load is at the bedrock level

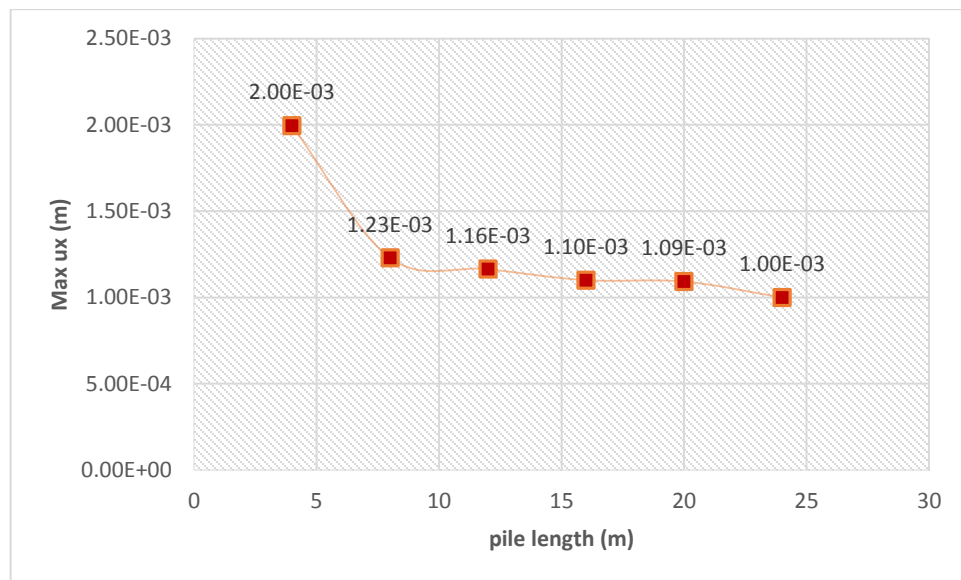


Figure 4-6 Pile head deflection of fixed headed pile

Comparison between Pile top displacement for free head and fixed head pile are shown in figure 4-6 below. The difference of pile displacement for 4m, 8m, 12m, 16m, and 20m is 38.5%, 8.2%, 13.79%, 4.37%,12.8% the deflection is almost the same other than 4m pile length. This is due to the fact that whether it is free head or fixed head pile; if the relevant parameters of the soil system remain same, the stiffness of soil does not alter. So fixity developed at the pile head (in case of a fixed head pile in the present study) does not noticeably or distinguishably effect of the soil system.

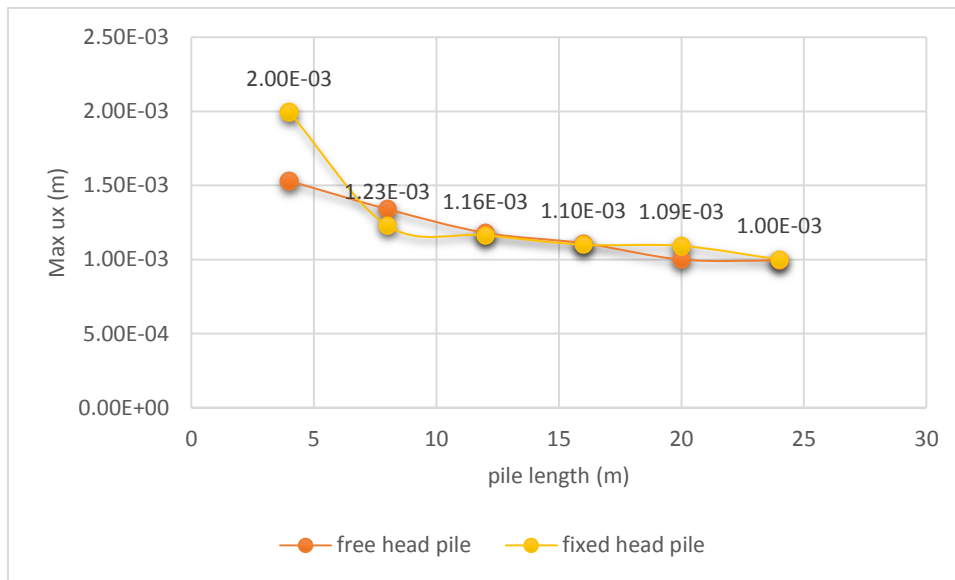


Figure 4-7 the effect of pile head fixity condition on maximum head deflection of pile

#### 4.4 Effect of batter angle

On the discussion of vertical pile shown in figure 3 for both pile head fixity conditions at 8m pile length show close result and chose for batter pile analysis using different batter angle to check using batter pile under earthquake condition have good or bad reputation

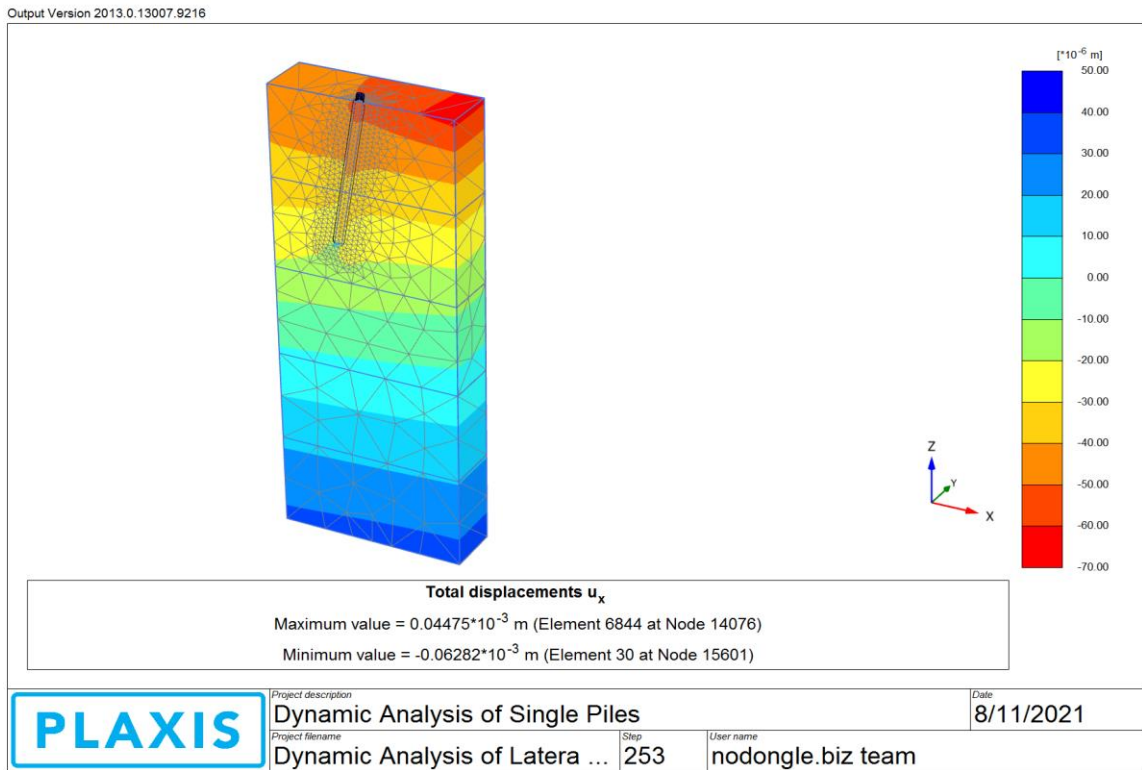


Figure 4-8 3D modeling negative batter pile

#### 4.5 Effect of Negative batter pile on Head Deflection of Pile

For the increasing in negative batter angle decreases the pile head displacement This behavior is due batter pile generally have higher horizontal stiffness, mainly due to the fact that inclined pile provide partial horizontal resistance and the upper soil support in a negative battered pile is enormous as shown in figure 4-8  $5^0$  and  $10^0$  batter angle gives less head deflection than the vertical pile. The reduction has similar pattern but with different reduction rate. Increasing batter angle from  $0^0$  to  $5^0$ m,  $5^0$  m to  $10^0$ m,  $10^0$ m to  $15^0$ m,  $15^0$ m to  $20^0$ m and  $20^0$ m to  $25^0$  the percentage of reduction in pile head displacement 43.0%, 3.5%, 46.6%, 2.25% and 99.4<sup>0</sup> % for negative batter pile foundation the reduction rate is almost similar at batter angle  $5^0$ - $10^0$  batter angle and show significant change in displacement  $25^0$  battered pile.

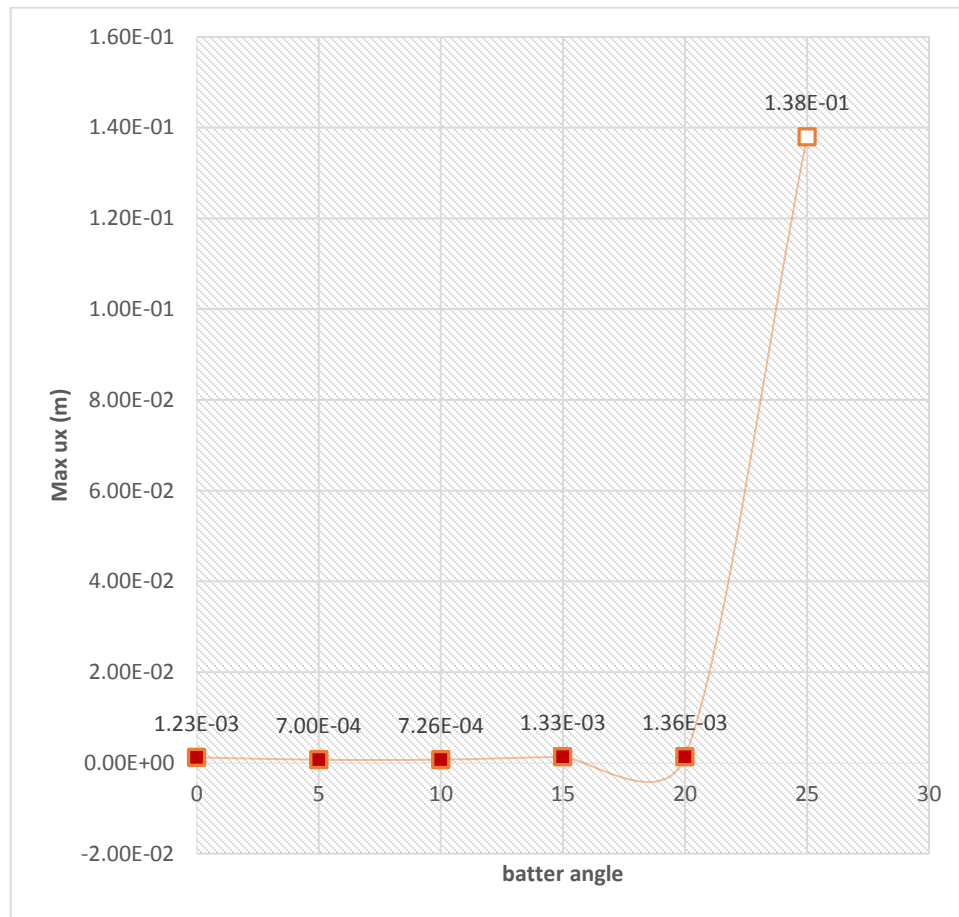


Figure 4-9 Pile top displacement Vs negative batter angle

L<sub>v</sub> et al. (2011) carried out experimental work to study the lateral bearing capacity of negative batter pile under different batter and different constraints at pile head. These piles were embedded in sand. The pile batter angle to vertical,  $\beta$ , is  $0^\circ$ ,  $10^\circ$  or  $20^\circ$ . The analysis indicates that the lateral capacity of the negative batter pile decreases as the batter angle decreases when the pile head is only horizontal movement (translational), the lateral capacity of the negative batter transitional pile is more than that of the positive batter.

#### 4.6 Effect of positive batter pile on Head Deflection of Pile

A pile is said to have a positive (+ve) batter if its inclination with the vertical is opposite to the direction of loading show on figure 4-10

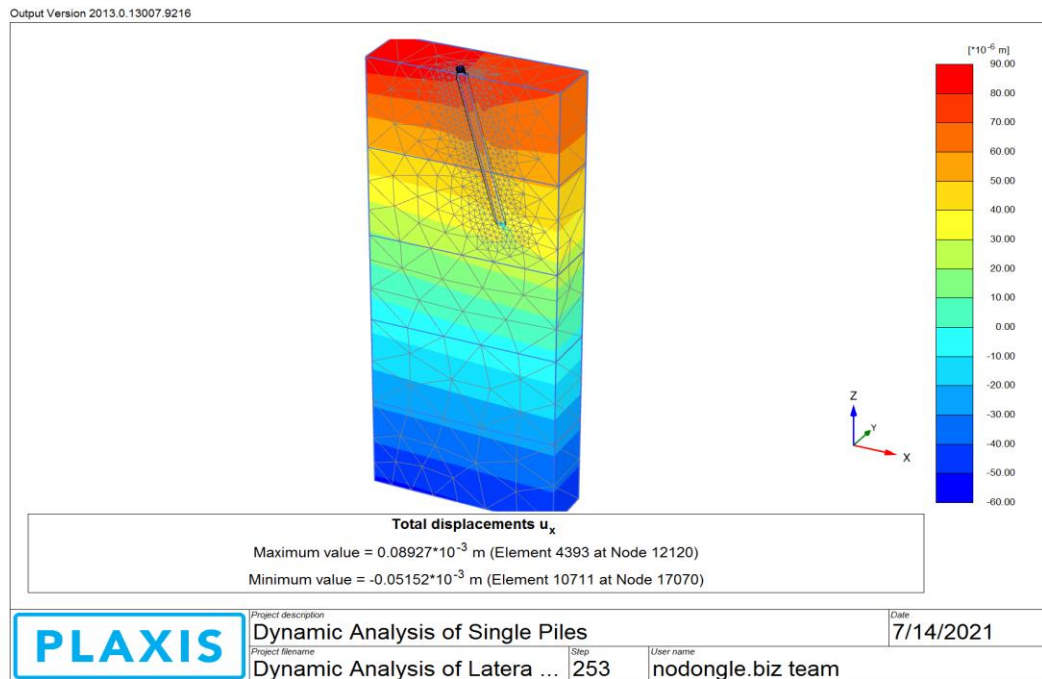


Figure 4-10 3D modeling positive batter pile

For the increasing in positive batter angle increasing the pile head displacement This behavior is due the soil reaction at the ground level is zero for positive batter pile as shown in figure4-11 the pile head displacement has increase when the batter angle increase the vertical pile has shown small displacement than positive batter pile. The reduction has similar pattern but with different reduction rate. Increasing batter angle from  $0^0$  to  $5^0$ m,  $5^0$  m to  $10^0$ m,  $10^0$ m to  $15^0$ m,  $15^0$ m to  $20^0$ m and  $20^0$ m to  $25^0$  the percentage of reduction in pile head displacement 63.4%, 37.56%, 1.99%, 13.73% and 98.43<sup>0</sup> % for negative batter pile foundation the reduction rate is almost similar at batter angle  $10^0$ - $20^0$  batter angle and show significant change in  $25^0$  From the analysis result it is shown in Figure 4-11 the load inclined at beyond  $25^0$  gives very large deformation.

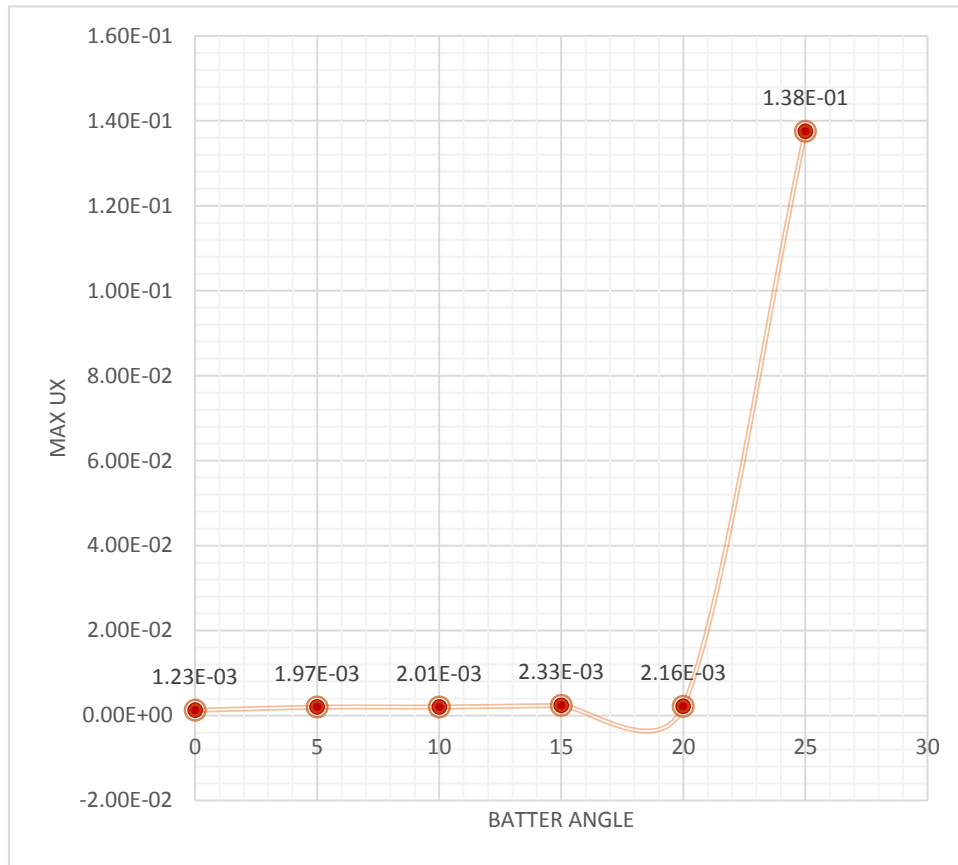


Figure 4-11 Pile top displacement Vs batter angle

It is reported that negative batter piles offer more lateral resistance than positive batter piles. This is explained by the fact that the soil reaction at ground level is zero for a positive batter pile and maximum for a negative batter pile, indicating that the upper soil support in a negative batter is enormous so that negative batter pile has larger lateral resistance.

Table 4-3 comparison pile top displacement for negative and positive batter pile under earthquake loading

Pile length	Batter angle(0°)	Pile top Dis negative batter pile(mm)	Pile top dis for positive batter pile(mm)	Show large Displacement
8m	0°	1.23E-3	1.23E-3	-

8m	5 <sup>0</sup>	7.00E-4	1.97E-3	Positive
8m	10 <sup>0</sup>	7.26E-4	2.01E-3	Positive
8m	15 <sup>0</sup>	1.33E-3	2.33E-3	Positive
8m	20 <sup>0</sup>	1.36E-3	2.16E-3	Positive
8m	25 <sup>0</sup>	1.38E-1	1.38E-1	Same

#### 4.7 Final displacement for free head and fixed head single pile

Figure 4-11 show that comparison between the final displacement free head pile and fixed head pile the final displacement is for short pile is greater than long pile because of the stiffness of soil around the ground have less resistance and pile has short length it has less fixity condition and displaced after the earthquake excitation in case of fixed head pile in the has small final displacement the long flexible pile final displacement almost similar or close for both fixed and free head single pile this is due to the soil and pile parameter used in the analysis is the same for both condition. Free head pile has displaced more than fixed head pile condition it's due to fixed head pile the pile head is restricted for any kind of rotation. The reduction rate is 3.29% for short pile and in case of long pile 12.72%, 0.79% 17.12%, 23.15% for consecutive pile length

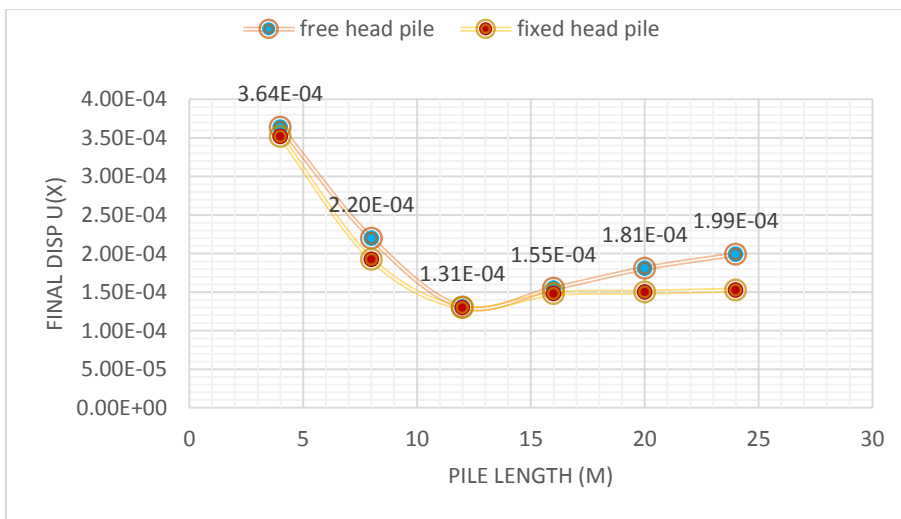


Figure 4-12 the effect of pile head fixity condition on the final displacement of pile

## 5. SUMMARY AND CONCLUSION

### 5.1 Summary

The main objective of this thesis was to study the behavior of laterally loaded pile foundation embedded in medium dense sand soils considering the effect of pile length, pile head fixity, and Pile batter angle under earthquake loading condition using a Plaxis 3D model. The main conclusions and recommendations drawn through the numerical modelling of laterally loaded pile developed in this study are summarized in this chapter.

In this study investigate the behavior of laterally loaded pile under dynamic lateral loading. As shown in chapter-3, a Plaxis 3D model has been developed to study the behavior of laterally loaded pile. In addition, to ensure the reliability of the results obtained by validated by using an experimental data conducted on offshore wind turbine by (Hetland & Ekisund, 2015) to make a comparison with current study of laterally loaded piles.

The result of the analysis show that pile length and batter angle affect the head deflection of vertical pile under dynamic loading condition

In this study the increase in a pile, length decreases the pile head displacement This behavior is due to increase in the depth of fixity and an increase in the relative stiffness of the soil-pile system due to increase in the embedded length of the pile. It noted that increased batter angle decreased the pile top displacement A positive batter pile has less resistance to lateral load than a negative batter pile for earthquake loading.

## 5.2 Conclusion

In this thesis, numerical studies have been conducted to investigate the behavior of vertical piles and batter piles embedded in the sand when subjected to lateral earthquake loading. The main conclusions and recommendations drawn through the numerical modeling of vertical and batter pile foundation developed in this study are summarized and draw conclusions in this chapter. The most important observations regarding the numerical modeling analysis are summarized

the short rigid pile has a larger deflection than the long flexible pile under both free head and fixed head condition This behavior is due to an increase in the depth of fixity and an increase in and an increase in the relative stiffness of the soil-pile system due to an increase in the embedded length of the pile also short rigid behavior resulting pile rotation. The percentage of head deflection of short for free head and fixed head condition 38.5% and 12.4% respectively as a pile length the analysis result also show that the of length the embedment length greater than the effective pile length commonly termed as flexible piles, the exact pile length  $L$ , has no influence on their response to lateral loads seismic load.

A positive batter pile has less resistance to lateral load than a negative batter also piles for earthquake loading It noted that increased batter angle decreased the pile top displacement until reaching at angle  $25^{\circ}$  (for both negative and positive batter pile) after that deflection become increased. Negative batter piles have more resistance to lateral load than vertical piles and positive battered pile.

### **5.3 Recommendation**

The work explored in this research is only on the effect of single piles, which have the basic behavior on group batter, but a combination of batter and vertical pile may have more efficiency for the combination of vertical and lateral load effects on pile group.

Further analysis on batter piles subjected earthquake loading in clay soil is useful.

## REFERENCES

- American Petroleum Institute. (2003). *Recommended Practice for Planning, Designing and Constructing Fixed Offshore Platforms-Working Stress Design*. Washington, D.C.: API Publishing Services.
- Banerjee, P., & Davis, T. (1978). The Behavior of Axially and Laterally Loaded Piles Embedded in Non-Homogeneous Soils. *Geotechnique*, 28, 309-326.
- Bhushan, K., Haley, S., & Fong, P. (1975). Lateral Load Test of Drilled Piers in Stiff Clay. *J.Geot.Engr. Div. ASCE*, 969-985.
- Boomintahn, A., & Ayothiraman, R. (2006). Dynamic Respose of Laterally Loaded Piles in Clay. *Institute of Civil Engineeners, Deotechnical Engineering I59. GE3*, pp. 233-241. ICE.
- Desai, C., & Appel, G. (1976). 3D Analysis of LAtterally Loaded Structure. *2nd International Confrence on Numerical Methods in Geomechanics*, (pp. 405-416). Blacksburg.
- Dobry, R., & Voucetic, M. (1987). Dynamic Response and Seismic Respose of Soft Clay Depaosits. *International Symposium Geotechnical Engineering of Soft Soils*, 2, pp. 51-87. Mexico City.
- Douglas, D., & Davis, E. (1964). The Movement of Burried Footings due to Moment and Horizontal Load and the Movement of Anchore Plates. *Geotchnique*, 115-134.
- El Naggar, M. H., & Bentely, K. J. (2000). Dynamic Analysis of Laterally Loaded Piles and Dynamic p-y Curves. *Canada Geotechnical Engineering Journal*, 37, 1166-1183.
- EL Naggar, M., & Novak, M. (1996). Nonlinear Analysis for Dynamic Lateral Pile Response. *Soil Dynamics and Earthquake Engineering (15)*, 233-244.
- Elnashai, A., & Di Sarini, L. (2015). *Fundamentals of Earthquake Engineering from Source to Fragility, 2nd Ed*. West Sussex, UK: John Wiley & Sons, Ltd.
- Faruque, M., & Desai, C. (1982). 3D Matrail and Geometric Nonlinear Analysis of Piles. *2nd international Methods on Numerical Methods of offshore Piling*, (pp. 553-575).

- Gaul, R. (1958). Model Study of a Dynamic Laterally Loaded Pile. *J.S.M.F.D ASCE*.
- Geogradis, M. (1983). Development of p-y curves for layered soils. *Geotechnical Practice in Offshore Engineering* (pp. 536-545). ASCE.
- Ghazzaly, O., Hwong, S., & O'Neal, M. (1976). Approximate Analysis of a Pile Under Dynamic Lateral Loading. *Computers and Structures*, 363-368.
- Gazetas G., "Analysis of Machine Foundation Vibration: State of Art," *Soil Dynamics and Earthquake Engineering*." Vol. 2, No. 1, pp. 1-41, 1983.
- Gazetas G., "Foundation Vibration," In: Fang H. Y. (editor.), "Foundation Engineering Handbook." Van Nostrand Reinhold, 1991.
- Gazetas G., "Seismic design of foundations and soil-structure interaction." *Proceedings of 1st European Conference on Earthquake Engineering and Seismology*, 2006.
- Hatényi, M. (1946). *Beams on Elastic Foundations*. Baltimore,MD: Waverly Press.
- Hayashi, S. (1973). A New Methods of Evaluating Sessmic Stability of Steel Structures. *Proceeding Fifth World Confrence Earthquake Engineering*, (pp. 2602-2605). Rome.
- Idriss, I., & Seed, H. (1968). Seismic response of Horizontal Soil Layers. *J.S.M.F.D SM4, 94*, 1003-1031.
- Ishitashi, I., & Zhang, X. (1993). Unified Dynamic Shear Moduli and Damping Ratios of Sand and Clay. *Soils and Foundations*, 1, 182-191.
- Kokushu, T., Yoshida, Y., & Eshashi, Y. (1982). Dynamic Properties of Soft Clay for Wide Strain Range. *Soils and Foundations*, 20(2), 45-60.
- Kramer, S. (1996). *Geotechnical Earthquake Engineering*. Upper Saddle River , N.J, USA: Prentice-Hall,Inc.
- Lee, P., & Gilbert, L. (1979). Behavior of Laterally Loaded Pile in a Soft Clay. *Offshore Technology Confrence*.
- Mardfekri, M., Gardoni, P., & Rosset, J. (2013). Modelling Laterally Loaded Single Piles Accounting for Nonlinear Soil-Pile Interaction. *J.Eng.(3)*, 1-7.

- Matlock, H. (1970). Correlation for Design of Laterally Loaded Piles in Soft Clay. *Proceedings Offshore Technology Conference*. Houston, TX.
- McClelland, B., & Focht, J. (1958). Soil Modulus for Laterally Loaded Piles. *Trans. Ame. Soc. Civ. Eng.*, 1049-1063.
- Morison, J., O'Brien, M., Johnson, J., & Schaff, S. (1950). The forces Exerted by surface Waves on Piles. *Petroleum Trans. Amer. Ins. Met. & Pet. Engrs.*, 189, 149-154.
- Mousa, A., & Christu, P. (2018). Evolution of Analysis Methods for Laterally Loaded Piles through Time. *Advances in Analysis and Design of Deep Foundation* (pp. 65-95). Cairo, Egypt: Springer. doi:DOI 10.1007/978-3-319-61642-1
- Nair, K. (1969). Dynamic and Earthquake Forces on Deep Foundations. *ASTM, STP*, pp. 229-261.
- Novak, M. (1974). Dynamic Stiffness and Damping of Piles. *Canadian Geotechnical Journal*, 574-598.
- Novak, M., & El-Sharnouby, B. (1983). Stiffness and Damping Constants of Single Piles. *J. Geotech. Div. ASCE*, 961-984.
- Novak, M., & Sheta, M. (1980). Approximate Approach to Contact Problem of Piles. *Dynamic response of Pile Foundations: Analytical Aspects* (pp. 53-79). Florida: Geotechnical Engineering Division, ASCE.
- Novak, M., Nogami, T., & Aboull-Ella, F. (1978). Dynamic Soil Reaction from Plain Strain Use. *J. Engr. mech. Div.*, 953-979.
- Penzien, J., Shaffey, C., & Parmelee, R. (1964). Seismic Analysis of Bridge on Long Piles. *J. Eng. Mech. Div. EM3*, 223-254.
- Poulos, H. (1971). Behaviour of Laterally Loaded Piles. *J. Soil Mechanics and Foundation Div. ASCE*, 733-751.
- Poulos, H. (1971). Behaviour of Laterally Loaded Piles. *J. Soil Mechanics Foundation Div. ASCE*, 711-731.

- Poulos, H., & Davis, E. H. (1980). *Pile Foundation Analysis and Design*. Rainbow- Bridge Book Co.
- Prakash, S., & Gupta, L. (1970). A study of Natural Frequency of Pile Groups. *Second South East Asian Regional Conference Soil Engineering*, (pp. 401-410). Singapore.
- Prakash, S., & Sharma, H. (1969). Analysis of Pile Foundations Against Earthquakes. *Indian Concr. J.*, 205-220.
- Prakash, S., & Sharma, H. (1990). *Pile Foundation in Engineering Practice*. 111 River Street Hoboken, NJ: John Wiley and Sons, Inc.
- Randolph, M. (1981). The Response of Flexible Pile to Lateral Loading. *Geotechnique*, 247-259.
- Reese, L., & Matlock, H. (1956). Non-Dimensional Solution for Laterally Loaded Piles with Soil Modulus assumed Proportional to Depth. *8th Texas Conference on Soil mechanics and Foundations*, (pp. 1-41). Austin.
- Reese, L., & Welch, R. (1975). Lateral Loading of Deep Foundation in Stiff Clay. *J. Geot. Engr. Div. ASCE*, 633-649.
- Reese, L., Cox, W., & Koop, F. (1974). Analysis of Laterally Loaded Piles in Sand. *Proceedings Offshore Technology Conference, OTC 2080*, pp. 473-483. Houston, TX.
- Reese, L., Cox, W., & Koop, F. (1975). Field Testing and Analysis of Laterally Loaded Piles in a Stiff Clay. *VII Annual Offshore Technology Conference* (pp. 672-690). Houston, TX: OTC 2312.
- Richart, F. E. (1962). Foundations Vibrations. *Trans. ASCE*, 127, 863-890.
- Richarts, F., Hall Jr, J., & Woods, R. (1970). *Vibrations of Soils and Foundations*. Englewood Cliffs, N.J., USA: Prentice-Hall, Inc.
- Seed, H., & Martin, G. (1966). The Seismic Coefficient in Earth Dam Design. *J.S.M.F.D.*, 92 SM3, 25-58.

- Sun, J., Golesorkhi, R., & Seed, H. (1988). *Dynamic Moduli and Damping Ratio for Cohesive Soils*. University of California, Earthquake Engineering Research Center, Berkeley.
- Trochanis, A., Bielak, J., & Christiano, P. (1991). Three Dimensional NonLinear Study of Piles. *J. Geotech. Engr.*, 429-447.
- Tucker, R. (1964). Lateral Analysis of Piles with Dynamic Behavior. *Confrence on Deep Foundations*, (pp. 157-171). Mexico City.
- Wolf, J. (1985). *Dynamic Soil-Structure Interaction*. Englewood Cliffs, N.J., USA: Prenticen-Hall,Inc.
- Zhand, L., McVey, M., & Lai, P. (1999). Centerfuge Modelling of Laterally Loaded Single Batter Piles in Sand. *Candian Geotechnical Journal* 36(6), 1074-1084.
- Zhang, Y., Conte, J., Yang, Z., Elgamal, A., Bielak, J., & Acero, G. (2008). Two Dimensional Non-Linear Earthquake Response Analysis a Bridge-Foundation-Ground System. *Earthquake Spectra* 24(3), 343.

## APPENDEIX

### APPENDEIX A

Stiffness of soils are known to relate to the effective stress level in the soil (Benz (2006)). Different correlations are used in literature. For simplicity, it is here chosen to relate soil stiffness to the effective vertical stress, seeing as this can be found directly without the use of  $K_0$ .

The equation was found to be:

$$E_0 = 6000 (\sigma_v)^{0.48}$$

Using equation (1) it is possible to discretize the stiffness in the finite element model, and get a better estimate of the deformation characteristics of the system.

### Initial Frequency

Anticipated Shear wave velocity for medium dense sand;

$V_s$  150 m/sec

$$W1 = 0.13 \text{ Hz}$$

$$W2 = 2.73 \text{ Hz}$$

Predominant Frequency of Hollister (1989) earthquake Load using seismosignal. The predominant period is 0.075 and the dominant amplitude hence the dominate frequency shall be

$$f_i = 13.3 \text{ Hz}$$

$$n = 102.40$$

Damping ratio for medium sand

$$\xi = 5\%$$

for steel pile

$$\xi = 0.5 \%$$

## **Soil parameters**

In order to perform the analysis, a wide range of soil properties are used. These values are extracted mainly from Obrzud and Truty (2012) and Bowles (1997).

### **Young's modulus**

Soil Young's modulus (E), commonly referred to as soil elastic modulus, is an elastic soil parameter and a measure of soil stiffness. It is defined as the ratio of the stress along an axis over the strain along that axis within the elastic strain range.

### **Poisson's ratio**

Poisson's ratio is the ratio of transverse contraction to a longitudinal extension. According to Bowles (1997), the value of Poisson's ratio of a soil lies between 0.2-0.5. The detailed values are given in Table 3-2. In this study, the values of Poisson's ratio used are 0.2, and 0.3.

## APPENDIX B

### PLAXIS 3D OUTPUT

Pile top displacement for free head and fixed vertical and better pile

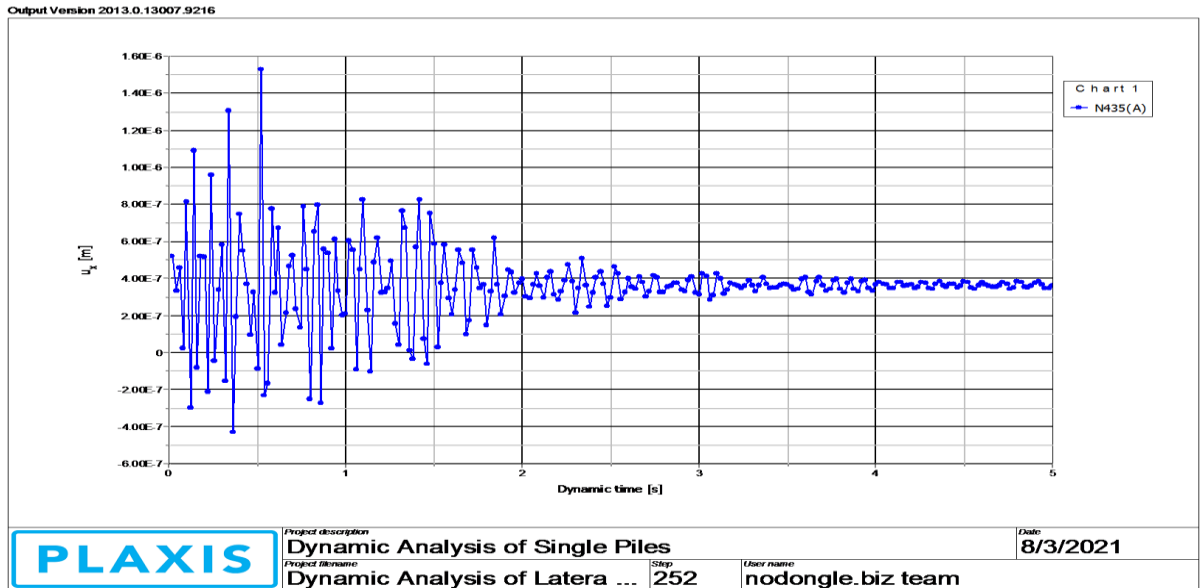


Figure B- 1 Pile head displacement for 4m free headed pile

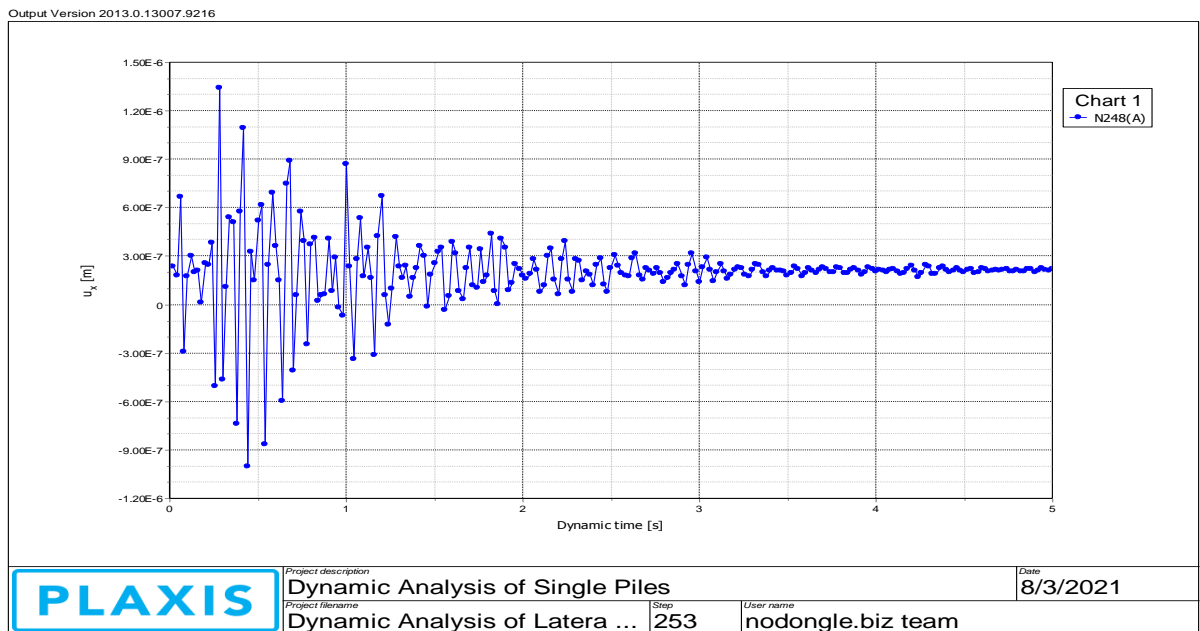


Figure B- 2 Pile head displacement 8m free headed pile

Output Version 2013.0.13007.9216

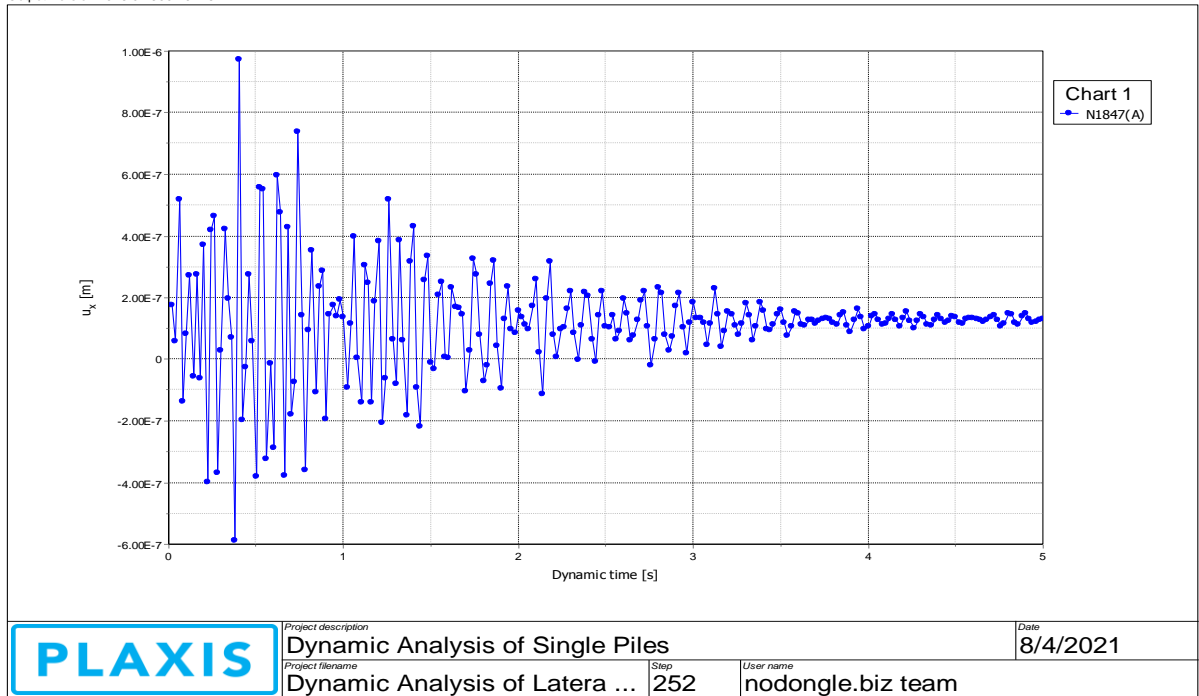


Figure B- 3 Pile head displacement 12m free headed pile

Output Version 2013.0.13007.9216

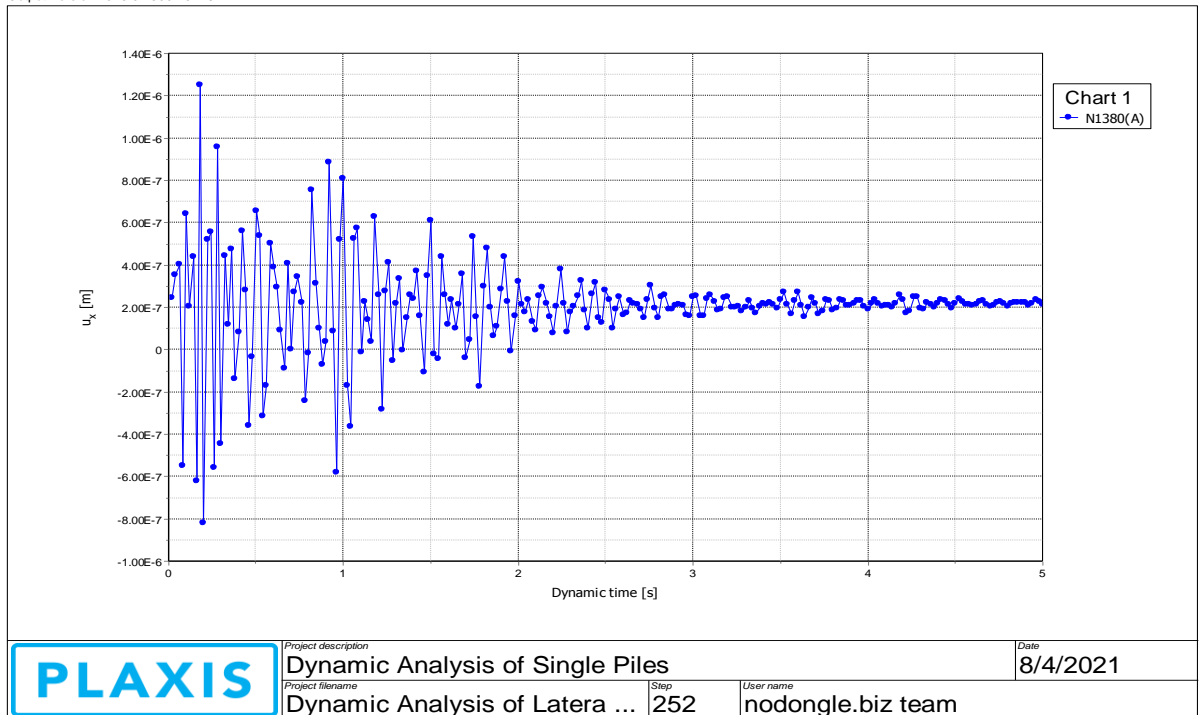


Figure B- 4 Pile head displacement 20m free headed pile

Output Version 2013.0.13007.9216

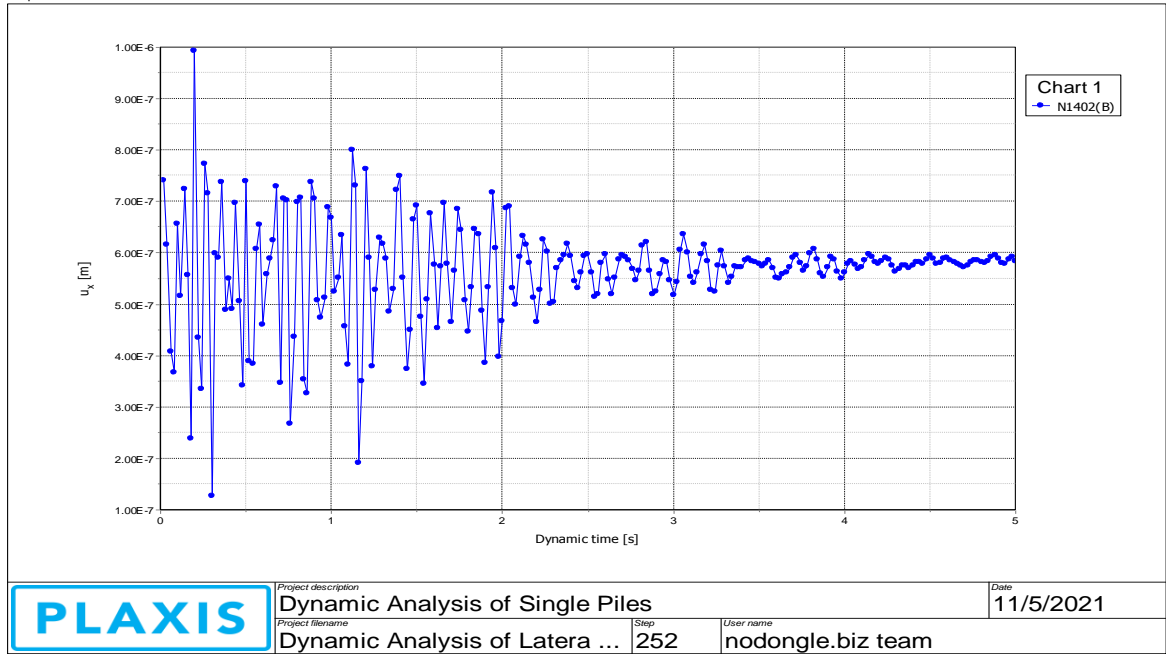


Figure B- 5 Pile head displacement 24m free headed pile

Output Version 2013.0.13007.9216

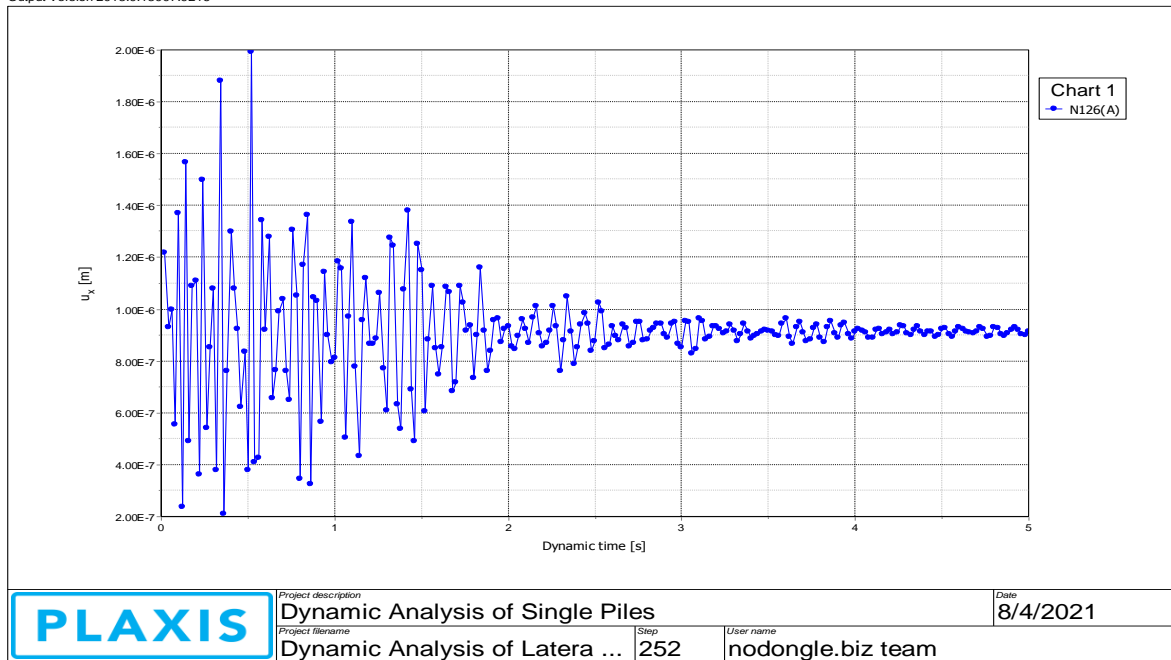


Figure B- 6 Pile head displacement 4m fixed headed

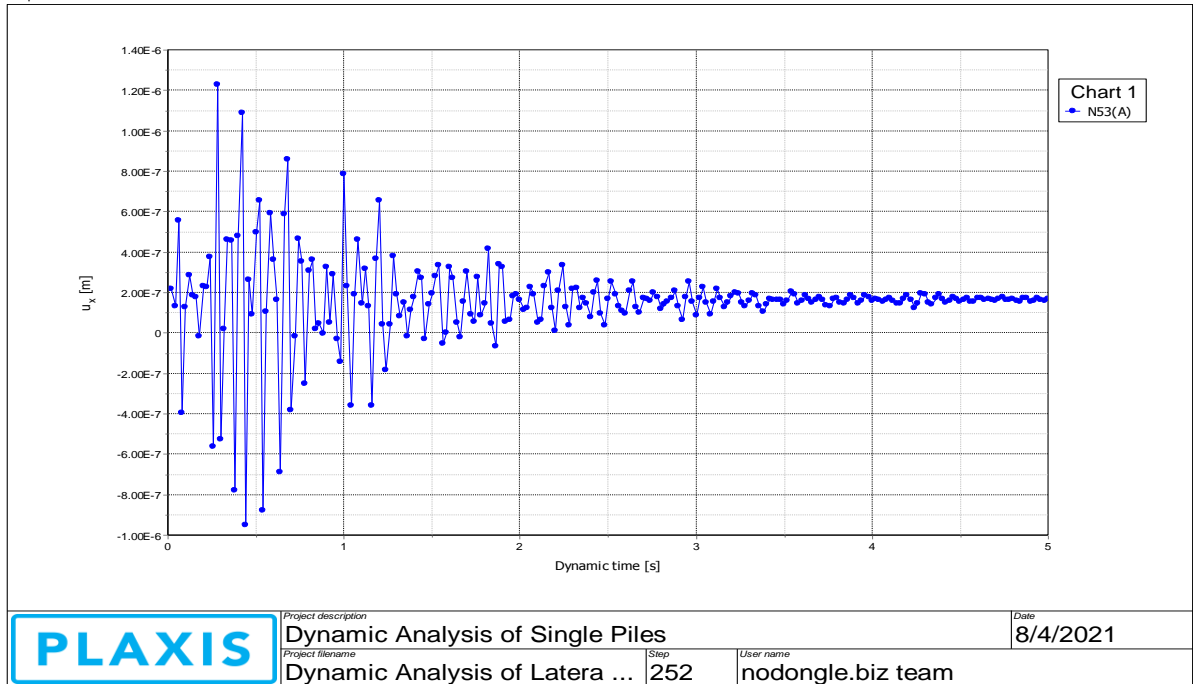


Figure B- 7 Pile head displacement 8m fixed headed

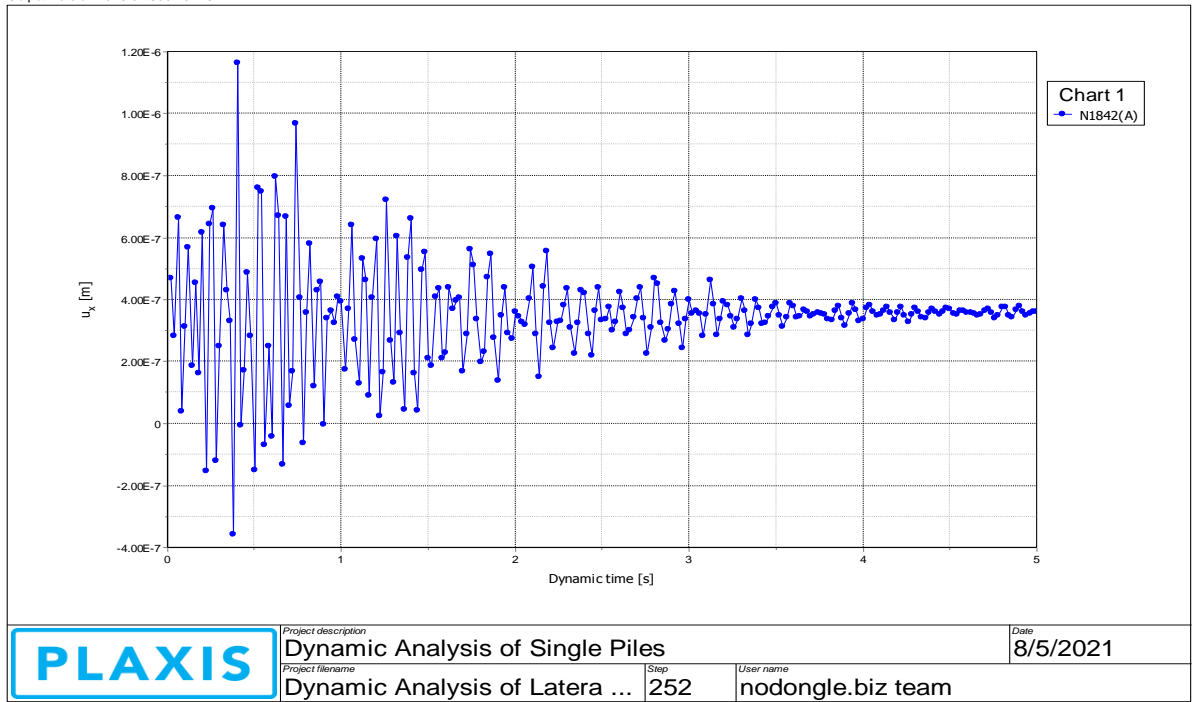


Figure B- 8 Pile head displacement 12m fixed headed

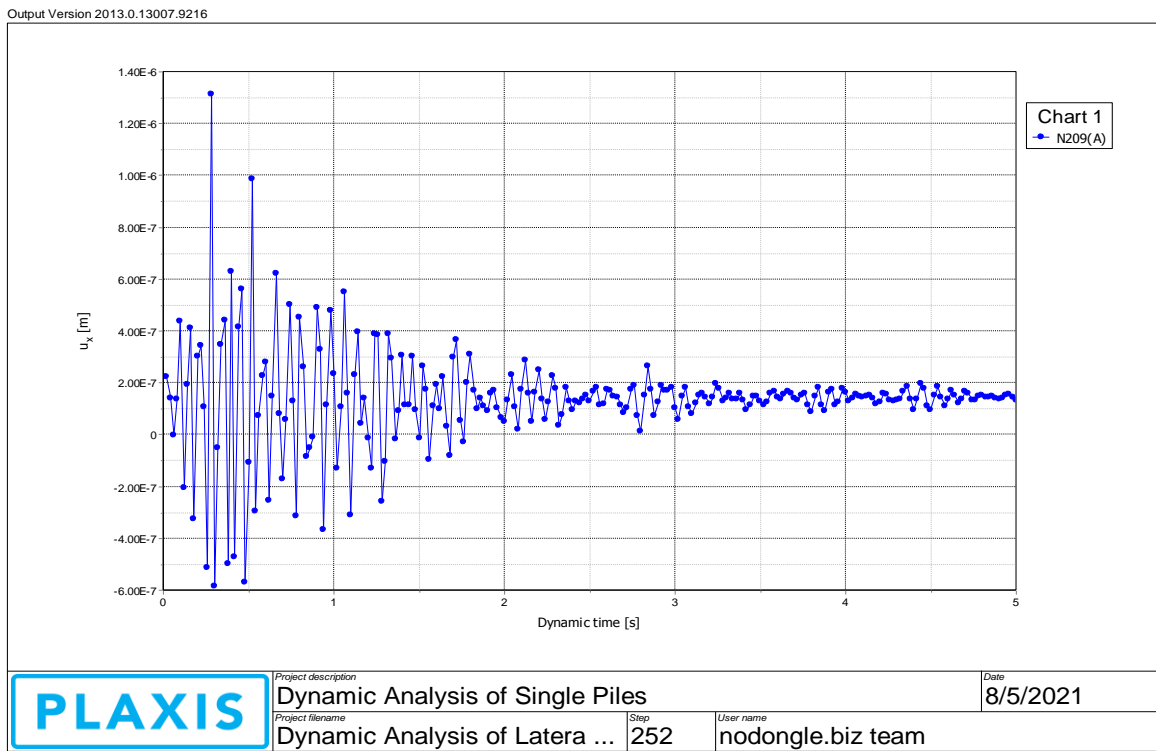


Figure B- 9 Pile head displacement 16m fixed headed

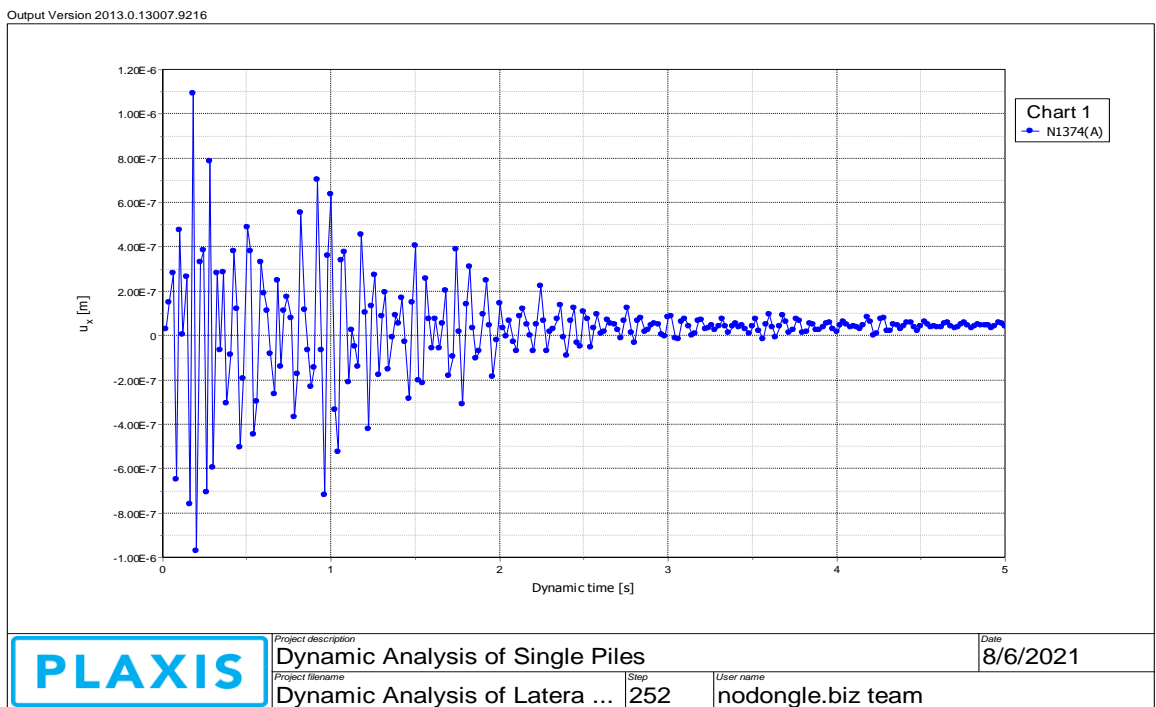


Figure B- 10 Pile head displacement 20m fixed headed

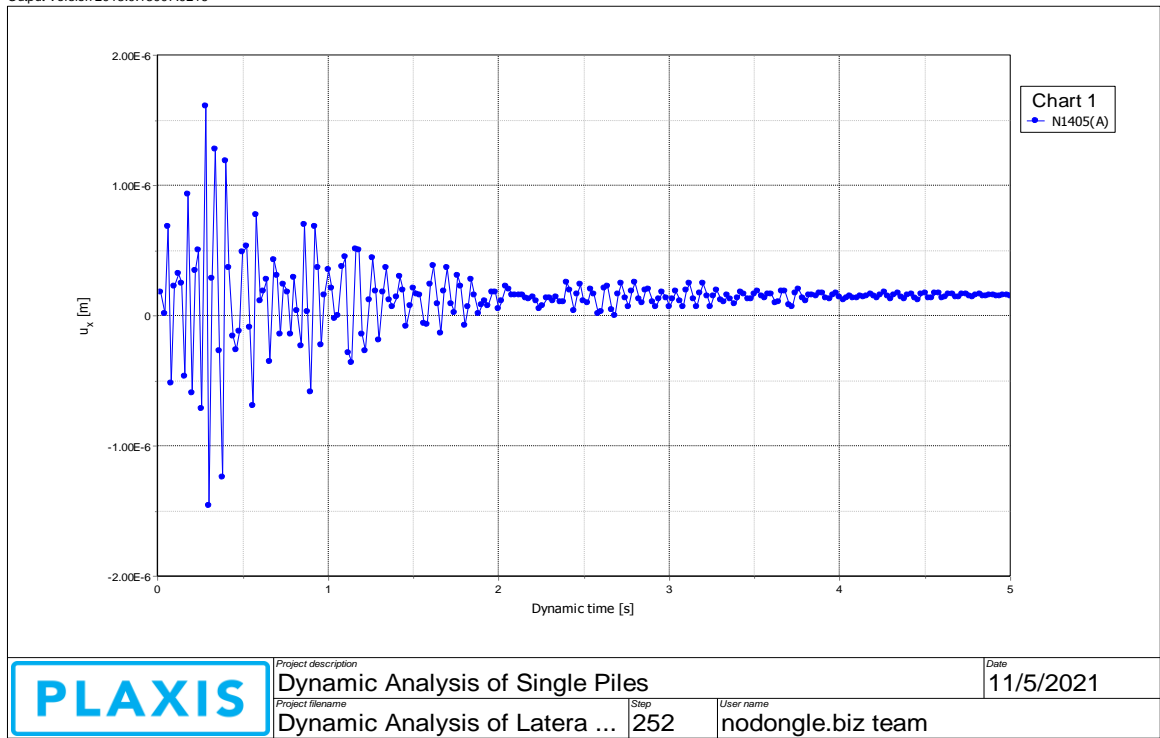


Figure B- 11 Pile head displacement 24m fixed headed